Dynamics and Stability of Tethered Satellites at Lagrangian Points†

by

J. Peláez,
Technical University of Madrid (UPM), 28040 Madrid, Spain

Workshop on Stability and Instability in Mechanical Systems: Applications and Numerical Tools

Thursday, 4 December 2008, Barcelona

† Supported by ESTEC Contract 21259

Dynamics and Stability of Tethered Satellites at Lagrangian Points†

by

Claudio Bombardelli, **Dario Izzo**,

ESTEC-ESA, Noordwijk, 2201 AZ, The Netherlands

Enrico C. Lorenzini, Davide Curreli,

University of Padova, Padova, 35131, Italy

M. Sanjurjo-Rivo, Fernando R. Lucas, J. Peláez,

Technical University of Madrid (UPM), 28040 Madrid, Spain

Daniel J. Scheeres,

The University of Colorado, Boulder, CO 80309-0429, USA

M. Lara

Real Observatorio de la Armada, 11110 San Fernando, Spain

Final Report for the Advanced Concept Team

† Supported by ESTEC Contract 21259

In a tethered system, two masses orbiting at different heights share a common orbital frequency Ω_0 $\Rightarrow$ The third Kepler law is broken by the tether tension

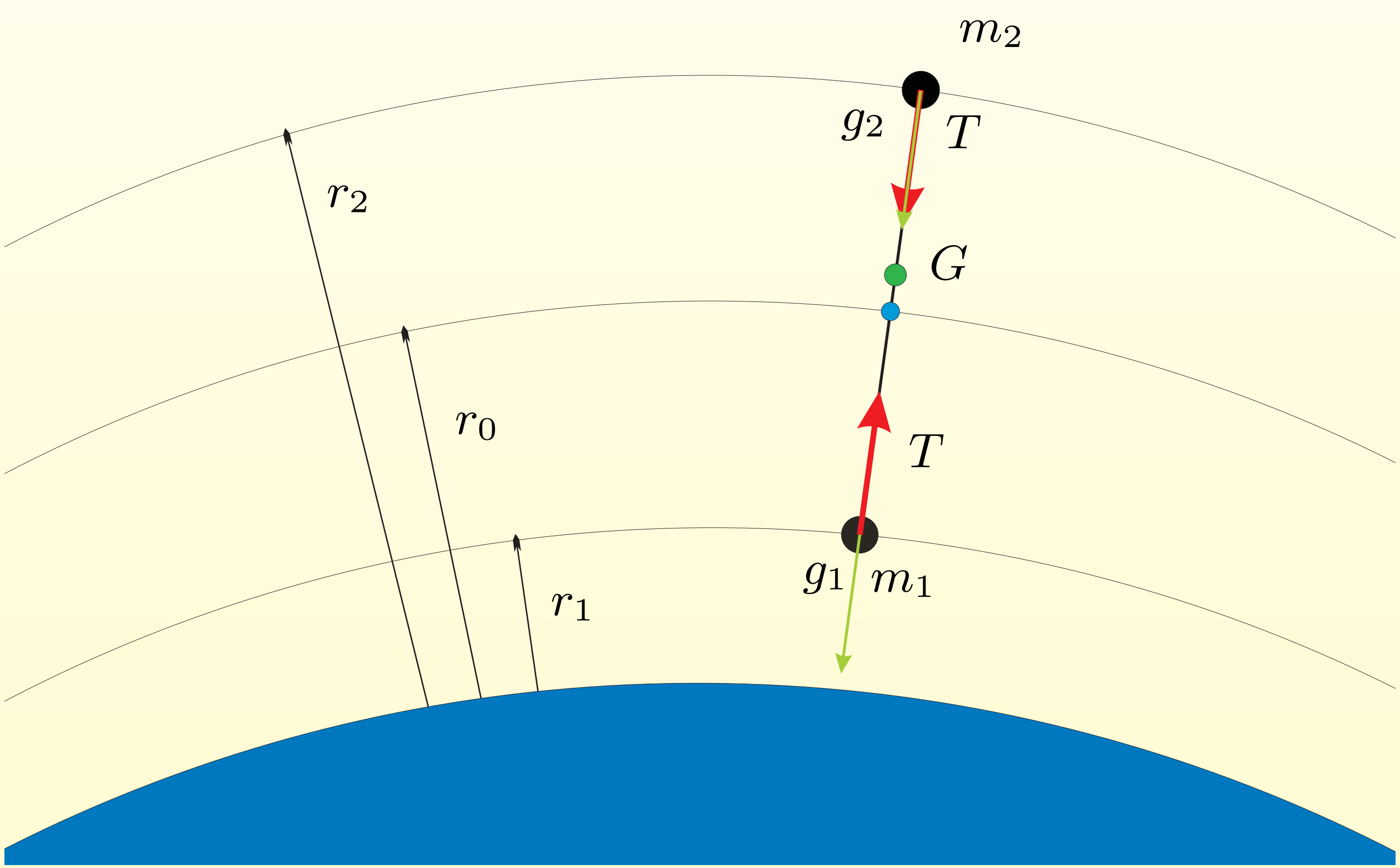

Stable equilibrium along the local vertical

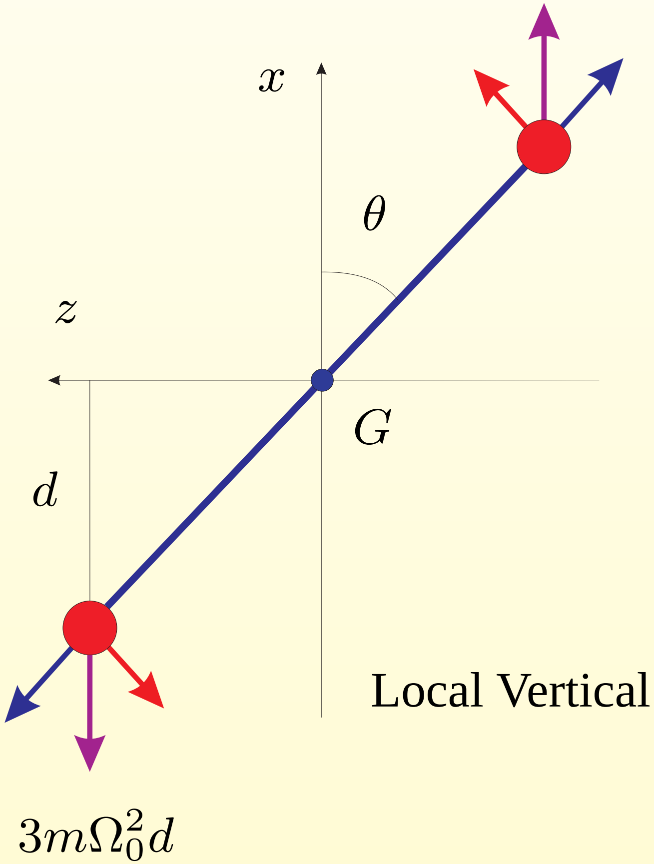

Any deviation θ from the local vertical gives place to a torque. In effect, the gravity gradient force breaks down in

- one component along the tether, which is basically balanced by the tether tension
- one component orthogonal to the tether, which provides the restoring torque. This torque leads the tether again to the local vertical

Thus, the local vertical is a stable equilibrium position for the tethered system

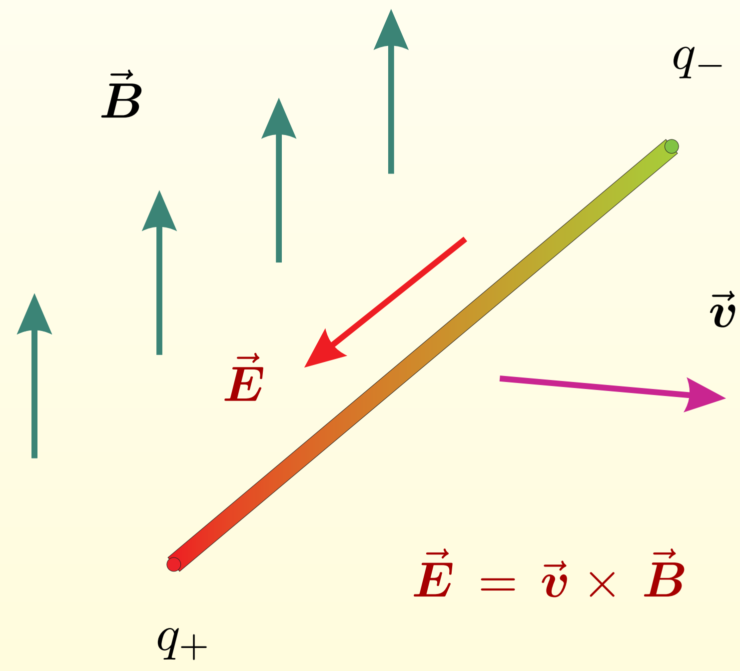

Conductive rod

In a frame attached to the rod, a motional electric field appears

$$\vec{E} = \vec{v} \times \vec{B}$$

It is induced by the magnetic field $\vec{B}$ inside which the rod is moving. For a conductive rod moving in the vacuum, a redistribution of surface charge takes place, leading to a vanishing electric field inside the rod. Thus, a steady state is reached with no motion of charged particles in the rod.

If the rod is moving inside a plasma environment, this picture changes drastically

Electrodynamic tethers in a plasma environment

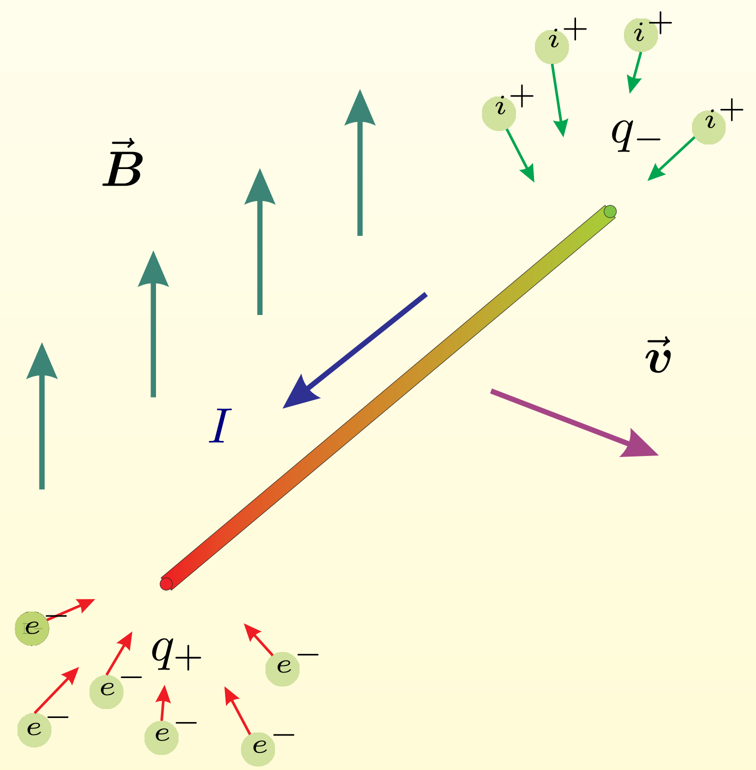

The ionospheric plasma makes the electrons begin to be attracted by the anodic end of the rod. Similarly, the ions will be attracted by the cathodic end. Some of these charges will be trapped by the rod and they produce a current I which flows inside the conductive material. The amount of current I can be increased with the help of plasma contactors placed in the tethers ends. However, the interaction between the tether current I and the magnetic field $\vec{B}$ gives place to forces acting on the rod. They will break (or accelerate) its motion (in the figure they are breaking the motion). Their resultant is: $\vec{F} = \vec{I} \times \vec{B}\, L$

Electrodynamic tethers in a plasma environment

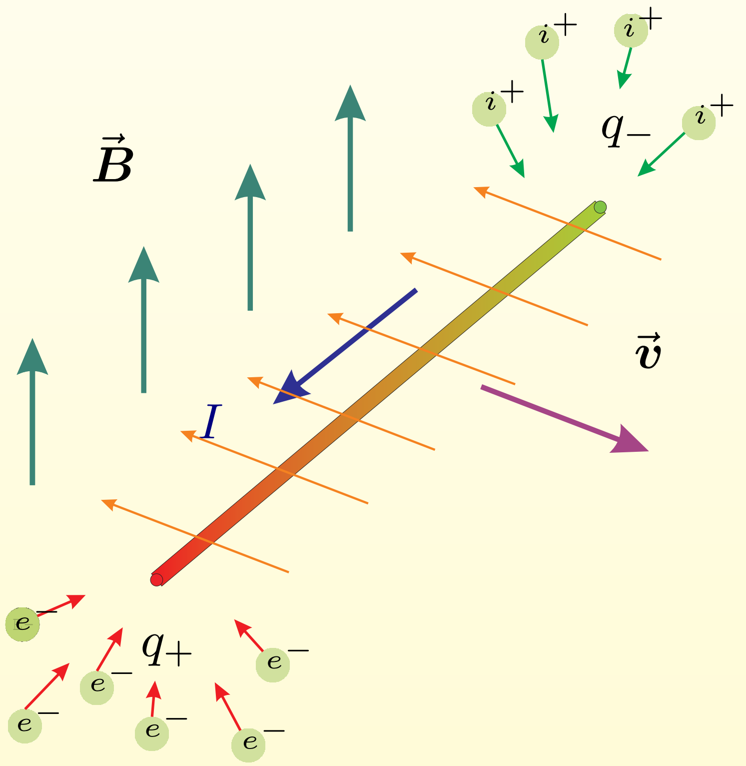

The ionospheric plasma makes the electrons begin to be attracted by the anodic end of the rod. Similarly, the ions will be attracted by the cathodic end. Some of these charges will be trapped by the rod and they produce a current I which flows inside the conductive material. The amount of current I can be increased with the help of plasma contactors placed in the tethers ends. However, the interaction between the tether current I and the magnetic field $\vec{B}$ gives place to forces acting on the rod. They will break (or accelerate) its motion (in the figure they are breaking the motion). Their resultant is: $\vec{F} = \vec{I} \times \vec{B}\, L$

The two basic tether configurations

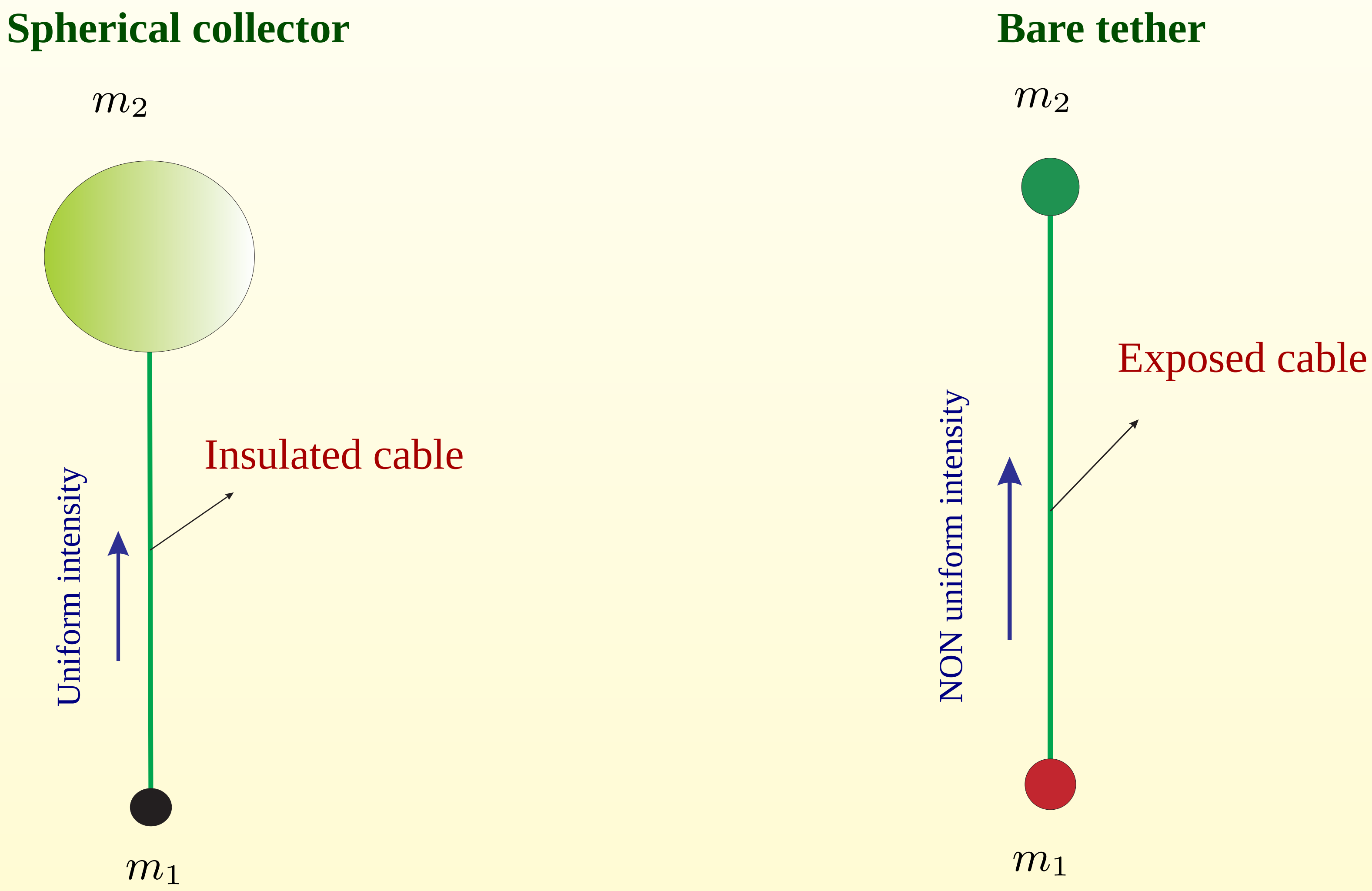

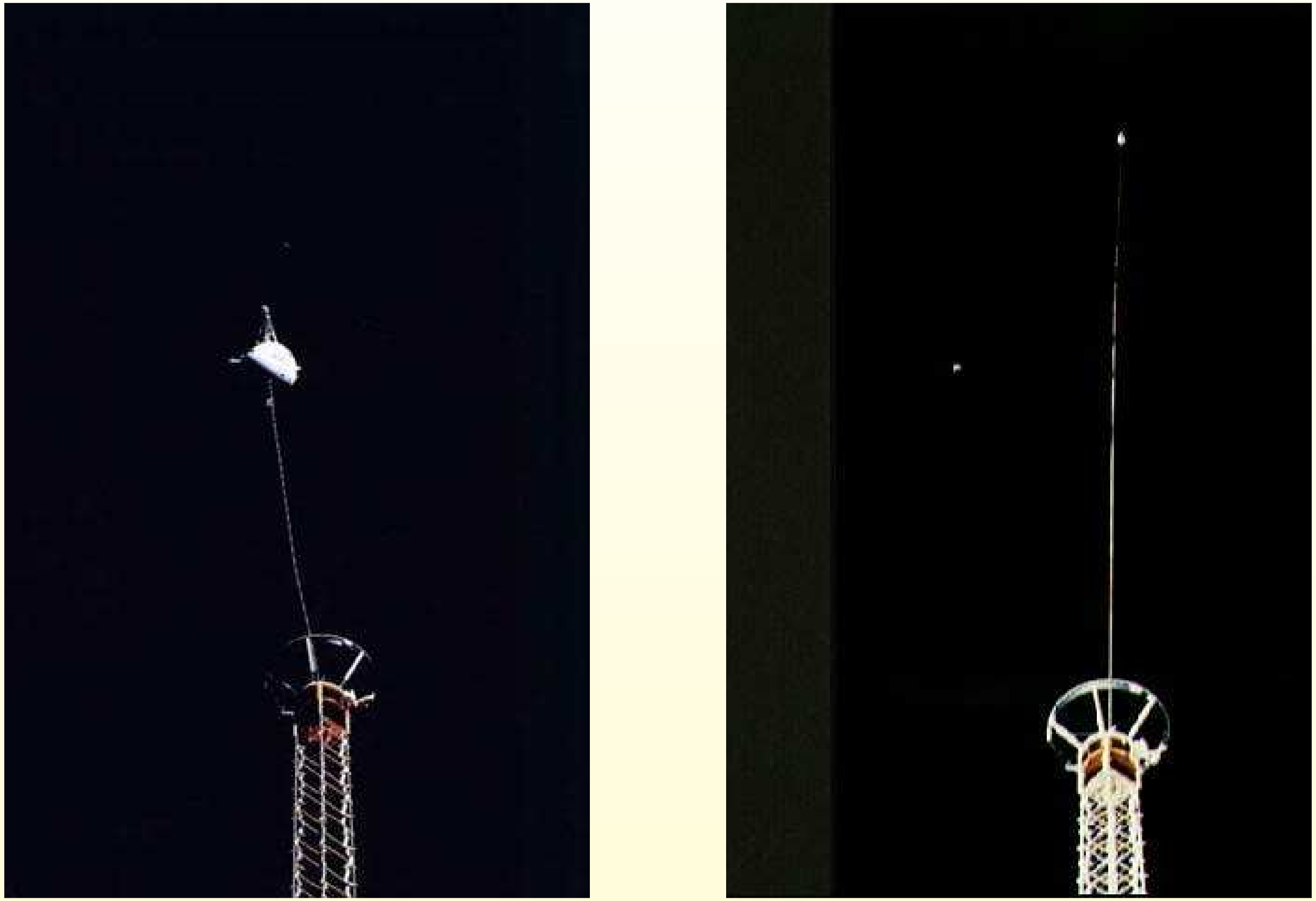

TSS-1R. The Tether is partially deployed

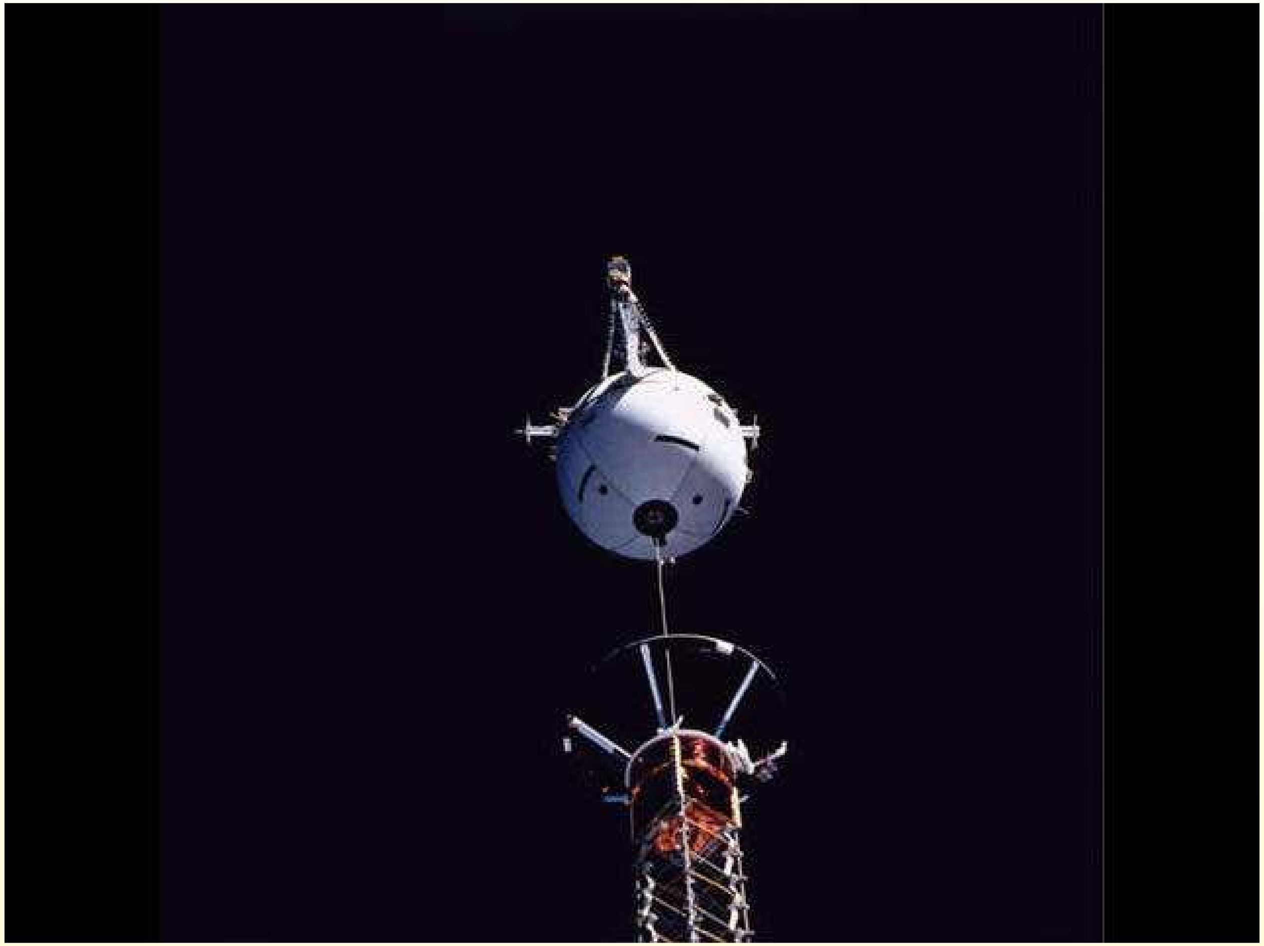

STS-46 Tethered Satellite System 1 (TSS-1) satellite deployment from OV-104

The satellite is reeled out via its thin Kevlar tether into the blackness of space during deployment operations from the payload bay of Atlantis. At the bottom of the frame is the satellite upper boom including (bottom to top) the 12-m deployment boom, tip can, the docking ring, and concentric ring damper. The Langmuir probe and the dipole-field antenna are stowed at either side of the TSS-1 satellite.

Background: Tethered satellites and Lagrangian Points

- The Earth-Moon external point (L_2). Excellent scenario for many different missions
- Tethers are useful in some specific missions
  * Stabilization at Lagrange points (Colombo, Farquhar, Misra)
- ED tethers: may produce power and propulsion in appropriate environments
  * Jovian world (Sanmartín et all., Peláez and Scheeres, . . .)
  * plasma collection is better with straightened tethers
- Tether's stabilization needs mechanical tension
  * Close to a body: gravity gradient (self balanced EDT)
  * Far from body: fast rotating tethers
- Dynamics may be quite different from mass-point satellites
  * coupled roto-traslational motion (long tethers)
  * varying length

Outline of Presentation

- Gentil Introduction
- Inert Tethers and Periodic Motions
- Io Exploration with Electrodynamic Tethers
- Stability of tethered satellites at lagrangian collinear points

• *Dynamics of tethered libration-points satellites*, by

Manuel Sanjurjo Rivo, Fernando R. Lucas & Jesús Peláez,

XI Jornadas de Trabajo en Mecánica Celeste, 25—27 June 2008, Albergue de la Real Fábrica, Ezcaray, La Rioja, Spain

• *Dynamic behavior of a fast-rotating tethered satellite*, by

M. Lara & Jesús Peláez,

XI Jornadas de Trabajo en Mecánica Celeste, 25—27 June 2008, Albergue de la Real Fábrica, Ezcaray, La Rioja, Spain

• *On the dynamics of a tethered system near the colineal libration points*, by

M. Sanjurjo-Rivo, F. R. Lucas, J. Peláez, C. Bombardelli, E. C. Lorenzini, D. Curreli, D. J. Scheeres & M. Lara,

AIAA paper 2008-7380, The **2008 AAS/AIAA Astrodynamics Specialist Conference and Exhibit**, 18—21 Agosto 2008 Hawaii Convention Center and Hilton Hawaiian Village, Honolulu, Hawaii, USA

• *Io exploration with electrodynamic tethers*, by

C. Bombardelli, E. C. Lorenzini, D. Curreli, M. Sanjurjo-Rivo, F. R. Lucas, J. Peláez, D. J. Scheeres & M. Lara,

AIAA paper 2008-7384, The **2008 AAS/AIAA Astrodynamics Specialist Conference and Exhibit**, 18—21 Agosto 2008 Hawaii Convention Center and Hilton Hawaiian Village, Honolulu, Hawaii, USA

Abstracts sent:

• *Plasma torus exploration with electrodynamic tethers*, by

E. C. Lorenzini, D. Curreli, C. Bombardelli, M. Sanjurjo-Rivo, F. R. Lucas, J. Peláez, D. J. Scheeres & M. Lara,

19th AAS/AIAA Space Flight Mechanics Meeting, February 8—12, 2009, Savannah, Georgia, USA

Conclusions

- **Gentil Introduction:** We have developed the theory that permit the analysis theoretical and the simulations of tethers, of constant or varying length, inert or electrodynamic, rotating or non-rotating in the environment provided for a binary system. Some results are completely new and there is nothing similar in the literature.

- **Inert Tethers and Periodic Motions:** The influence of the tether length in the existence and stability of periodic motions associated to Halo orbits has been studied in detail for inert tethers. Some results are completely new and open interesting research lines and possibilities.

- **Io Exploration with Electrodynamic Tethers:** All the analysis is an important novelty. At least two different, and important, research lines have been set up.

- **Stability of tethered satellites at lagrangian collinear points:** We show that the Hill approach permits to clarify some obscure details underneath the previous analysis. An interesting application for the Mars satellites —Deimos or Phobos— can be deduced from our analysis.

Deimos and Phobos

Mars - Deimos

Magnitude	Value	Unit
L_T	10	km
x_E	22.34	km
Δx	200	m
k_ξ	4	
T	72	hours
m	1000	kg
ϕ	45	deg
Λ	0.1	

Mars - Phobos

Magnitude	Value	Unit
L_T	5	km
x_E	16.96	km
Δx	125	m
k_ξ	3	
T	72	hours
m	1000	kg
ϕ	45	deg
Λ	0.1	

Gentil Introduction

GOAL: TO GAIN AN INSIGHT INTO THE DYNAMICS OF FAST ROTATING TS

1. Derive the equations of motion of tethered satellites
   - CRTBP approximation
   - inert tethers, constant length
   - coupled (5-DOF) rotational-traslational motion

2. Fast rotating tethers
   - Average over the (fast) rotation angle

3. Motion “close” to the smaller primary: Hill’s approach
   - In some interesting cases, rotational and translational motion decouple!

4. Show relevant characteristics of specific applications

Inertial motion of an inert tether

- Only gravitational forces
- Dumbbell model $\quad\Rightarrow\quad$ rigid body dynamics:

$$T = \tfrac{1}{2}\, m\,(\dot{\boldsymbol{x}} \cdot \dot{\boldsymbol{x}}) + \frac{1}{2}\boldsymbol{\Omega} \cdot \mathbf{I} \cdot \boldsymbol{\Omega}, \qquad V = -\int_m \frac{\mu}{\|\boldsymbol{y}\|}\,\mathrm{d}m$$

  - m total mass, $\mathbf{I}$ central inertia tensor
  - $\boldsymbol{x}$ position of c.o.m., $\boldsymbol{y}$ position of mass elements
  - $\boldsymbol{\Omega}$ tether's rotation vector
  - μ gravitational parameter of the attracting body

- Lagrangian approach: $\quad \mathcal{L} = T - V \quad\to\quad \dfrac{\mathrm{d}}{\mathrm{d}t}\left(\dfrac{\partial \mathcal{L}}{\partial \dot{q}_j}\right) - \dfrac{\partial \mathcal{L}}{\partial q_j} = 0,$
  - $\dot{q}_j = \mathrm{d}q_j/\mathrm{d}t$, q_j: generalized coordinates

The dumbbell model

- Inertial frame $Oxyz$
- Tether-attached frame: origin G, unit vectors $(\boldsymbol{u}_1, \boldsymbol{u}_2, \boldsymbol{u}_3)$,
  - $\boldsymbol{u}_1 = \boldsymbol{u}, \qquad \boldsymbol{u}_2 = \boldsymbol{k} \times \boldsymbol{u} / \|\boldsymbol{k} \times \boldsymbol{u}\|, \qquad \boldsymbol{u}_3 = \boldsymbol{u}_1 \times \boldsymbol{u}_2,$
  - $\dot{\boldsymbol{u}} = \boldsymbol{\Omega} \times \boldsymbol{u} \qquad \Rightarrow \qquad \boldsymbol{\Omega} = (\boldsymbol{\Omega} \cdot \boldsymbol{u}_1, \boldsymbol{\Omega} \cdot \boldsymbol{u}_2, \boldsymbol{\Omega} \cdot \boldsymbol{u}_3)^T$

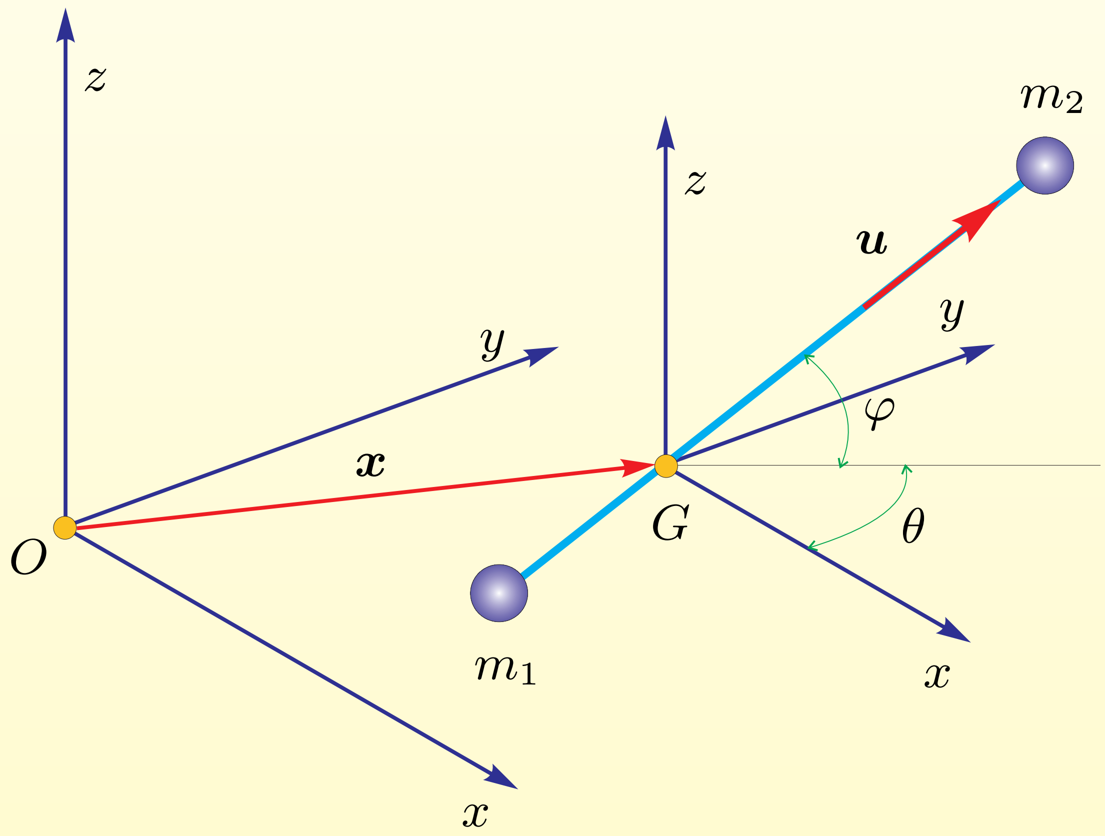

Gravitational Potential

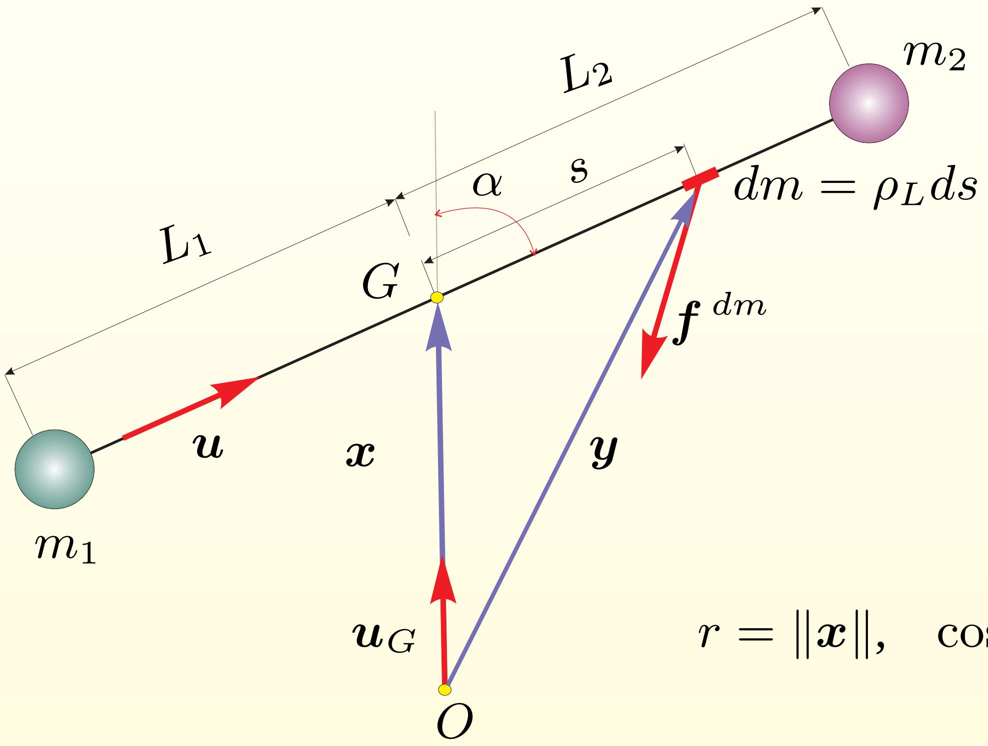

$$V = -\int_m \frac{\mu}{\|\boldsymbol{y}\|}\,\mathrm{d}m$$

$$r = \|\boldsymbol{x}\|, \quad \cos\alpha = \boldsymbol{u}\cdot\boldsymbol{x}/r$$

- Usual expansion of $\dfrac{1}{\|\boldsymbol{y}\|}$ in Legendre polynomials

$$V = -\frac{\mu}{r}\int_m \frac{\mathrm{d}m}{\sqrt{1+2(s/r)\cos\alpha + (s/r)^2}} = -\frac{\mu m}{r}\sum_{n\geq 0}^{\infty}\left(\frac{L}{r}\right)^n a_n\, P_n(\cos\alpha)$$

- $a_n = a_n(m_1, m_2, m_T)$ are functions of tether & end masses ($a_0 = 1$, $a_1 = 0$)

Kinetic analysis

- Kinetic energy: $$T = \frac{1}{2} m \left(\dot{\boldsymbol{x}} \cdot \dot{\boldsymbol{x}} \right) + \frac{1}{2} \boldsymbol{\Omega} \cdot \mathbf{I} \cdot \boldsymbol{\Omega}$$
  - Rotational motion (tether attached frame):
    - Inertia tensor (null moment of inertia around $\boldsymbol{u}$):

$$\mathbf{I} = \begin{pmatrix} 0 & 0 & 0 \\ 0 & \mathcal{I} & 0 \\ 0 & 0 & \mathcal{I} \end{pmatrix} \qquad \mathcal{I} = mL^2 a_2 = \frac{1}{12} mL^2 \left(3 \sin^2 2\phi - 2\Lambda \right)$$

    - $\phi = \phi(m_1, m_2, m_T), \quad \Lambda = m_T / m$
    - $\boldsymbol{\Omega} \cdot \dot{\boldsymbol{u}} = 0 \quad \Rightarrow \quad \boldsymbol{\Omega} \cdot \mathbf{I} \cdot \boldsymbol{\Omega} = \mathcal{I} \, \|\dot{\boldsymbol{u}}\|^2$
    - Position of the tether: $\boldsymbol{u} = (\cos\varphi \, \cos\theta, \cos\varphi \, \sin\theta, \sin\varphi)$

- Kinetic energy: $$T = \frac{1}{2} m \left(\dot{x}^2 + \dot{y}^2 + \dot{z}^2 \right) + \frac{1}{2} \mathcal{I} \left(\dot{\varphi}^2 + \dot{\theta}^2 \cos^2 \varphi \right)$$

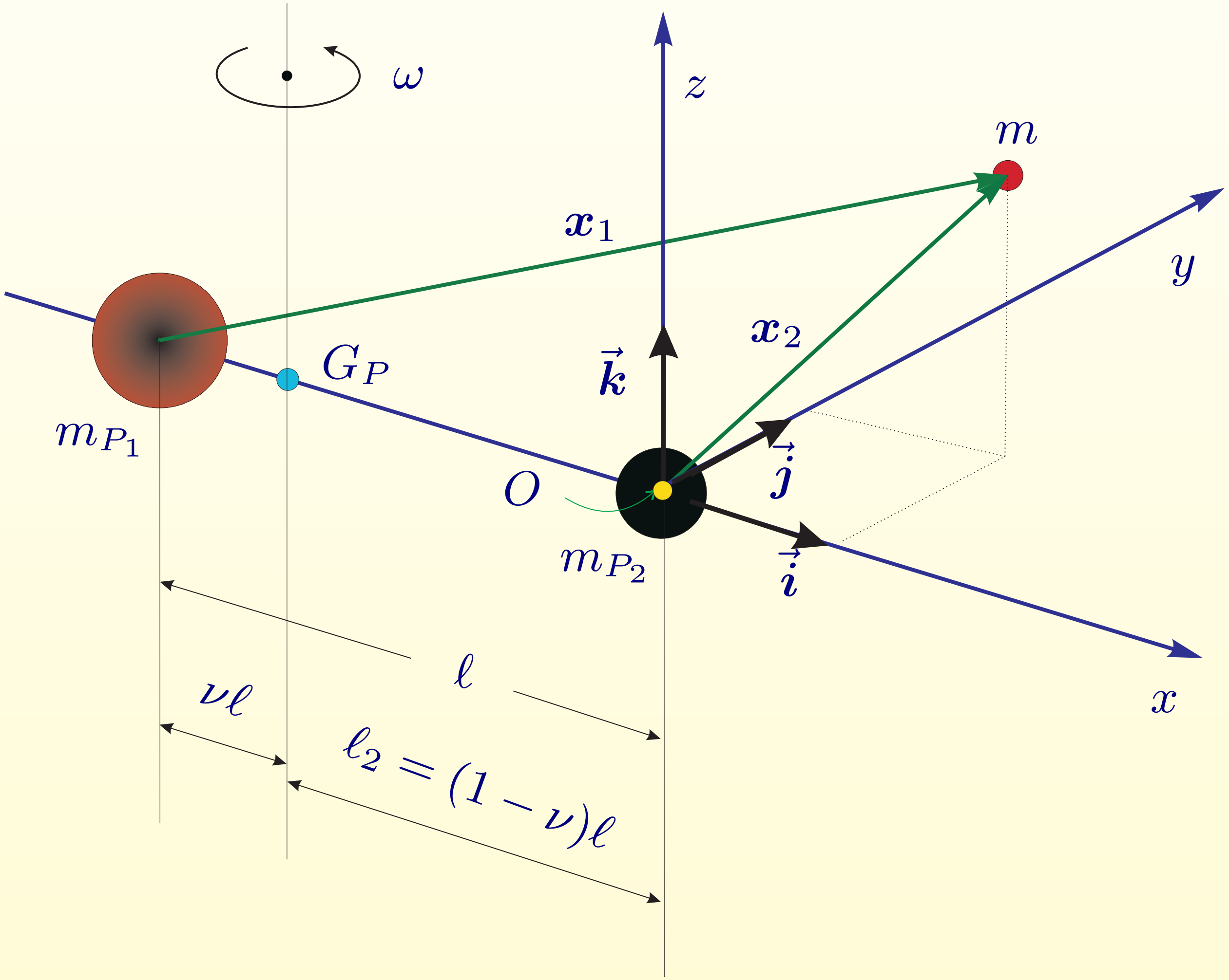

- + Perturbations acting on the c.o.m (ED forces, size, varying length . . .)
- + Attitude dynamics

Motion relative to the synodic frame

1. Two attractive bodies (primaries). Gravitational forces calculated under two assumptions: 1) spherical attracting bodies and, 2) small ratios for $\frac{L}{r_i}$
   - Gravitational potential V_i $(i = 1, 2)$ of each primary:

$$V_i = -\frac{m\mu_i}{r_i}\left[1 + (\frac{L}{r_i})^2\, a_2\, P_2(\cos\alpha_i) + \mathcal{O}(\frac{L}{r_i})^3\right], \qquad \cos\alpha_i = \boldsymbol{u}\cdot\boldsymbol{x}_i/r_i$$

2. Rotating frame $\Rightarrow$ inertia forces
   - Constant rotation rate ω in the z axis direction
   - Generalized potential includes
     - Coriolis term: $m\,\omega\,(x\,\dot{y} - y\,\dot{x})$
     - Rotation term: $m\,(\omega^2/2)\,(x^2 + y^2)$

Lagrangian function and non-dimensional variables

1. Lagrangian function

$$\frac{\mathcal{L}}{m} = \frac{1}{2}(\dot{x}^2 + \dot{y}^2 + \dot{z}^2) + \omega\,(x\,\dot{y} - y\,\dot{x}) + \frac{\omega^2}{2}\,(x^2 + y^2) + \frac{\mu_1}{r_1} + \frac{\mu_2}{r_2}$$
$$+L^2\,a_2\left[\frac{\mu_1}{r_1^3}\,P_2(\cos\alpha_1) + \frac{\mu_2}{r_2^3}\,P_2(\cos\alpha_2) + \frac{1}{2}[\dot{\varphi}^2 + \dot{\theta}^2\cos^2\varphi]\right] + \mathcal{O}(L^3/r^3)$$

   Here, $a_2 = \mathcal{I}/(m\,L^2)$, $\qquad 0 < a_2 < 1/4$

2. Generalized coordinates: x, y, z, φ, θ

3. We use non-dimensional variables with characteristics values: total mass of the system, distance ℓ between primaries, $\tau = \omega\,t$ (primaries' orbit period $= 2\,\pi$)

Governing equations for a constant length inert librating tether

$$- 2\dot{y} - (1-\nu)(1 - \frac{1+x}{\rho_1^3}) - x(1 - \frac{\nu}{\rho^3}) = \epsilon_0^2 \left\{ \frac{(1-\nu)}{\rho_1^5}[3(\boldsymbol{\rho}_1 \cdot \boldsymbol{u})(\vec{\boldsymbol{i}} \cdot \boldsymbol{u}) - (1+x)S_2(\alpha_1)] + \frac{\nu}{\rho^5}[3(\boldsymbol{\rho} \cdot \boldsymbol{u})(\vec{\boldsymbol{i}} \cdot \boldsymbol{u}) - xS_2(\alpha_2)]\right.$$

$$\ddot{y} + 2\dot{x} + y\frac{(1-\nu)}{\rho_1^3} - y(1 - \frac{\nu}{\rho^3}) = \epsilon_0^2 \left\{ \frac{(1-\nu)}{\rho_1^5}[3(\boldsymbol{\rho}_1 \cdot \boldsymbol{u})(\vec{\boldsymbol{j}} \cdot \boldsymbol{u}) - yS_2(\alpha_1)] + \frac{\nu}{\rho^5}[3(\boldsymbol{\rho} \cdot \boldsymbol{u})(\vec{\boldsymbol{j}} \cdot \boldsymbol{u}) - yS_2(\alpha_2)] \right\}$$

$$\ddot{z} + z\frac{\nu}{\rho^3} + z\frac{(1-\nu)}{\rho_1^3} = \epsilon_0^2 \left\{ \frac{(1-\nu)}{\rho_1^5}[3(\boldsymbol{\rho}_1 \cdot \boldsymbol{u})(\vec{\boldsymbol{k}} \cdot \boldsymbol{u}) - zS_2(\alpha_1)] + \frac{\nu}{\rho^5}[3(\boldsymbol{\rho} \cdot \boldsymbol{u})(\vec{\boldsymbol{k}} \cdot \boldsymbol{u}) - zS_2(\alpha_2)] \right\}$$

$$\ddot{\theta}\cos\varphi - 2(1+\dot{\theta})\dot{\varphi}\sin\varphi = 3\frac{(1-\nu)}{\rho_1^5}(\boldsymbol{\rho}_1 \cdot \boldsymbol{u})(\boldsymbol{\rho}_1 \cdot \boldsymbol{u}_2) + 3\frac{\nu}{\rho^5}(\boldsymbol{\rho} \cdot \boldsymbol{u})(\boldsymbol{\rho} \cdot \boldsymbol{u}_2)$$

$$\ddot{\varphi} + (1+\dot{\theta})^2 \sin\varphi\cos\varphi = 3\frac{(1-\nu)}{\rho_1^5}(\boldsymbol{\rho}_1 \cdot \boldsymbol{u})(\boldsymbol{\rho}_1 \cdot \boldsymbol{u}_3) + 3\frac{\nu}{\rho^5}(\boldsymbol{\rho} \cdot \boldsymbol{u})(\boldsymbol{\rho} \cdot \boldsymbol{u}_3)$$

$\nu \equiv$ reduced mass of the small primary, $\quad \varepsilon_0^2 = (\frac{L}{\ell})^2 a_2, \quad S_2(\alpha_i) = \frac{3}{2}(5\cos^2\alpha_i - 1)$

$$\cos\alpha_1 = \frac{\boldsymbol{\rho}_1}{\rho_1} \cdot \boldsymbol{u}, \qquad \cos\alpha_2 = \frac{\boldsymbol{\rho}}{\rho} \cdot \boldsymbol{u}$$

The Attitude Dynamics of the tether can be analyzed more intuitively using the Newton-Euler formulation. The core of the analysis is the angular momentum equation:

$$\frac{d\boldsymbol{H}_G}{dt} = \boldsymbol{M}_G$$

Here $\boldsymbol{M}_G$ is the resultant of the **external** torques applied to the center of mass G of the tethered system and $\boldsymbol{H}_G$ is the angular momentum of the system, at G, in the motion relative to the center of mass.

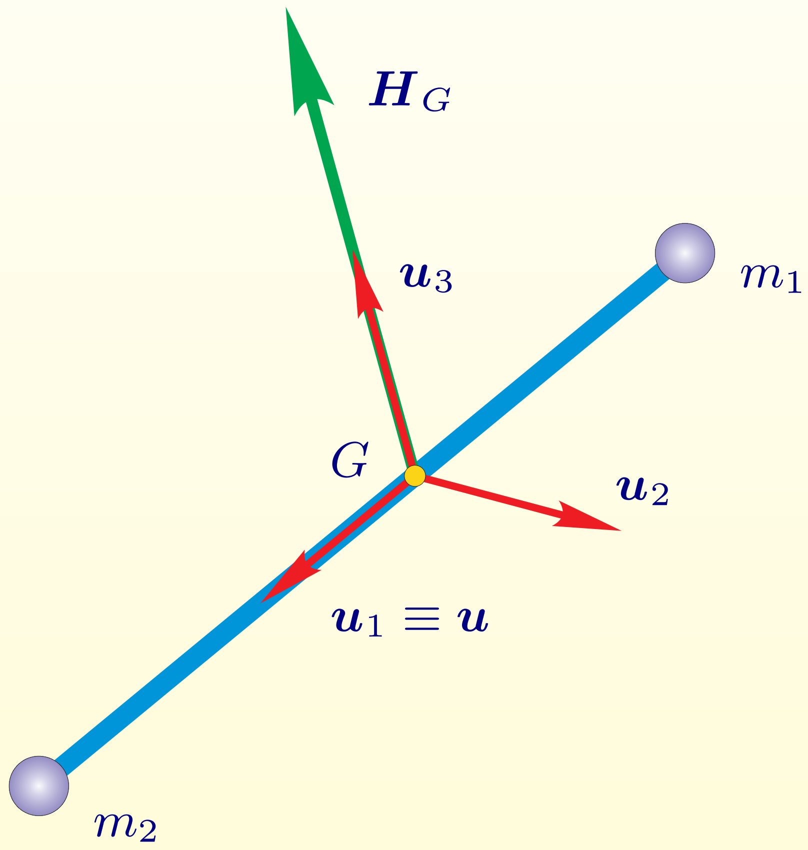

Rotating Tether Attitude Dynamics

In the **Dumbbell Model** the angular velocity of the tether and its angular momentum $\boldsymbol{H}_G$ are:

$$\vec{\boldsymbol{\Omega}} = \boldsymbol{u} \times \dot{\boldsymbol{u}} + \boldsymbol{u}\,(\boldsymbol{u} \cdot \boldsymbol{\Omega}\,), \qquad \boldsymbol{H}_G = \mathbf{I} \circ \boldsymbol{\Omega} = \mathcal{I}(\boldsymbol{u} \times \dot{\boldsymbol{u}})$$

Attached to the tether we take a reference frame $Gu_1u_2u_3$ where the unit vectors are given by:

$$\boldsymbol{u}_1 = \boldsymbol{u}, \qquad \boldsymbol{u}_2 = \frac{\dot{\boldsymbol{u}}}{\|\dot{\boldsymbol{u}}\|}, \qquad \boldsymbol{u}_3 = \boldsymbol{u}_1 \times \boldsymbol{u}_2$$

In this body frame the angular momentum is:

$$\boldsymbol{H}_G = \mathcal{I}\tilde{\Omega}_\perp \boldsymbol{u}_3, \qquad \text{where} \qquad \tilde{\Omega}_\perp = \|\boldsymbol{u} \times \dot{\boldsymbol{u}}\| = \|\dot{\boldsymbol{u}}\|$$

and the angular momentum equation takes the form:

$$\frac{d\tilde{\Omega}_\perp}{dt}\boldsymbol{u}_3 + \tilde{\Omega}_\perp \frac{d\boldsymbol{u}_3}{dt} = \frac{1}{\mathcal{I}}\boldsymbol{M}_G$$

This way we obtain the following equations:

$$\frac{d\boldsymbol{u}_1}{dt} = \tilde{\Omega}_\perp \boldsymbol{u}_2$$

$$\frac{d\boldsymbol{u}_3}{dt} = \frac{M_2}{\tilde{\Omega}_\perp \mathcal{I}} \boldsymbol{u}_2$$

$$\frac{d\tilde{\Omega}_\perp}{dt} = \frac{M_3}{\mathcal{I}}$$

We introduce the Tait-Bryant angles (or Cardan angles) as generalized coordinates. Notice that, from a mathematical point of view, we have a four-orden system of ODE'S.

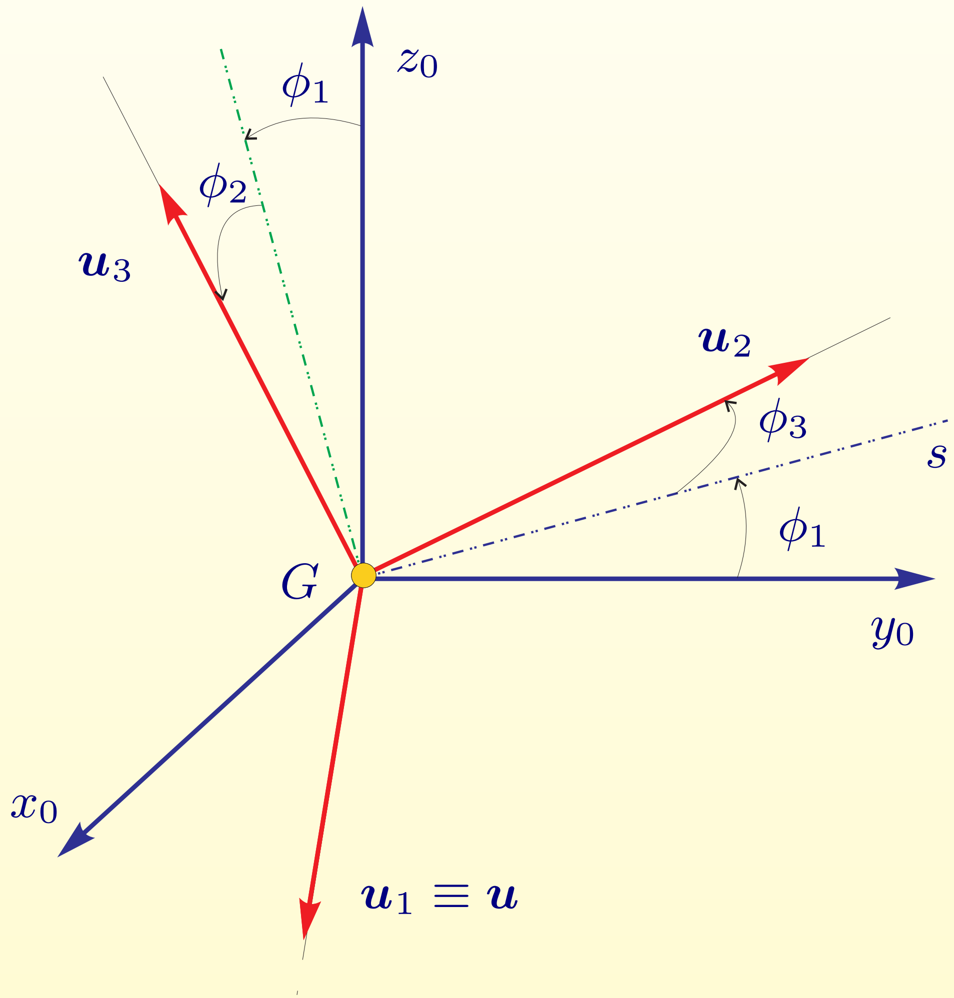

Rotating Tether Attitude Dynamics

In terms of the Bryant angles the unit vectors $\boldsymbol{u}_1$ and $\boldsymbol{u}_3$ are given by

$$\boldsymbol{u}_1 = (\cos\phi_2\cos\phi_3,\ \cos\phi_1\sin\phi_3 + \sin\phi_1\sin\phi_2\cos\phi_3,\ \sin\phi_1\sin\phi_3 - \cos\phi_1\sin\phi_2\cos\phi_3)$$

$$\boldsymbol{u}_3 = (\sin\phi_2,\ -\sin\phi_1\cos\phi_2,\ \cos\phi_1\cos\phi_2)$$

The equations governing the time evolution of the Bryant angles are:

$$\frac{d\phi_1}{d\tau} = -\frac{M_2}{\omega^2\mathcal{I}}\cdot\frac{1}{\Omega_\perp}\cdot\frac{\cos\phi_3}{\cos\phi_2}$$

$$\frac{d\phi_2}{d\tau} = -\frac{M_2}{\omega^2\mathcal{I}}\cdot\frac{1}{\Omega_\perp}\cdot\sin\phi_3$$

$$\frac{d\phi_3}{d\tau} = \Omega_\perp + \frac{M_2}{\omega^2\mathcal{I}}\cdot\frac{1}{\Omega_\perp}\cdot\cos\phi_3\tan\phi_2$$

$$\frac{d\Omega_\perp}{d\tau} = \frac{M_3}{\omega^2\mathcal{I}}$$

where $\Omega_\perp = \tilde{\Omega}_\perp/\omega$ is the non-dimensional form of $\tilde{\Omega}_\perp$. These equations should be integrated from the initial conditions:

$$\text{at}\quad \tau = 0: \quad \phi_1 = \phi_{1\,0},\ \phi_2 = \phi_{2\,0},\ \phi_3 = \phi_{3\,0},\ \Omega_\perp = \Omega_{\perp\,0}$$

Fast Rotating Tether

For a **fast rotating tether** the value of $\Omega_\perp$ is large, $\Omega_\perp \gg 1$. There are two characteristic times:

1) the period of the orbital dynamics of both primaries, $\tau = \mathcal{O}(1)$ and

2) the period of the intrinsic rotation of the tether $\tau_1 = \Omega_\perp \tau = \mathcal{O}(1)$

For example, consider the governing equation

$$\frac{d\phi}{d\tau} = f(\phi_1, \phi_2, \phi_3, \Omega_\perp)$$

Its averaged equations form is:

$$< \frac{d\phi}{d\tau} >= \frac{1}{2\pi} \int_0^{2\pi} f(\phi_1, \phi_2, \phi_3, \Omega_\perp) d\tau_1$$

To integrate the function $f(\phi_1, \phi_2, \phi_3, \Omega_\perp)$ the slow variables $(\phi_1, \phi_2, \Omega_\perp)$ take constant values and the fast variable ϕ_3 is approximated by $\phi_3 \approx \tau_1 + \phi_{3_0}$.

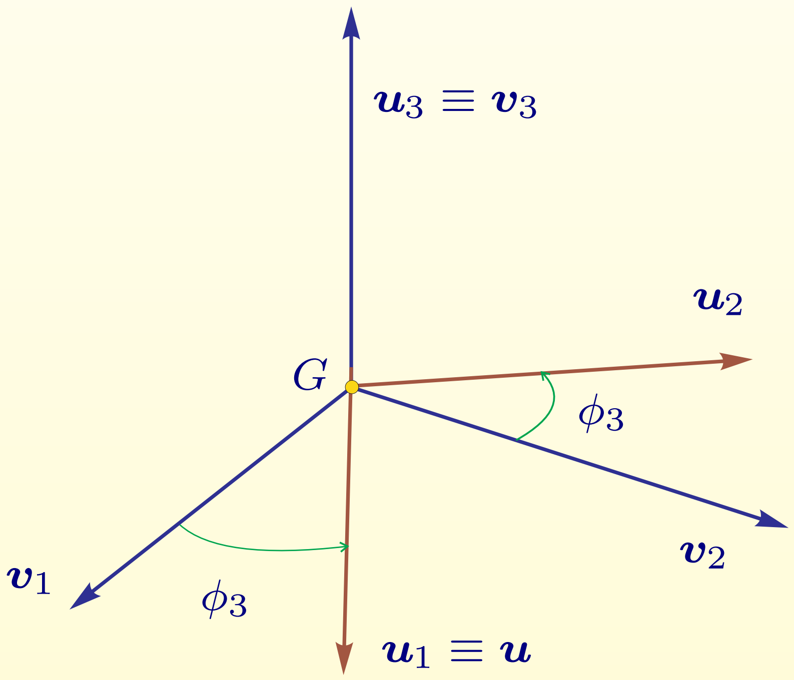

Stroboscopic frame

Averaged equations for an inert fast rotating tether

$$- 2\dot{y} - (1-\nu)\left(1-\frac{1+x}{\rho_1^3}\right) - x\left(1-\frac{\nu}{\rho^3}\right) = \frac{\epsilon_0^2}{2}\left\{ \frac{\nu-1}{\rho_1^5}\left[3(\sin\phi_2+\tilde{n})\sin\phi_2 - (1+x)S_2\left(\frac{\tilde{n}_1}{\rho_1}\right)\right] - \frac{\nu}{\rho^5}\left[3\tilde{n}\sin\phi_2 - xS_2\left(\frac{\tilde{n}}{\rho}\right)\right]\right\}$$

$$\ddot{y} + 2\dot{x} + y\frac{(1-\nu)}{\rho_1^3} - y\left(1-\frac{\nu}{\rho^3}\right) = \frac{\epsilon_0^2}{2}\left\{ \frac{1-\nu}{\rho_1^5}\left[3(\sin\phi_2+\tilde{n})\cos\phi_2\sin\phi_1 + yS_2\left(\frac{\tilde{n}_1}{\rho_1}\right)\right] + \frac{\nu}{\rho^5}\left[3\tilde{n}\cos\phi_2\sin\phi_1 + yS_2\left(\frac{\tilde{n}}{\rho}\right)\right]\right.$$

$$\ddot{z} + z\frac{\nu}{\rho^3} + z\frac{(1-\nu)}{\rho_1^3} = \frac{\epsilon_0^2}{2}\left\{ \frac{\nu-1}{\rho_1^5}\left[3(\sin\phi_2+\tilde{n})\cos\phi_2\cos\phi_1 - zS_2\left(\frac{\tilde{n}_1}{\rho_1}\right)\right] - \frac{\nu}{\rho^5}\left[3\tilde{n}\cos\phi_2\cos\phi_1 - zS_2\left(\frac{\tilde{n}}{\rho}\right)\right.\right.$$

$$\frac{d\phi_1}{d\tau} = \left(1+\frac{\cos\phi_1\cos\phi_2}{2\Omega_\perp}\right)\frac{\sin\phi_2\cos\phi_1}{\cos\phi_2} + \frac{3}{2}\frac{(1-\nu)}{\Omega_\perp}\frac{(\sin\phi_2+\tilde{n})(\cos\phi_2+\tilde{b})}{\rho_1^5\cos\phi_2} + \frac{3}{2}\frac{\nu}{\Omega_\perp}\frac{\tilde{n}\,\tilde{b}}{\rho^5\cos\phi_2}$$

$$\frac{d\phi_2}{d\tau} = -\left(1+\frac{\cos\phi_1\cos\phi_2}{2\Omega_\perp}\right)\sin\phi_1 + (y\cos\phi_1 + z\sin\phi_1)\left\{\frac{3}{2}\frac{(1-\nu)}{\Omega_\perp}\frac{(\sin\phi_2+\tilde{n})}{\rho_1^5} + \frac{3}{2}\frac{\nu}{\Omega_\perp}\frac{\tilde{n}}{\rho^5}\right\}$$

$$\frac{d\Omega_\perp}{d\tau} = \sin\phi_1\sin\phi_2\cos\phi_1$$

where the quantities $(\tilde{n}, \tilde{b})$ and the fast variable ϕ_3 are given by

$$\tilde{n} = x\sin\phi_2 - (y\sin\phi_1 - z\cos\phi_1)\cos\phi_2$$

$$\tilde{b} = x\cos\phi_2 + (y\sin\phi_1 - z\cos\phi_1)\sin\phi_2$$

$$\frac{d\phi_3}{d\tau} = \Omega_\perp - \left(1+\frac{\cos\phi_1\cos\phi_2}{2\Omega_\perp}\right)\frac{\sin^2\phi_2\cos\phi_1}{\cos\phi_2} - \frac{3}{2}\frac{(1-\nu)}{\Omega_\perp}\frac{(\sin\phi_2+\tilde{n})(\cos\phi_2+\tilde{b})}{\rho_1^5}\tan\phi_2 - \frac{3}{2}\frac{\nu}{\Omega_\perp}\frac{\tilde{n}\,\tilde{b}}{\rho^5}\tan\phi_2$$

Remember: for a FRT the non-dimensional variable $\Omega_\perp$ is a large number, that is, $\Omega_\perp \gg 1$.

The Hill approach for fast rotating tethers

• Frequently, the parameter ν is small. The Hill approximation give us the right order of magnitude of distance to the small primary. We introduce this approximation by means of the change of variables:

$$x = \ell\,\nu^{1/3}\,\xi, \qquad y = \ell\,\nu^{1/3}\,\eta, \qquad z = \ell\,\nu^{1/3}\,\zeta, \qquad \rho = \ell\,\nu^{1/3}\,\hat{\rho}$$

• For a FRT the parameter $\Omega_\perp$ is large ($\Omega_\perp \gg 1$). For example, taking Jupiter and Io as primaries, $T_p \approx 1.769$ days. If $T_{FRT} \approx 25$ minutes then $\Omega_\perp > 100$. It is reasonable to take the limit $\Omega_\perp \to \infty$ in the governing equations.

• The tether's characteristic length, $\lambda = \dfrac{a_2}{2}\left(\dfrac{L}{\nu^{1/3}\,\ell}\right)^2$ appears in a natural way in the problem (here $\nu = \mu/(\mu_1 + \mu)$ is the reduced mass of the small primary or central body).

The Hill approach for fast rotating tethers

$$\ddot{\xi} - 2\dot{\eta} = (3 - \frac{1}{\hat{\rho}^3})\xi - \frac{\lambda}{\hat{\rho}^5}\left\{3\tilde{N}\sin\phi_2 - \xi S_2(\frac{\tilde{N}}{\hat{\rho}})\right\}$$

$$\ddot{\eta} + 2\dot{\xi} = -\frac{\eta}{\hat{\rho}^3} + \frac{\lambda}{\hat{\rho}^5}\left\{3\tilde{N}\cos\phi_2\sin\phi_1 + \eta S_2(\frac{\tilde{N}}{\hat{\rho}})\right\}$$

$$\ddot{\zeta} = -\zeta(1 + \frac{1}{\hat{\rho}^3}) - \frac{\lambda}{\hat{\rho}^5}\left\{3\tilde{N}\cos\phi_2\cos\phi_1 - \zeta S_2(\frac{\tilde{N}}{\hat{\rho}})\right\}$$

$$\frac{d\phi_1}{d\tau} = \cos\phi_1\tan\phi_2$$

$$\frac{d\phi_2}{d\tau} = -\sin\phi_1$$

$$\tilde{N} = \xi\sin\phi_2 - (\eta\sin\phi_1 - \zeta\cos\phi_1)\cos\phi_2$$

These equations should be integrated from the initial conditions:

$$\text{at} \quad \tau = 0: \quad \xi = \xi_0,\ \eta = \eta_0,\ \zeta = \zeta_0,\ \dot{\xi} = \dot{\xi}_0,\ \dot{\eta} = \dot{\eta}_0,\ \dot{\zeta} = \dot{\zeta}_0,\ \phi_1 = \phi_{10},\ \phi_2 = \phi_{20}$$

If the initial conditions are $\phi_{10} = \phi_{20} = 0 \quad \Rightarrow \quad \phi_1(\tau) = \phi_2(\tau) \equiv 0.$

The Hill approach for fast rotating tethers

TETHER ROTATION PARALLEL TO THE PRIMARIES PLANE:

$$
\begin{aligned}
\xi'' - 2\,\eta' &= 3\,\xi - \frac{\xi}{\rho^3} - \frac{3}{2}\,\lambda\,\frac{\xi}{\rho^5}\left(1 - 5\,\frac{\zeta^2}{\rho^2}\right)\\
\eta'' + 2\,\xi' &= -\frac{\eta}{\rho^3} - \frac{3}{2}\,\lambda\,\frac{\eta}{\rho^5}\left(1 - 5\,\frac{\zeta^2}{\rho^2}\right)\\
\zeta'' &= -\zeta - \frac{\zeta}{\rho^3} - \frac{3}{2}\,\lambda\,\frac{\zeta}{\rho^5}\left(3 - 5\,\frac{\zeta^2}{\rho^2}\right)
\end{aligned}
$$

Formally equal to a Hill-J_2 problem:

- J_2 helps to stabilize high inclination orbits
- we have control over L and, therefore, over λ!
- λ might take “high” values with feasible tether lengths
  - $\lambda = 0.01 \quad \Rightarrow \quad$ Metis: $L \approx 7.2$ km ($R_\oplus \approx 50$ km)
  - $\ldots$when consistent with our $\mathcal{O}(L/r)^3$ approximation

Hill+oblateness long-term dynamics

- Studied since the dawn of the space era (Lidov, Kozai)
- β: ratio J_2 to third body perturbations ($\beta^2 \propto a^{-5}$)

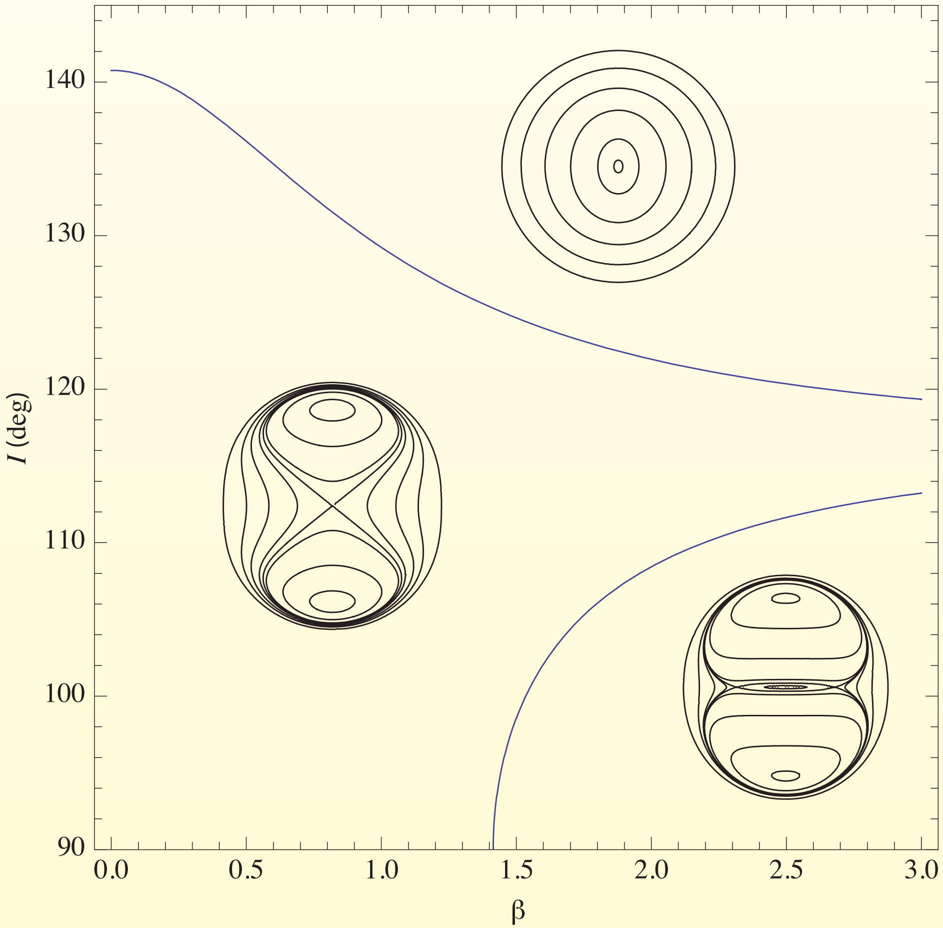

The END of this Gentil Introduction

Inert Tethers and Periodic Motions

Inert tethers and periodic motions

In the CRTBP for a mass particle there are three well known families of periodic motion originated from the collinear points:

- 1) Lyapunov periodic orbits, starting from highly unstable small ellipses with retrograde motion around the collinear points
- 3) Eight-shaped orbits
- 2) Halo orbits bifurcated from the Lyapunov family

Figure is an sketch of three starting orbits

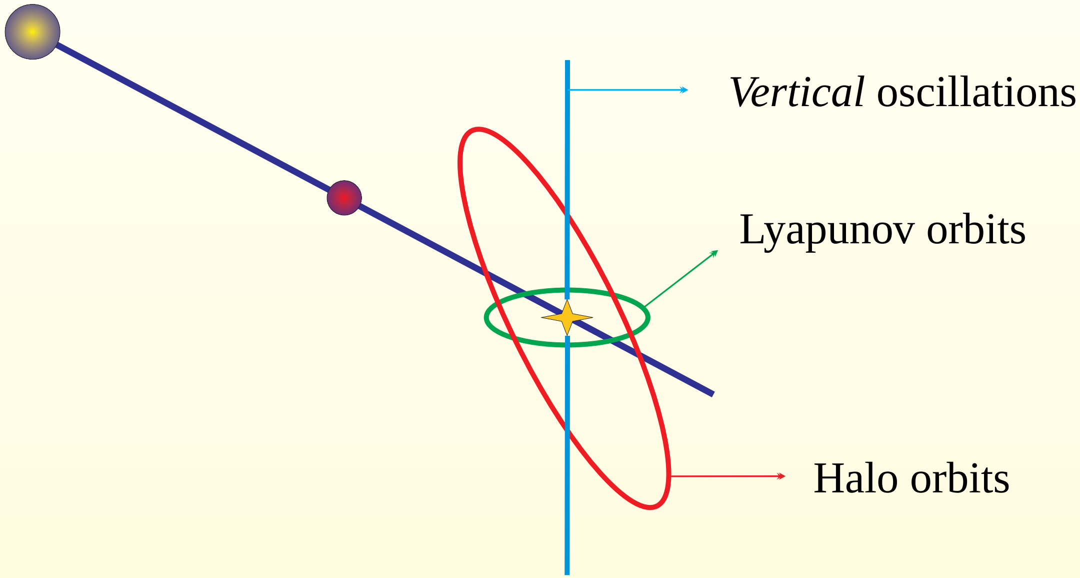

We carried out numerical explorations of the tethered-satellite problem. More precisely, we discuss how the known periodic solutions of the Hill problem are modified in the case of tethered satellites. The most favorable configuration is found for tethers rotating parallel to the plane of the primaries, a case in which the attitude of the tethered-satellite remains constant on average. In this case, the effect produced by a non-negligible tether's length is equivalent to introducing a J_2 perturbation on the primary at the origin, or intensifying it if the primary at the origin is an oblate body, and it is shown that either lengthening or shortening the tether may lead to orbit stability. Promising results are found for eight-shaped orbits, but regions of stability are also found for Halo orbits.

Summary

• Lyapunov orbits: there is no beneficial effects on orbit stability by using tethered satellites

• Eight-shaped orbits: the presence of the tether in general, reduces instability. Stability regions are found for certain lengths of the tether when the Jacobi constant remains below roughly $C = 3$.

• Halo orbits: stability regions for the tethered satellites are generally found, even when starting from highly unstable orbits of the Hill problem. The general effect of lengthening the tether is to narrow and twist the Halo, sometimes converting the Halo in a thin, eight-shaped orbit. However, depending on the Jacobi constant value of the starting Halo orbit, the required length of the tether to stabilize the orbit may be small and the stabilized orbit may retain most of the Haloing characteristics.

Two different motivations to use a tether: 1) to stabilize unstable Halo orbits and 2) to take advantage of the tether; it enjoys the stability properties of some stable Halo orbits (for values of C close to the lower limit).
Therefore, **at first sight, the most promising regions are close to the Halo family's stability region of the Hill problem**, where tethers of few tenths of kilometers may stabilize Halo orbits of the simplified model. For specific applications one needs to check that the tether length required for stabilization is feasible, say of few tenths of km, and that the corresponding Halo orbit does not impact the central body.

Summary

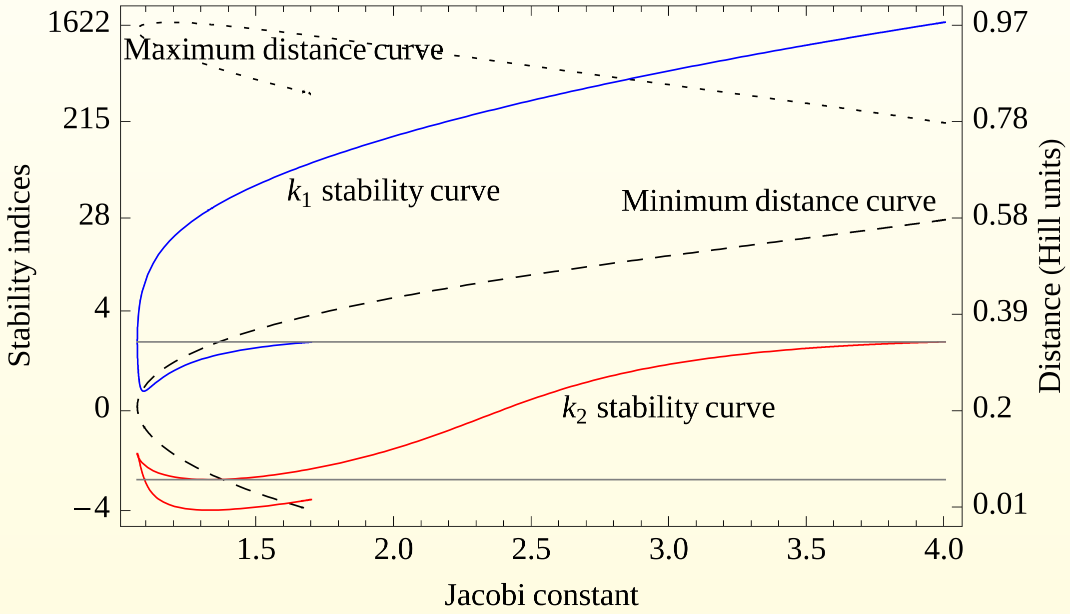

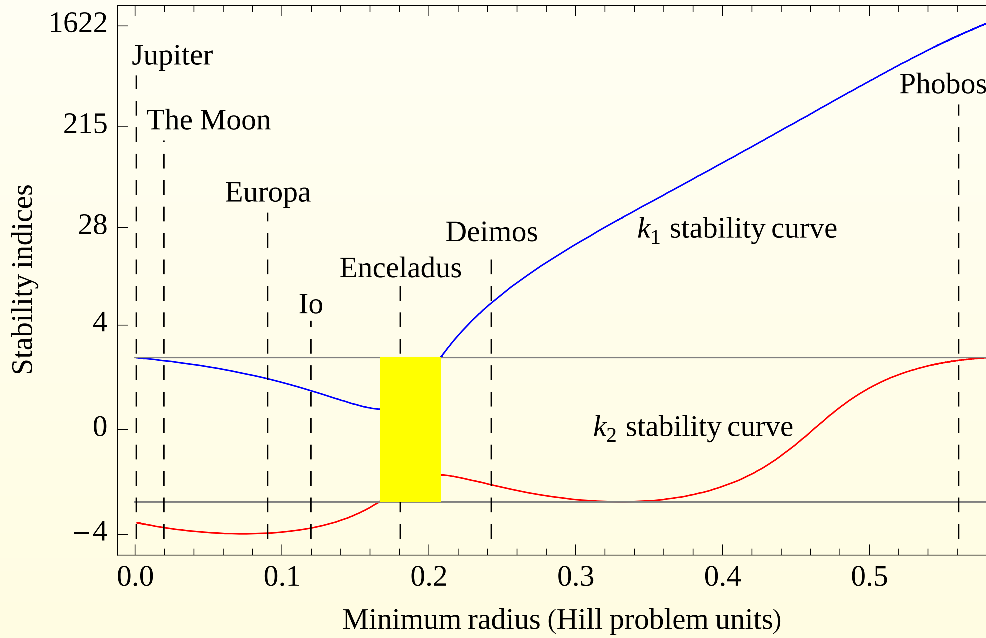

- Left: Stability diagram of the Halo family of the Hill problem (no tether) showing the maximum and minimum distance to the origin.

Right: Stability diagram of the Halo family of the Hill problem (no tether) as a function of the minimum distance to the origin.

Summary

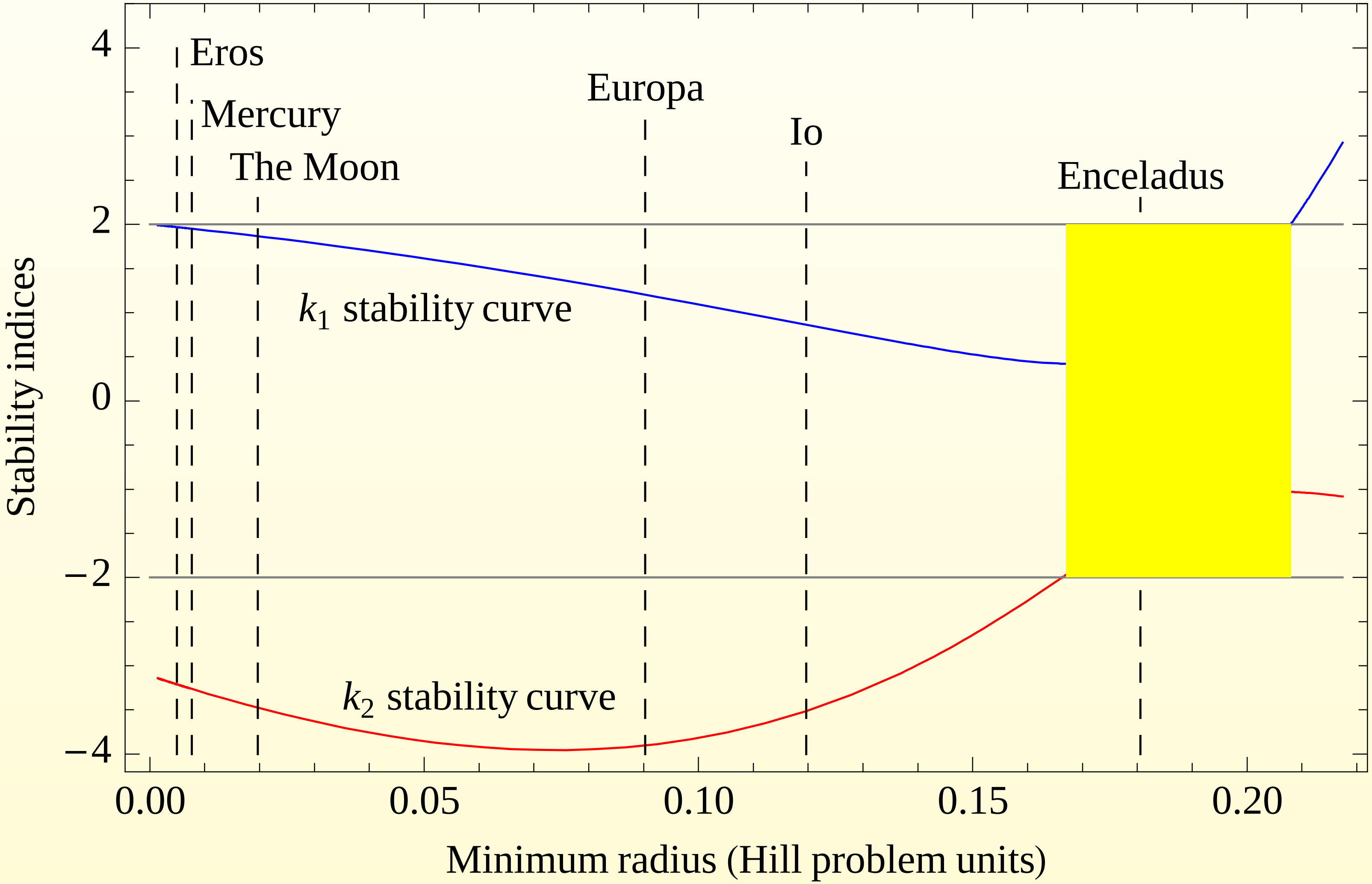

Right: Stability diagram of the Halo family of the Hill problem (no tether) as a function of the minimum distance to the origin.

Summary

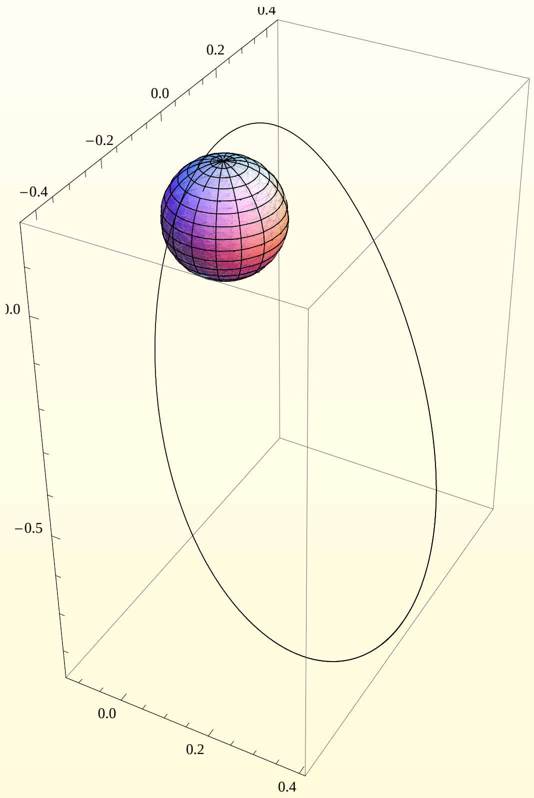

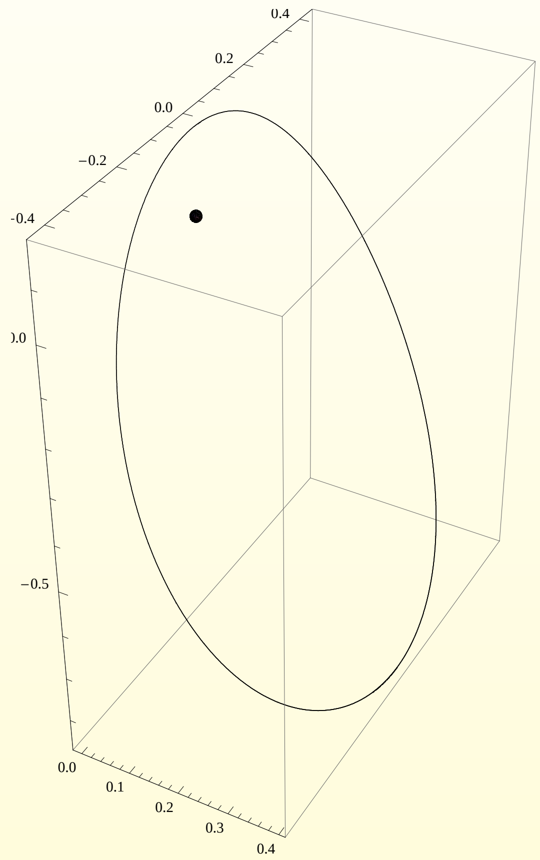

• Left: Halo orbit close to Io, stabilized with a tether length of $\sim$ 70 km. The minimum distance to Io is about one half of it radius.

Right: Halo orbit about Eros, stabilized with a tether length of $\sim$ 110 km.

The END of Inert Tethers and Periodic Motions

Io Exploration with Electrodynamic Tethers

Power and Masses of some RTG's

Mission	Thermal W	Electrical W	Mass (kg)
Pionner 10	2250	150	54.4
Voyager 1 y 2	7200	470	117
Ulysses	4400	290	55.5
Galileo	8800	570	111
Cassini	13200	800	168

Problems of the RTG's

- Very high cost: from $40,000 to $400,000 per W
- High potential risk
- Limited power (mass grows strongly)

ANY SATELLITE CAN BE DEORBITED WITH AN ELECTRODYNAMIC TETHER WORKING IN THE GENERATOR REGIME

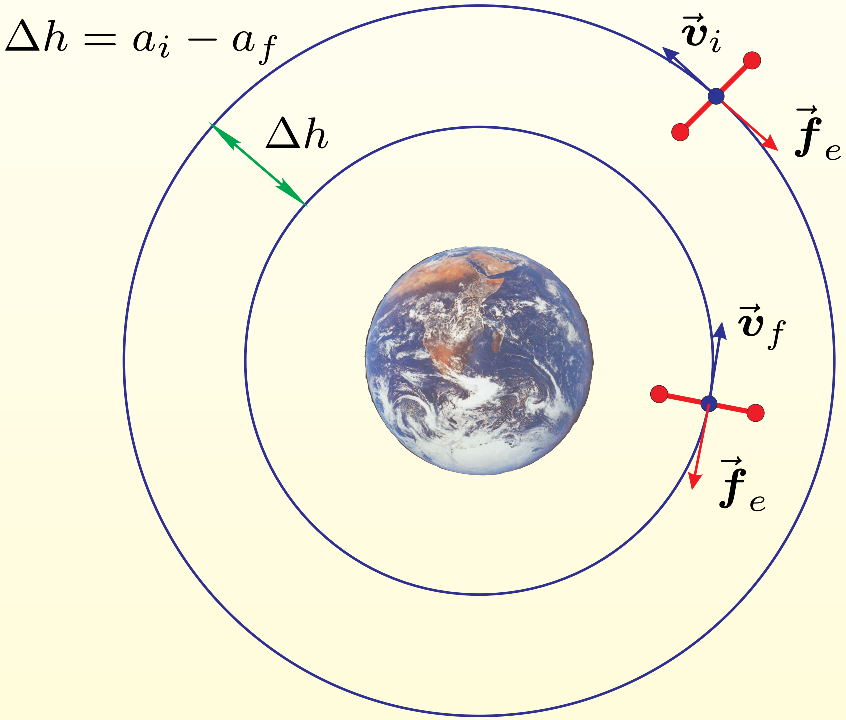

Deorbiting a satellite

The mechanical energy lost in the deorbiting process is

$$\Delta E = \frac{m\mu}{2a_f a_i}\Delta h \approx \frac{m\mu}{2a_f^2}\Delta h(1 - \frac{\Delta h}{a_f})$$

and it is invested in several task. Basically:

- to attract the electrons from the infinity to the tether
- ohmics loss in the tether when the current is flowing
- some useful work that we can obtain in the form of electrical energy (charging batteries, for example)

We need: magnetic field and plasma environment. Both are present in Jupiter.

THE ELECTRODYNAMIC TETHER IS ABLE TO RECOVER A SIGNIFICANT FRACTION OF THE MECHANICAL ENERGY LOST DURING THE DEORBITING PROCESS

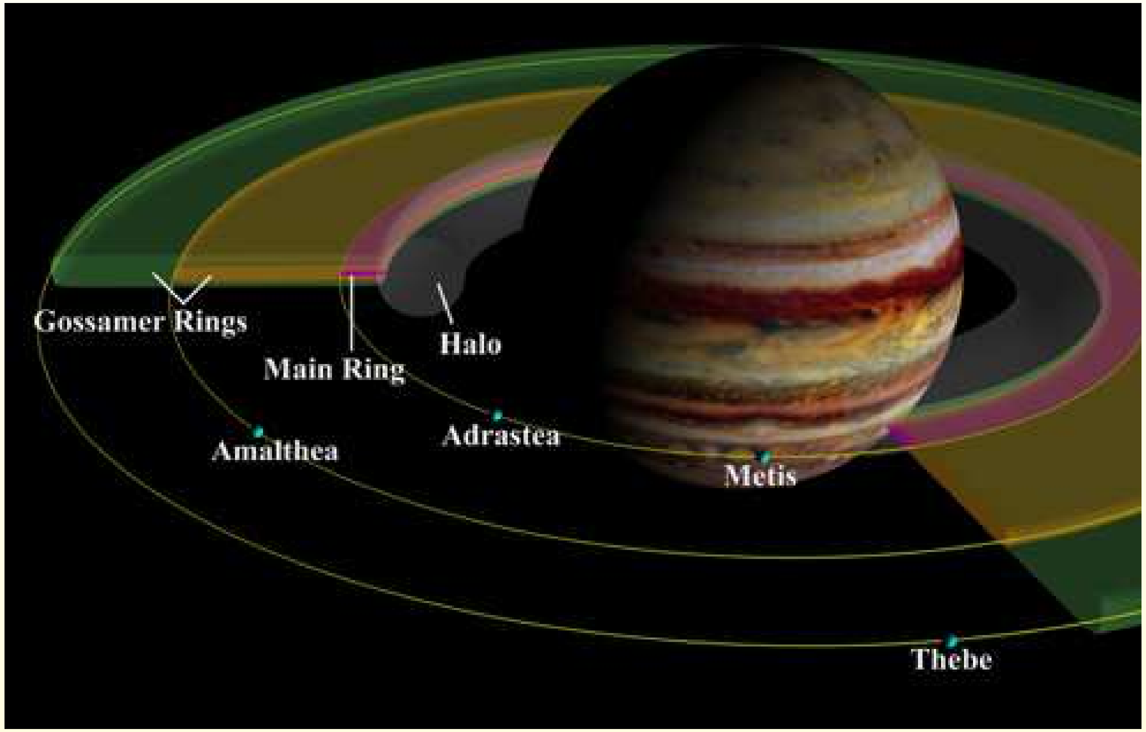

Jupiter inner moonlets

$$r_{\text{Adrastea}} = 128971 \text{ km}, \quad r_{\text{Metis}} = 127969 \text{ km}$$
$$r_{\text{Amalthea}} = 181300 \text{ km}, \quad r_{\text{Thebe}} = 221895 \text{ km}$$

The plasma environment is co-rotating with Jupiter (as a rigid body); the angular velocity is

$$\omega_J \approx 1.7579956104 \times 10^{-4}\text{s}^{-1}$$

The orbital velocity in a circular orbit of radius r is $v_c = \sqrt{\frac{\mu}{r}}$($\mu = 1.26686536 \times 10^{17}\text{m}^3/\text{s}^2$). It exists an orbital radius for which the orbital period coincides with the sideral period of Jupiter (about 9.925 hours); it is the stationary radius (r_s) given by

$$r_s = \left(\frac{T\sqrt{\mu}}{2\pi}\right)^{\frac{2}{3}} \approx 160009.4329 \text{ km}$$

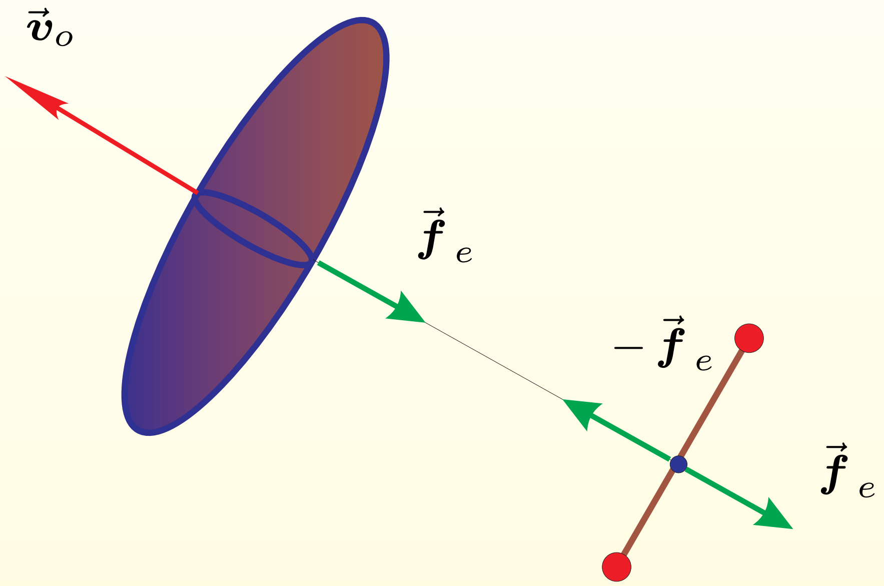

Amalthea: $m = 2.09 \times 10^{18}$ kg, $a_f = 181300$ km

The cable can be removed by using the gravitational attraction of Amalthea to link the tether system and the small Jupiter moon. The tether system moves in an equilibrium position relative to the primaries: Jupiter + Amalthea

We tray to deorbit one of the Jupiter moonlets. We joint the tether and the moonlet with a cable. $\vec{F}_e$ is the electrodynamic drag acting on the tether. This force is transmitted thought the cable to the small Jupiter moon that will be deorbited.

$$\Delta h = \frac{2\Delta E a_f^2}{m\mu}$$

To deorbit Amaltea 1mm ($\Delta h = 1$mm) implies a loss of mechanical energy about

$$\Delta E \approx 4 \times 10^{15}\text{J} \approx 1.1 \times 10^9\text{Kwh}$$

From a practical point of view the reserve of energy is unbounded

Equilibrium Positions at the Synodic Frame

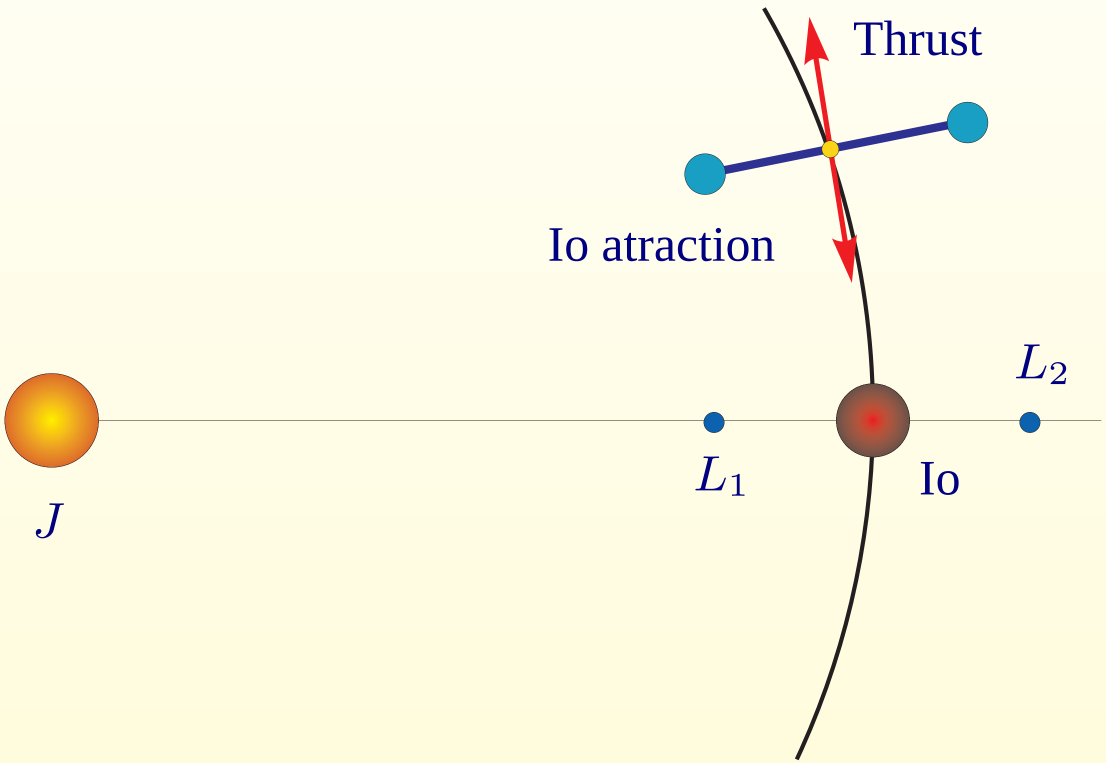

- *A permanent tethered observatory at Jupiter. Dynamical analysis*, **by J. Peláez and D. J. Scheeres**, Proceedings of the 17th AAS/AIAA Space Flight Mechanics Meeting Sedona, Arizona, Vol. 127 of Advances in the Astronautical Sciences, 2007, pp. 1307–1330
- *On the control of a permanent tethered observatory at Jupiter*, **by J. Peláez and D. J. Scheeres**, Paper AAS07-369 of the 2007 AAS/AIAA Astrodynamics Specialist Conference, Mackinac Island, Michigan, August 19-23, 2007

Equilibrium Positions

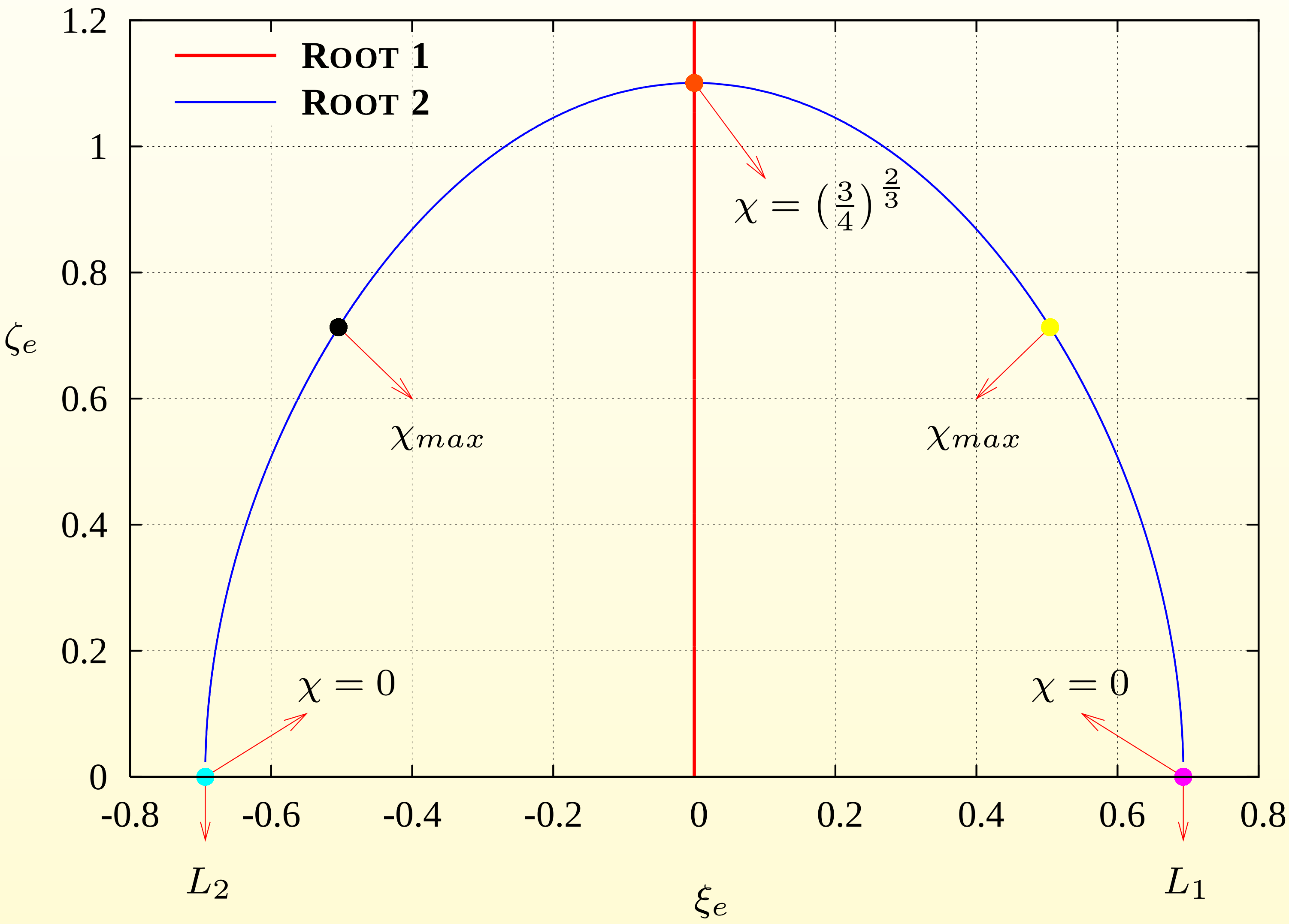

Equilibrium Positions on the plane (ξ_e, ζ_e)

EQUILIBRIUM POSITIONS (AMALTEA)

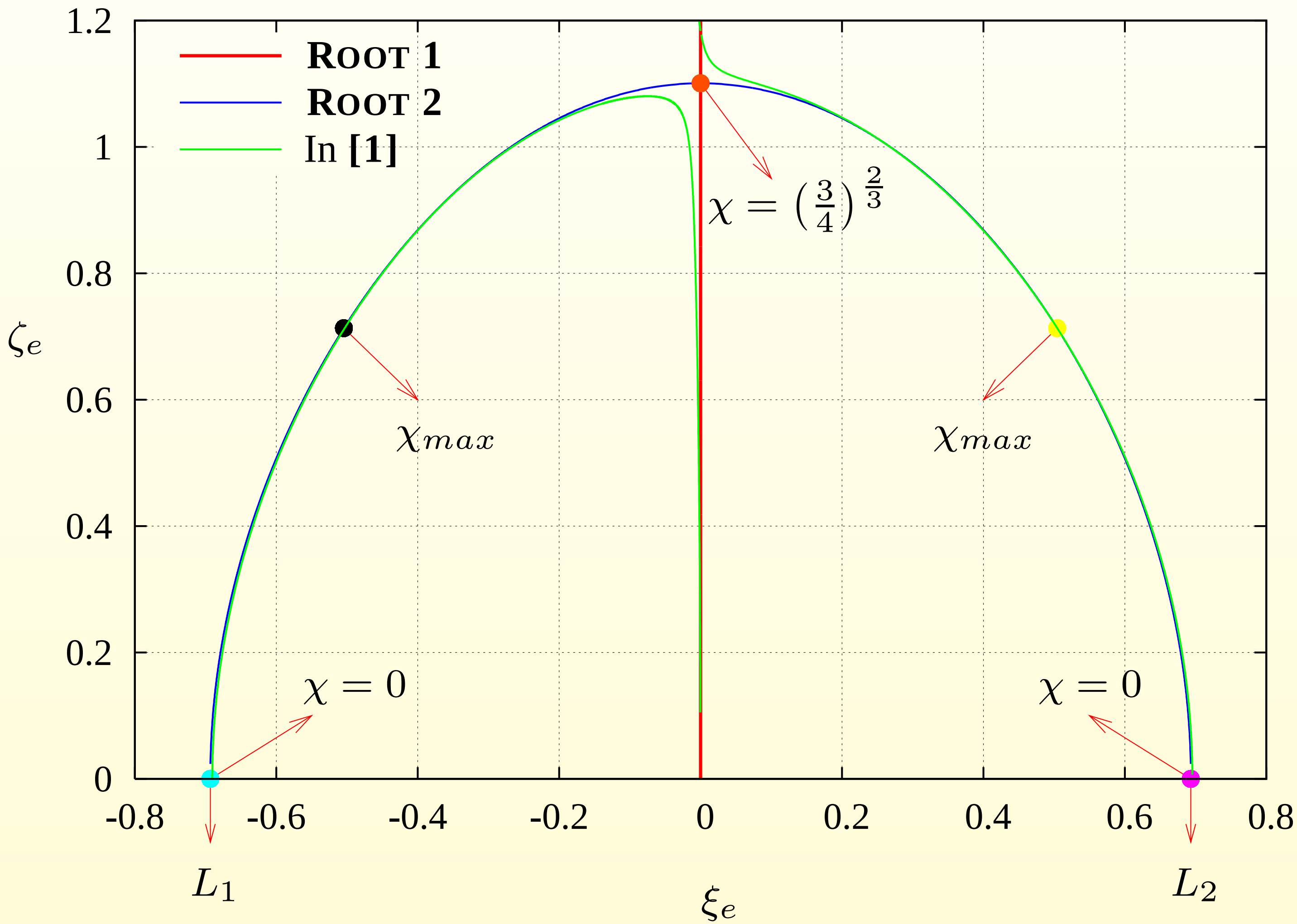

Comparison with the results summarized in **[1]**

[1] A permanent tethered observatory at Jupiter. Dynamical analysis, by **J. PELÁEZ & D. J. SCHEERES**, (Paper AAS07-190) of *The 2007 AAS/AIAA Space Flight Mechanics Meeting, Sedona, AZ, January 2007.*

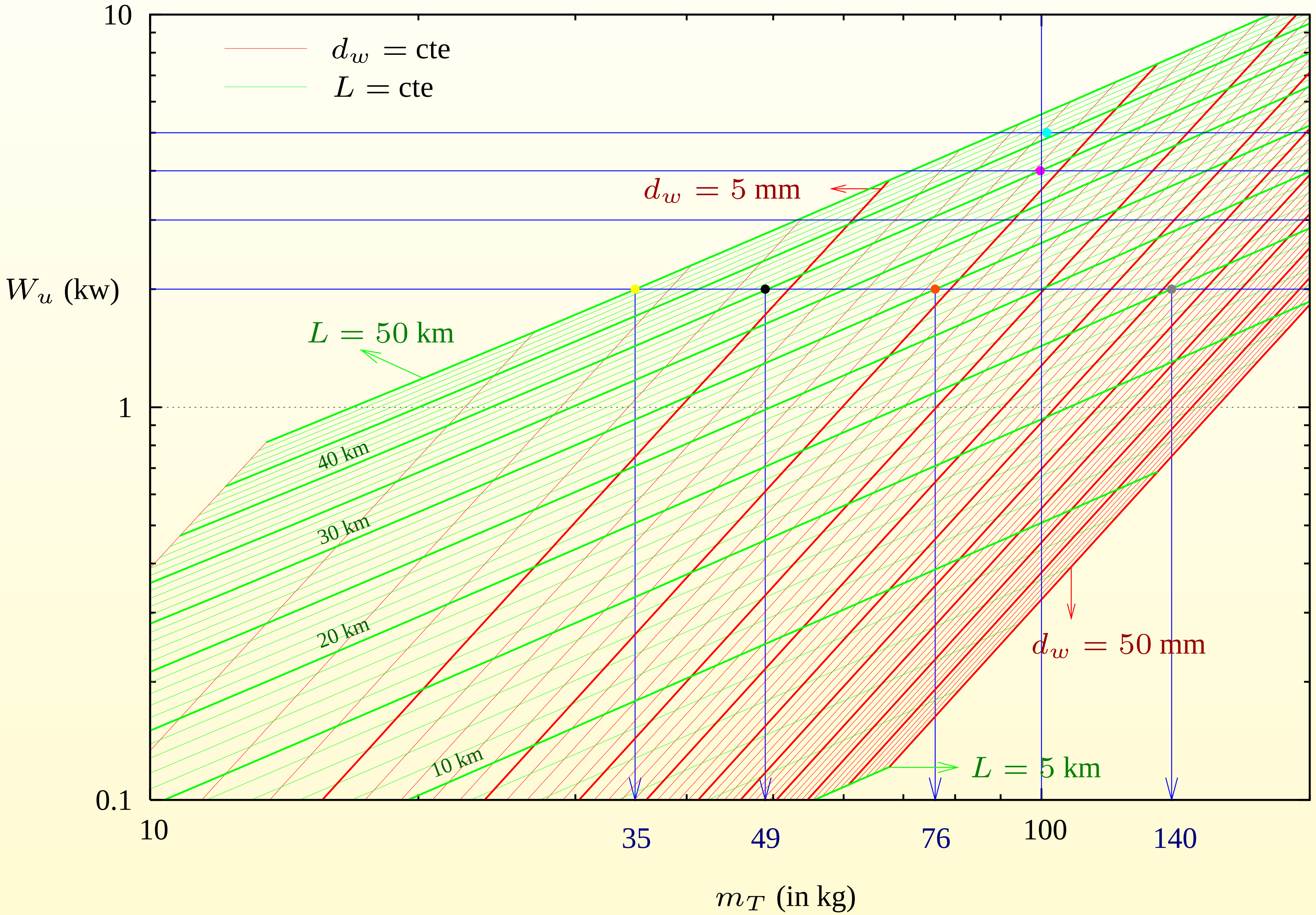

DIFFERENT OPTIMUM CONFIGURATIONS AT METIS ($h = 0.1$ MM)

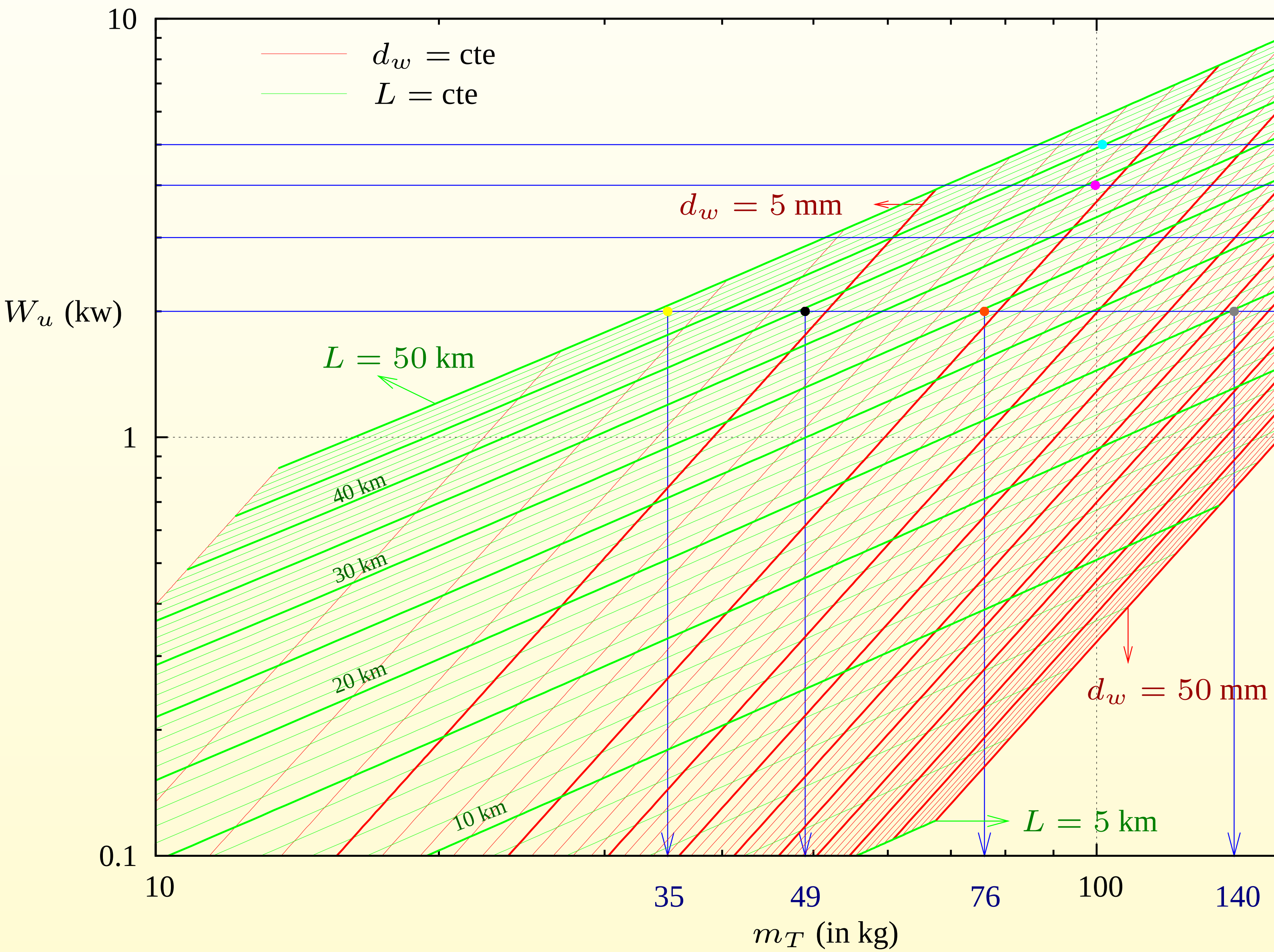

DIFFERENT OPTIMUM CONFIGURATIONS AT METIS ($h = 0.1$ MM)

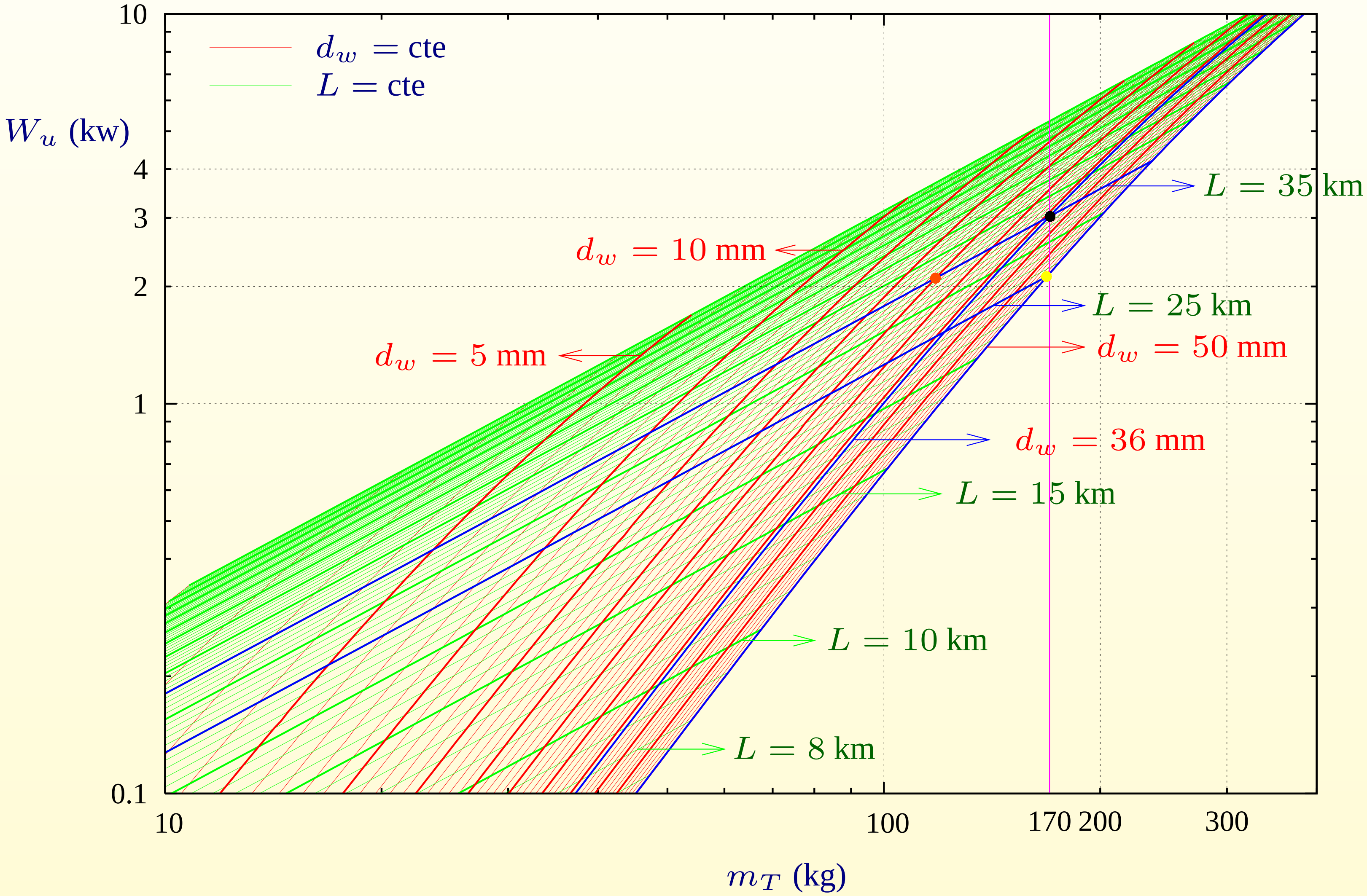

Different optimized configurations in Io ($h = 0.05$ mm)

THREE DIFFERENT CONFIGURATION

	A	B	C
L (km)	25	35	35
d_w (mm)	50	25	36
m_T (kg)	169	117	170
Z_C (Oh)	640	1265	886
W_u (w)	2100	2100	3000
I_{sc} (A)	10.94	5.53	7.89
I_{av} (A)	1.43	1.04	1.49
ϕ^* (deg)	39.7	40.06	40.06
$\chi \cdot 10^3$	5.79	5.91	8.43
d_e (km)	200,052	198,119	165,803
T (mN)	5.28	7.4	7.4

Three possible designs

- Aluminum tape 0.05 mm thick
- Self-balanced
- Mass of the S/C 500 kg
- Tether mass $\leq$ 170 kg
- $\chi \in [0, 0.115]$ STABLE
- Power from 2 – 3 kw
- distance d_e large
- Tether tension small $\approx$ mN
- Appropriate for the scientific exploration of the Io plasma torus

ROTATING ELECTRODYNAMIC TETHER ORBITING IO

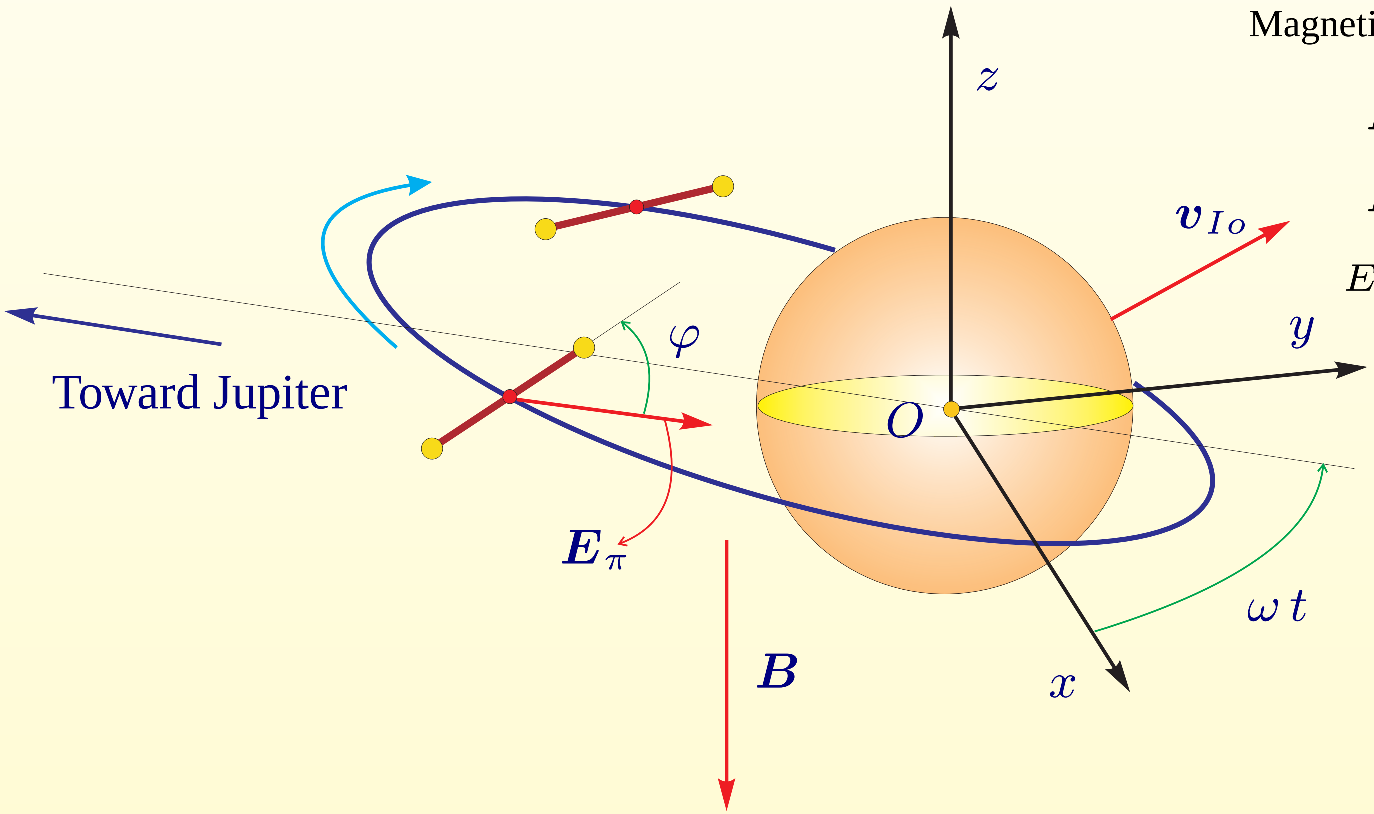

We take an inertial frame $Oxyz$ (origin Io)

Orbital velocity of Io: $\boldsymbol{v}_{Io} \approx 17.33$ km/s

Plasma velocity at Io orbit ≈ 74.17 km/s

Orbital velocity of S/C (around Io) ≈ 1 km/s

Magnetic field $\boldsymbol{B} \approx 2 \cdot 10^{-6}$ T

$$\boldsymbol{E} \approx (\boldsymbol{v}_{Io} - \boldsymbol{v}_{pl}) \times \boldsymbol{B}$$

$$\boldsymbol{E} = E_\pi(\cos\omega t, \sin\omega t, 0),$$

$$E_\pi \approx 0.12 \text{ V/m}$$

Power Generation Io

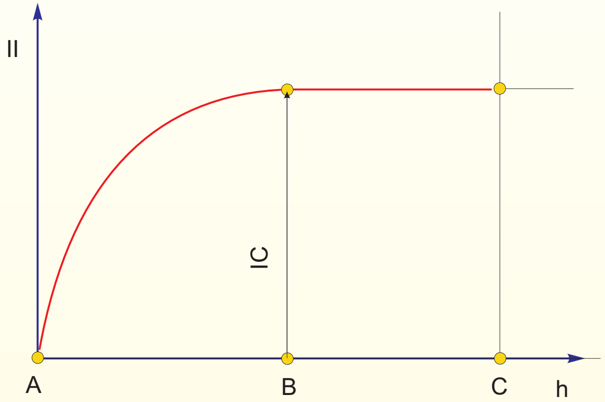

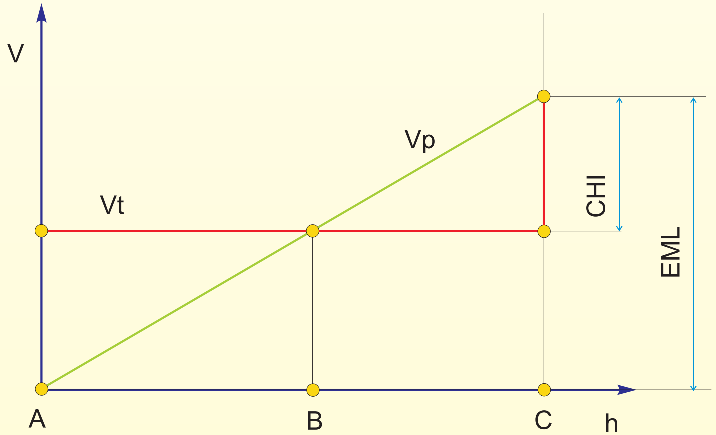

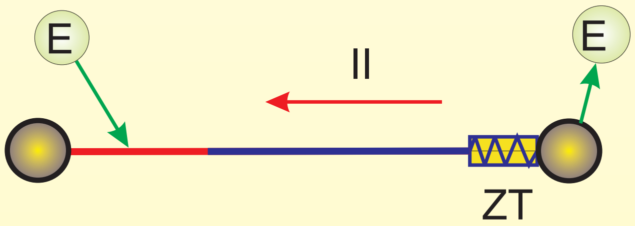

Power generation: assumptions

- small values of n_∞ no Ohmic effects
- negligible ion losses at the cathodic segment
- control impedance Z_C at the cathodic end
- OML regime
- control parameter $\zeta = \dfrac{z^*}{L} = 1 - \dfrac{Z_C\, I_C}{E_m L}$

Results of the analysis

- $I_{av} = \frac{1}{L}\int_0^L I(z)dz = I_0\,(1 - \frac{2}{5}\zeta)\zeta^{3/2}$
- $\dot{W} = Z_C I_C^2 = I_0 E_m L(1-\zeta)\zeta^{3/2}$

$$I_0 = \frac{4d_w}{3\pi} e n_\infty \sqrt{\frac{2eE_m L^3}{m_e}}$$

Optimum Power Generation

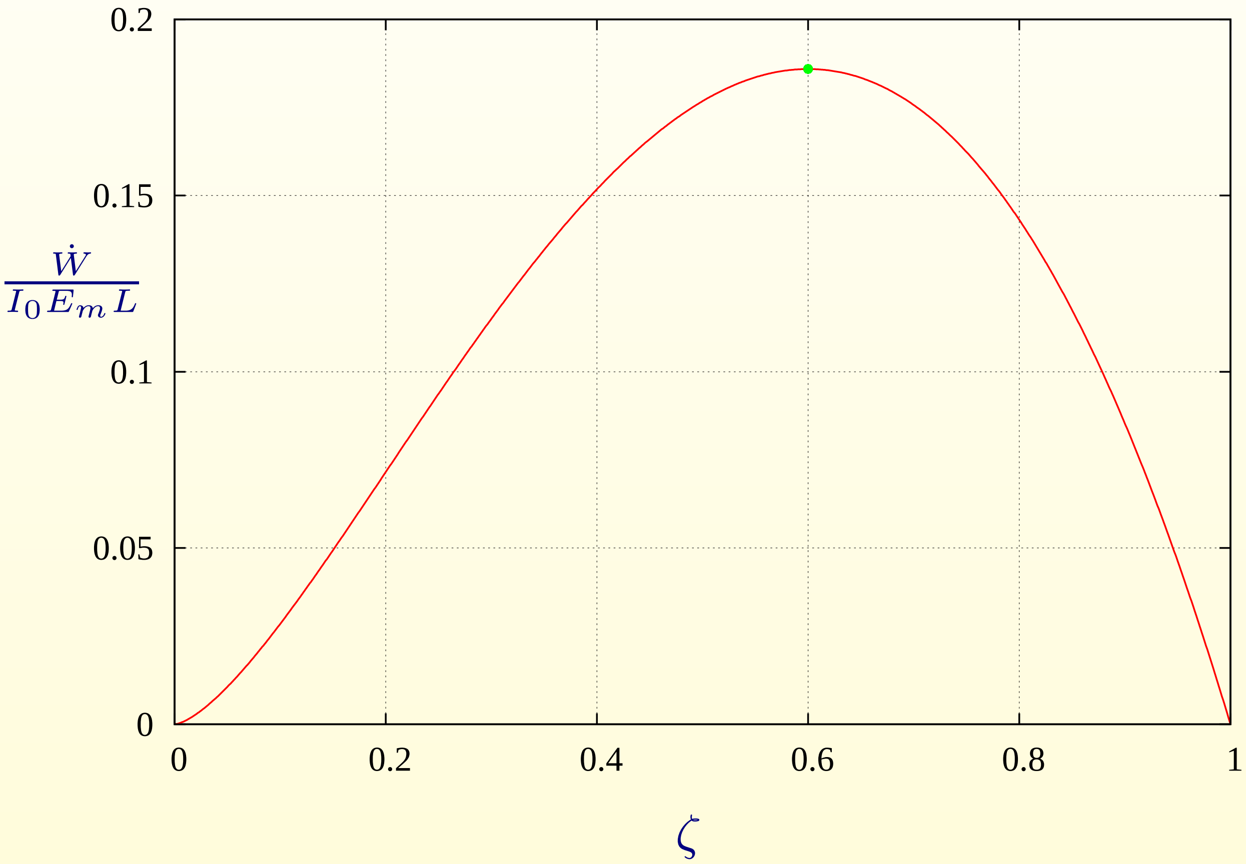

$$\zeta_{opt} = \frac{3}{5}, \qquad Z_C^{opt} = \frac{3\pi\sqrt{2}}{8} \cdot \frac{1-\zeta_{opt}}{\zeta_{opt}^{3/2}} \cdot \frac{1}{d_w n_\infty}\sqrt{\frac{m_e E_m}{e^3 L}} = \frac{\pi\sqrt{30}}{12} \cdot \frac{1}{d_w n_\infty}\sqrt{\frac{m_e E_m}{e^3 L}}$$

Rotating electrodynamic tether orbiting Io

$$\dot{W}_{av} = \frac{1}{\pi}\int_{-\pi/2}^{\pi/2} \cos^{3/2}\varphi\, d\varphi \cdot \frac{4d_w}{3\pi} n_\infty \sqrt{\frac{2E_\pi^3 L^5 e^3}{m_e}} \left[(1-\zeta)\,\zeta^{3/2}\right]$$

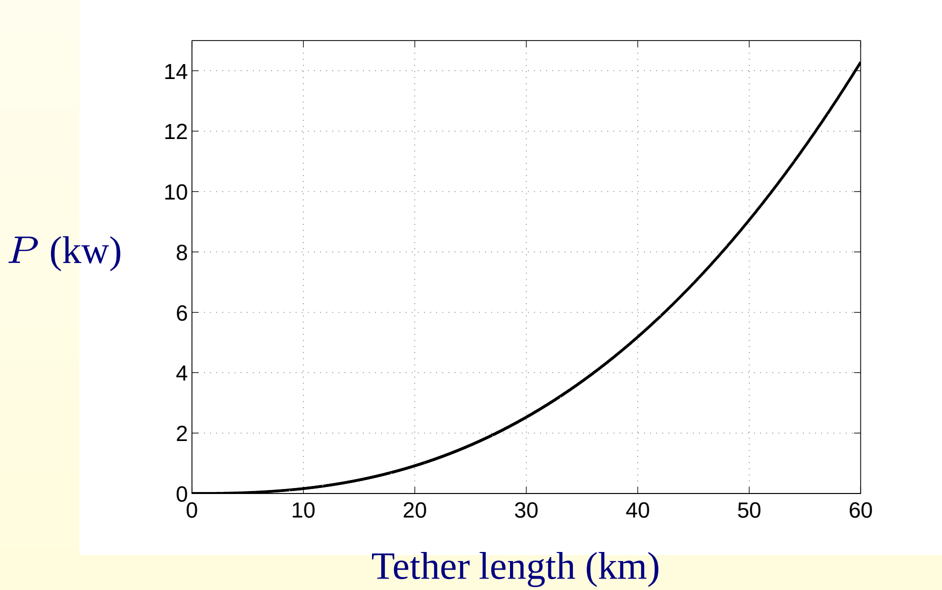

First order approximation of averaged generated power for a 5 cm wide tape tether of different lengths in Io orbit.

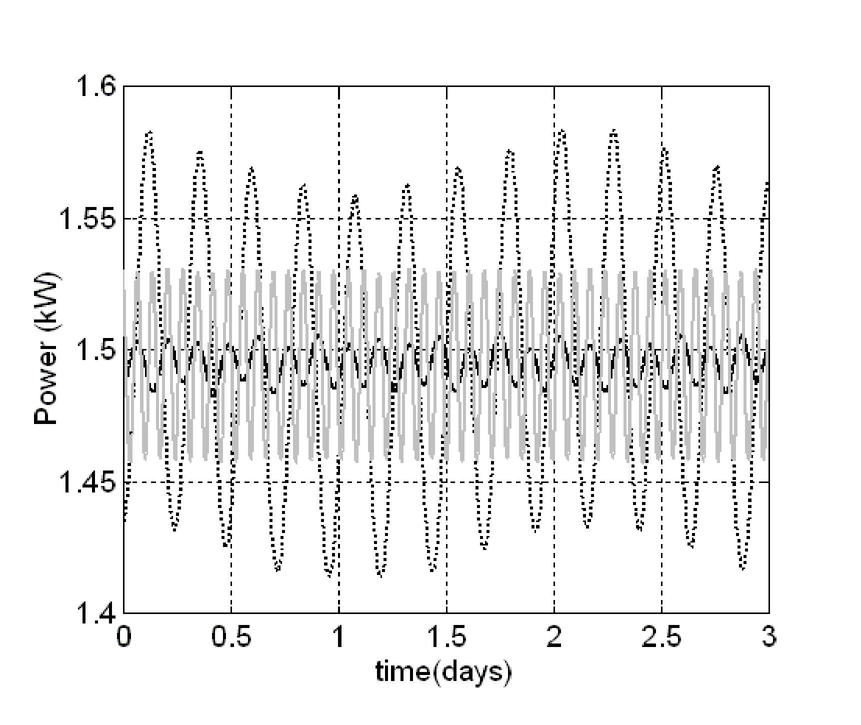

Power generated with a 25 km long 5 cm wide tape tether along circular retrograde orbits of different radii: $r = 1.1\ r_{Io}$ (grey solid line), $r = 2.0\ r_{Io}$ (dark solid line), and $r = 3.0\ r_{Io}$ (dark dotted line).

Power Generation in Ionian Orbit

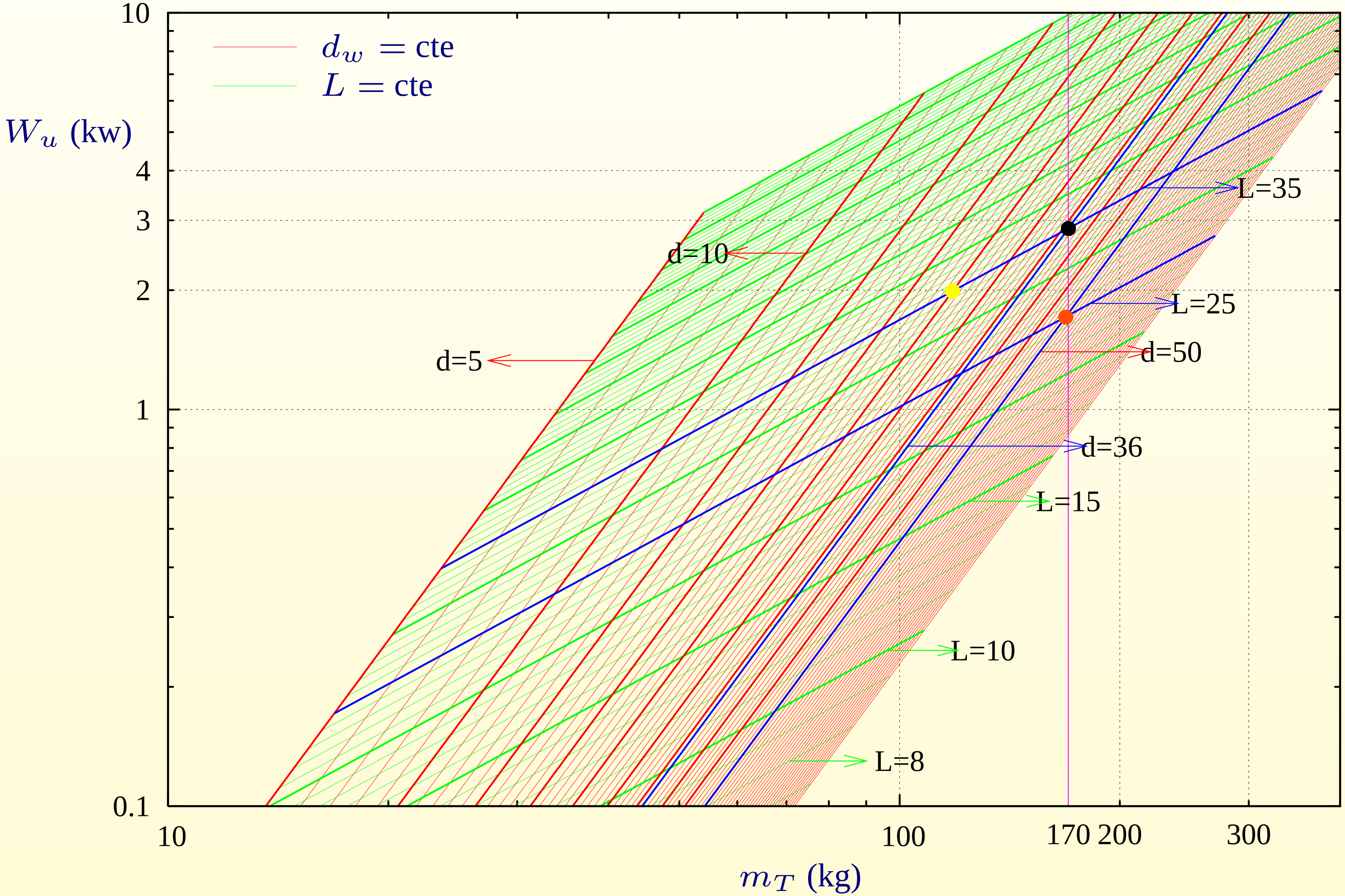

Different optimized configurations in Io ($h = 0.05$ mm)

ORBIT STABILITY

- Io is the Galilean moon more affected by the gravitation of Jupiter
- Lara & Russel[a] shows that **retrograde equatorial** orbits around Europe are stable when eccentricity and semimajor axis are smaller than critical values.
- Their results have been numerically extended to Io: if the apocenter is less than 3.5 r_{Io} the equatorial retrograde orbit is stable for at least a year

$$\boldsymbol{F}_{av} = \frac{1}{\pi}\int_{-\pi/2}^{\pi/2} L\, I_{av}\,(\boldsymbol{u}\times\boldsymbol{B})d\varphi = \frac{1}{\pi}L\left[\int_{-\pi/2}^{\pi/2} I_{av}\,\boldsymbol{u}\,d\varphi\right]\times\boldsymbol{B}$$

When the load impedance is controlled for maximum power generation ζ =cte:

$$\int_{-\pi/2}^{\pi/2} I_{av}\,\boldsymbol{u}\,d\varphi = \frac{1}{E_\pi}\int_{-\pi/2}^{\pi/2} I_{av}\,\cos\varphi\,\boldsymbol{E}_\pi\,d\varphi = \frac{\boldsymbol{E}_\pi}{E_\pi}\cdot\int_{-\pi/2}^{\pi/2} I_{av}\,\cos\varphi\,d\varphi$$

This way we have

$$\boldsymbol{F}_{av} = \frac{k'}{\sqrt{E_\pi}}(\boldsymbol{E}_\pi\times\boldsymbol{B}), \qquad k' \approx 0.0667\,d_w n_\infty\sqrt{\frac{L^5 e^3}{m_e}}\,(5-2\zeta)\zeta^{3/2}$$

The averaged force has a constant value, in a first approximation, on the synodic frame.

[a] *On the design of a science orbit about Europa*, Paper AAS 06-168, 16th AAS/AIAA Space Flight Mechanics Conference. Tampa, Florida,USA, January 2006

Orbit Stability

$$\boldsymbol{F} \approx F(-\sin\omega\, t, \cos\omega\, t, 0) \qquad \text{with} \qquad F = 0.0667\, d_w n_\infty B \sqrt{\frac{E_\pi L^5 e^3}{m_e}} \cdot (5 - 2\zeta)\, \zeta^{3/2}$$

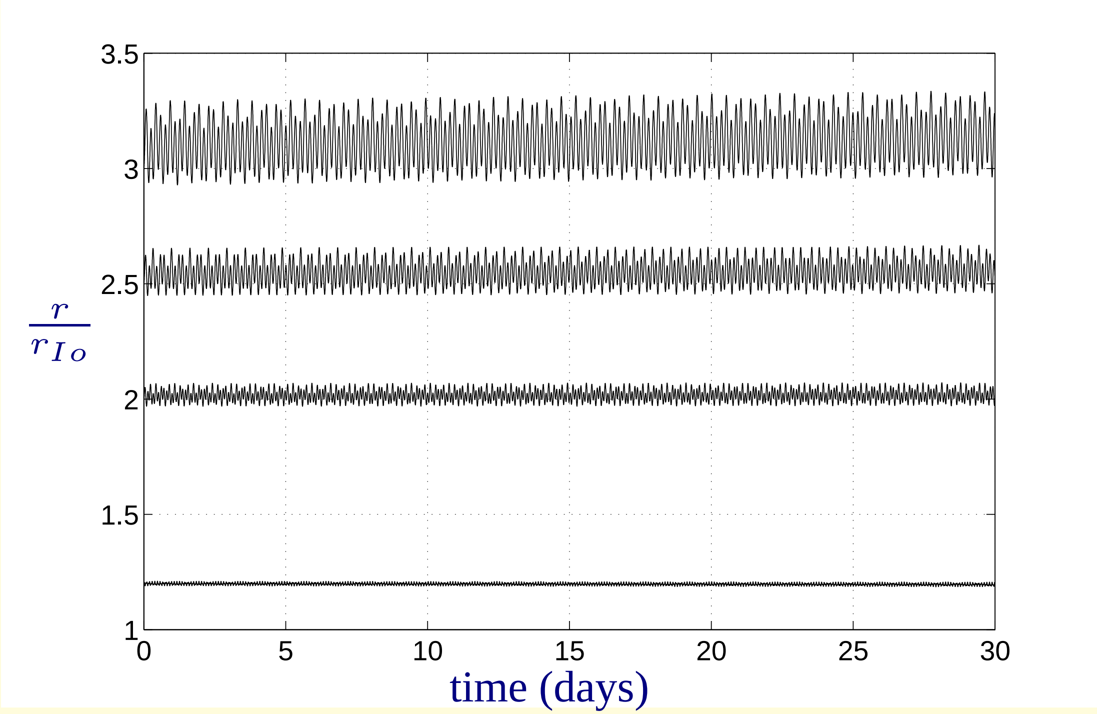

Evolution of orbital radius for circular retrograde orbits of different radii (1.2, 2.0, 2.5 and 3 Io radii) under the effect of the Lorentz force of a 25 km long 5 cm wide tape tether with power-optimized impedance control.

Orbit Control

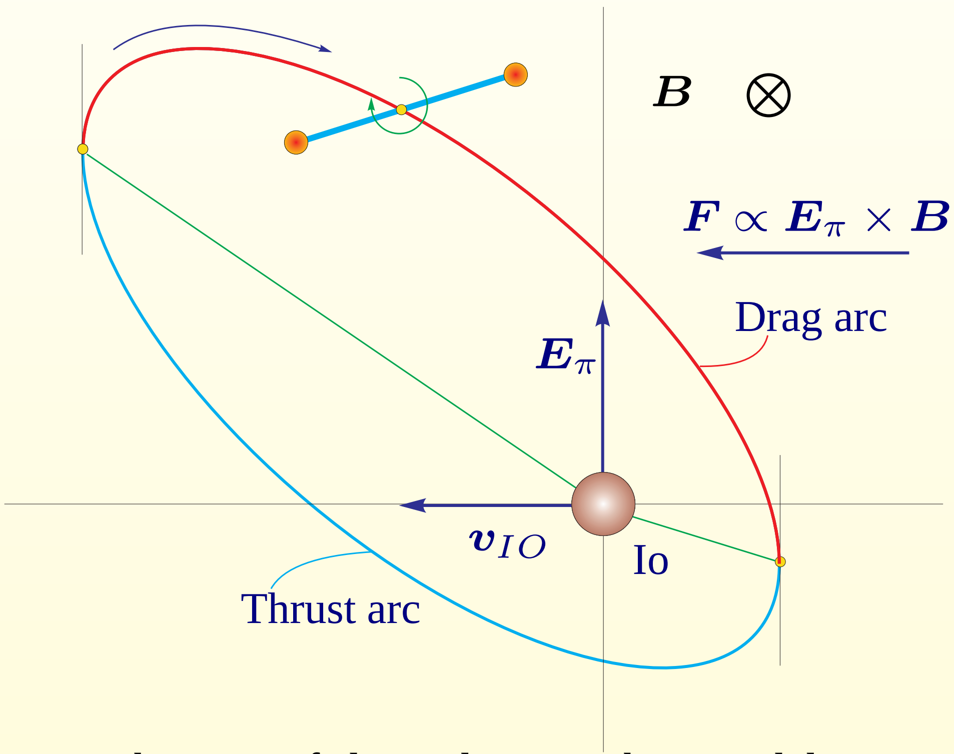

Schematic of electrodynamic thrust and drag arc for a generic Ionian orbit. We neglect the orbital velocity around Io in the determination of motional electric field

The main contribution to the motional electric field comes from Io orbital velocity rather than the spacecraft orbital velocity around Io. The Lorentz force is thrusting the S/C in part of the orbit (thrust arc) and braking it (drag arc) in the rest of the Ionian orbit.

Preliminary test with a simple control strategy: the control parameter ζ is switched to 1 (maximum Lorentz force) on thrust arcs and switched to 0 (no force) on drag arcs. A numerical simulation has been conducted assuming a 500 kg spacecraft equipped with a 25 km long and 5 cm wide electrodynamic tether starting from a low altitude retrograde circular orbit ($r = 1.2$ Io radii).

ORBIT CONTROL

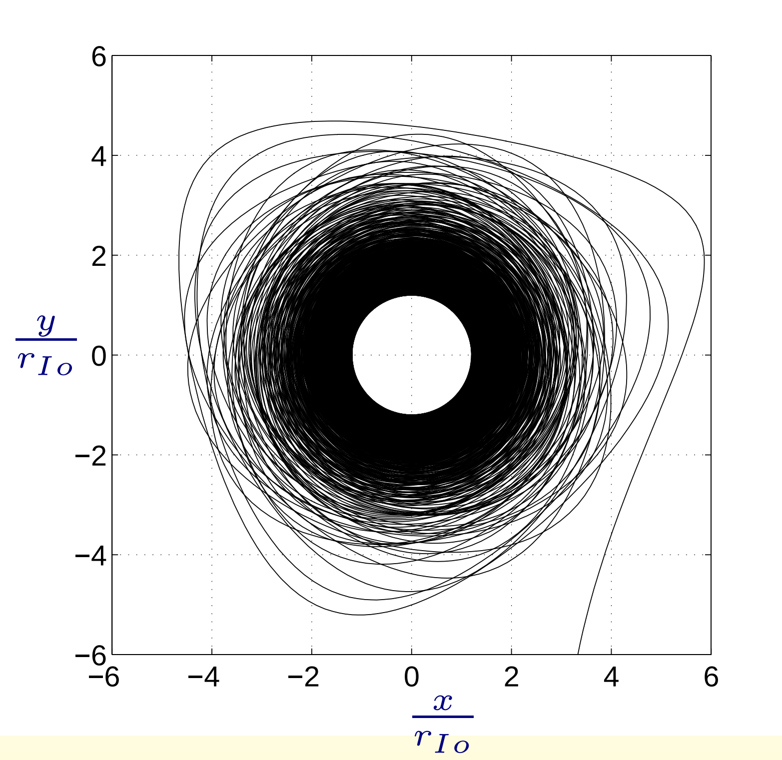

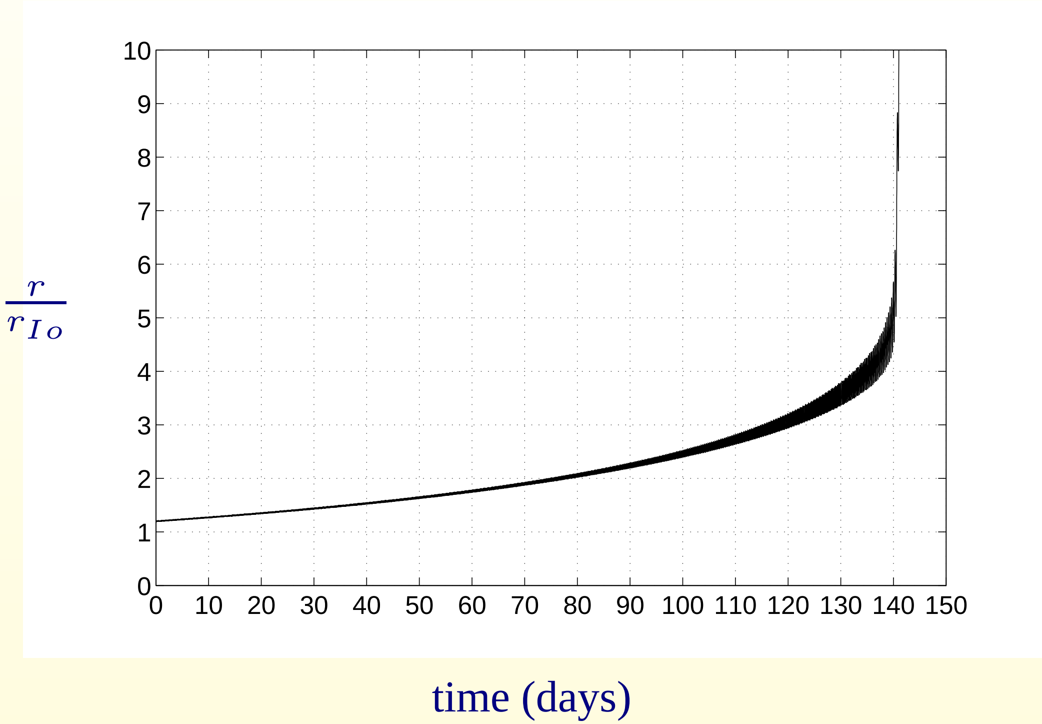

Spiral-out trajectory (left) and orbital radius evolution (right) for a 500 kg spacecraft propelled by a 25 km long 5 cm wide tape tether with simple current control strategy. Escape from Io gravitational field require less than 5 months, in this case.

The END of Io Exploration with Electrodynamic Tethers

Stability of tethered satellites at collinear lagrangian points

Previous analysis

- *The Stabilization of an Artificial Satellite at the Inferior Conjunction Point of the Earth-Moon System*, **G. Colombo**, Smithsonian Astrophysical Observatory Special Report No. 80, November 1961
- *The Control and Use of Libration-Point Satellites*, **R. W. Farquhar**, NASA TR R-346, September 1970. pp. 89-102
- *Tether Stabilization at a Collinear Libration Point*, **R. W. Farquhar**, The Journal of the Astronautical Sciences, Vol. 49, No. 1, January-March 2001, pp. 91-106.
- *Dynamics of a Tethered System near the Earth-Moon Lagrangian Points*, **A. K. Misra, J. Bellerose, and V. J. Modi**, Proceedings of the 2001 AAS/AIAA Astrodynamics Specialist Conference, Quebec City, Canada, Vol. 109 of Advances in the Astronautical Sciences, 2002, pp. 415–435.
- *Dynamics of a multi-tethered system near the Sun-Earth Lagrangian point*, **B. Wong and A. K. Misra**, 13th AAS/AIAA Space Flight Mechanics Meeting, Ponce, Puerto Rico, February 2003, Paper No. AAS-03-218.
- *Dynamics of a Libration Point Multi-Tethered System*, **B. Wong and A. K. Misra**, Proceedings of 2004 International Astronautical Congress, Paper No. IAC-04-A.5.09.

Equilibrium Positions at the Synodic Frame

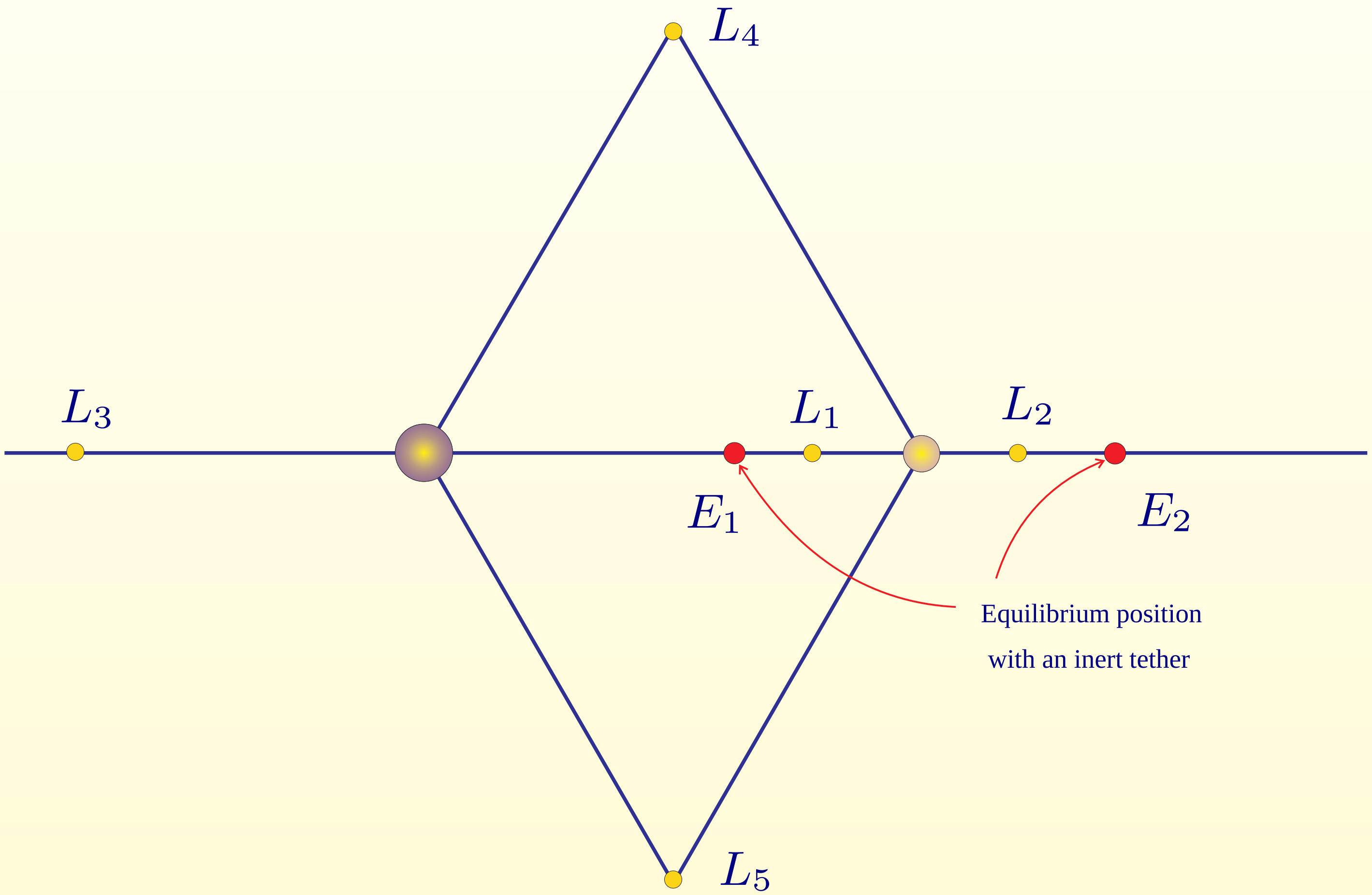

VARYING LENGTH INERT TETHER

$$\ddot{\xi} - 2\dot{\eta} - (3 - \frac{1}{\rho^3})\xi = \frac{\lambda}{\rho^5}\left\{3\tilde{N}\cos\varphi\cos\theta - \xi S_2(\frac{\tilde{N}}{\rho})\right\}$$

$$\ddot{\eta} + 2\dot{\xi} + \frac{\eta}{\rho^3} = \frac{\lambda}{\rho^5}\left\{3\tilde{N}\cos\varphi\sin\theta - \eta S_2(\frac{\tilde{N}}{\rho})\right\}$$

$$\ddot{\zeta} + \zeta(1 + \frac{1}{\rho^3}) = \frac{\lambda}{\rho^5}\left\{3\tilde{N}\sin\varphi - \zeta S_2(\frac{\tilde{N}}{\rho})\right\}$$

$$\ddot{\theta} + (1+\dot{\theta})\left[\frac{\dot{I}_s}{I_s} - 2\dot{\varphi}\tan\varphi\right] + 3\cos\theta\sin\theta = \frac{3\tilde{N}}{\rho^5}\frac{(-\xi\sin\theta + \eta\cos\theta)}{\cos\varphi}$$

$$\ddot{\varphi} + \frac{\dot{I}_s}{I_s}\dot{\varphi} + \sin\varphi\cos\varphi\left[(1+\dot{\theta})^2 + 3\cos^2\theta\right] = \frac{3\tilde{N}}{\rho^5}(-\sin\varphi[\xi\cos\theta + \eta\sin\theta] + \zeta\cos\varphi)$$

where $\rho = \sqrt{\xi^2 + \eta^2 + \zeta^2}$ and the quantity $\tilde{N}$ and the function $S_2(x)$ are given by

$$\tilde{N} = \xi\cos\varphi\cos\theta + \eta\cos\varphi\sin\theta + \zeta\sin\varphi, \qquad S_2(x) = \frac{3}{2}(5x^2 - 1)$$

$$\lambda = \left[\frac{L_d}{\ell}\right]^2 \cdot \frac{a_2}{\nu^{2/3}}, \qquad a_2 = \frac{I_s}{m\,L_d^2} \in [\frac{1}{12}, \frac{1}{4}]$$

where, ℓ is the distance between primaries, ν is the reduced mass of the small primary (usually $\nu \ll 1$), $m = m_1 + m_2 + m_T$ is the total mass of the system and I_s is the moment of inertia about a line normal to the tether by the center of mass G of the system; a_2 is of order unity and takes its maximum value $a_2 = 1/4$ for a massless tether with equal end masses ($m_1 = m_2$). For a tether of varying length the parameter λ is a function of time since the deployed tether mass m_d and the deployed tether length $L_d(t)$ are changing. Moreover, some terms of these governing equations involve the ratio:

$$\frac{\dot{I}_s}{I_s} = 2\frac{\dot{L}_d}{L_d} J_g, \qquad J_g = 1 - \frac{\Lambda_d\,(1 + 3\cos 2\phi)}{(3\sin^2 2\phi - 2\Lambda_d)}, \qquad \Lambda_d = \frac{m_d}{m}, \qquad \cos^2\phi = \left(\frac{m_1}{m} + \frac{\Lambda_d}{2}\right)$$

This formulation includes the mass of the tether through the parameter Λ_d and the mass angle ϕ. In order to neglect the tether mass, we only have to introduce the condition $\Lambda_d = 0$ in the above expressions. For a tether of constant length the parameter λ is also constant and the quotient $\dot{I}_s/I_s$ vanishes, that is, $\dot{I}_s/I_s = 0$. For the sake of simplicity we will assume a massless tether in what follows.

Extended Dumbbell Model. Hill approach

In the search of equilibrium position we will consider the tether tension given by

$$T_0 \approx \frac{m_1\, m_2}{m_1 + m_2}\omega^2 L_d \left[\dot{\varphi}^2 + \cos^2\varphi\{(1+\dot{\theta})^2 + 3\cos^2\theta\} - 1 + \frac{1}{\rho^3}\{3\left(\frac{\tilde{N}}{\rho}\right)^2 - 1\} - \frac{\ddot{L}_d}{L_d}\right]$$

This expression has been derived under the following assumptions: 1) inert tether, 2) massless tether, and 3) the Hill approach has been performed. At any equilibrium position, **tether tension must be positive** because a cable does not support compression stress and the above expression takes the form

$$T_0 \approx T_c\left[\cos^2\varphi\{1 + 3\cos^2\theta\} - 1 + \frac{1}{\rho^3}\{3\left(\frac{\tilde{N}}{\rho}\right)^2 - 1\}\right], \qquad T_c = \frac{m_1\, m_2}{m_1 + m_2}\omega^2 L_d$$

We will use this expression for checking the tether tension in a given steady solutions of the equations of motion; if the tension is positive the equilibrium position will exist; if negative, the equilibrium position will not exist.

Values of λ for Sun and different planets

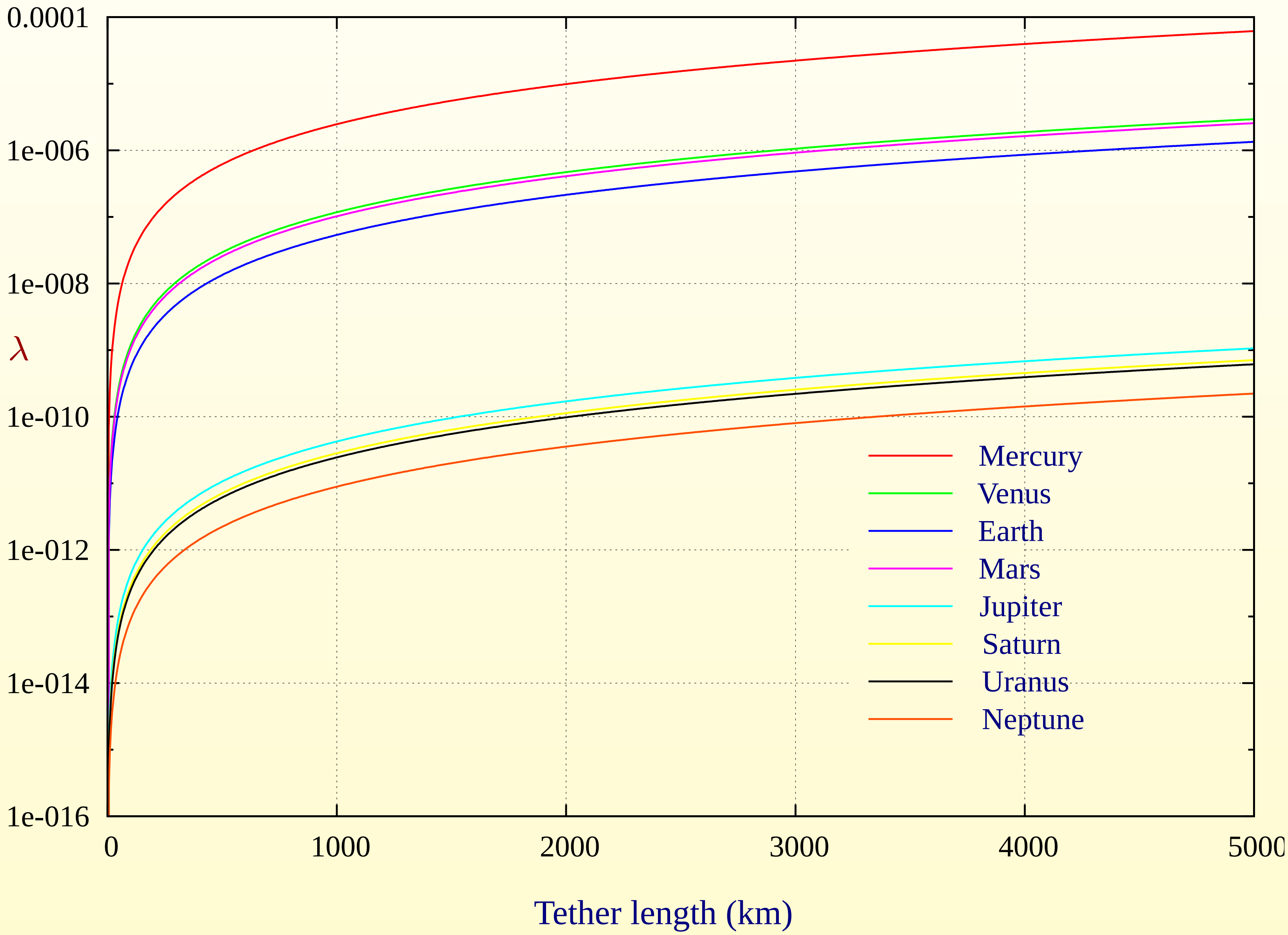

Values of λ for binary systems in the Solar System

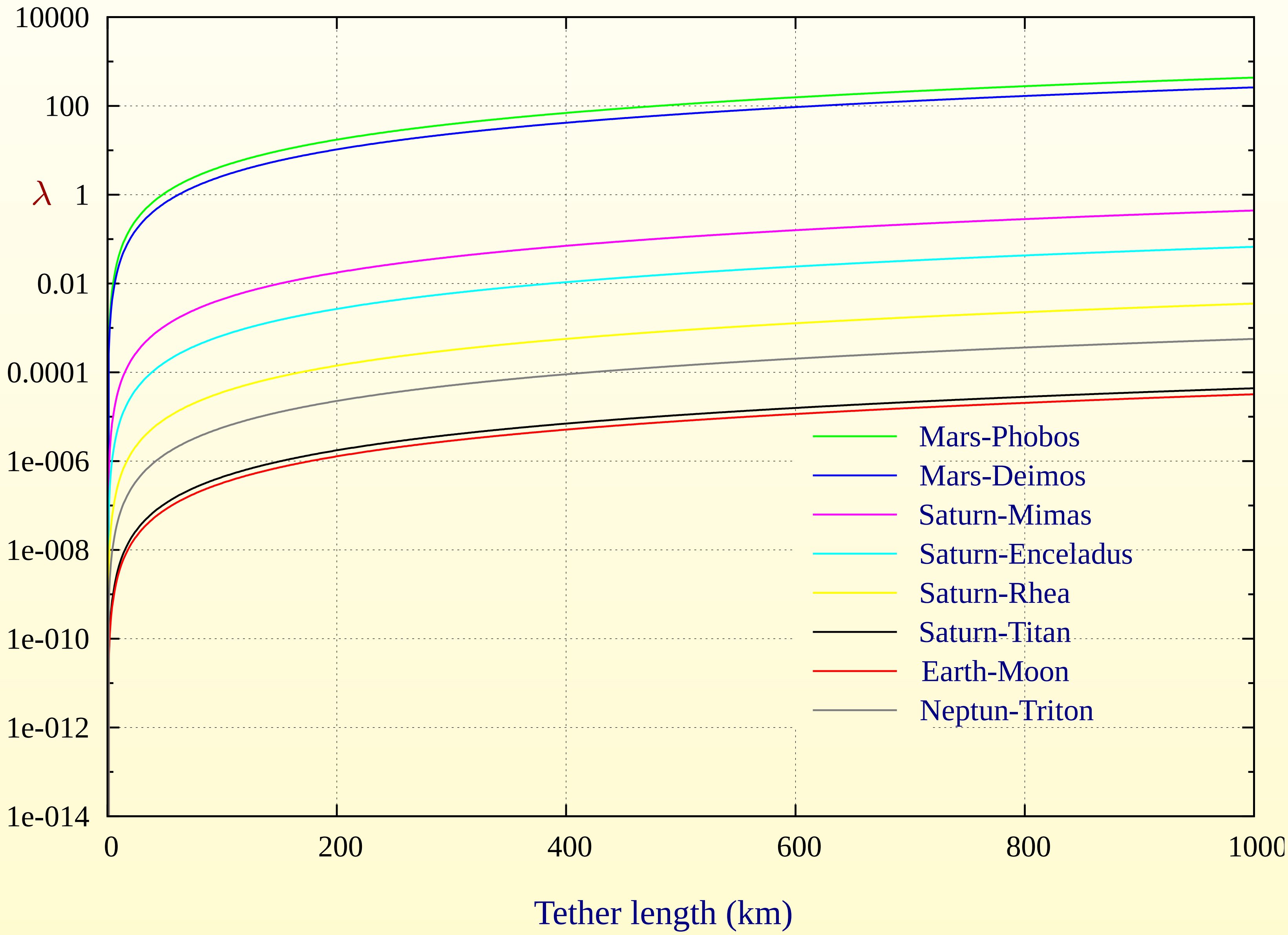

VALUES OF λ FOR BINARY SYSTEMS IN THE JOVIAN WORLD

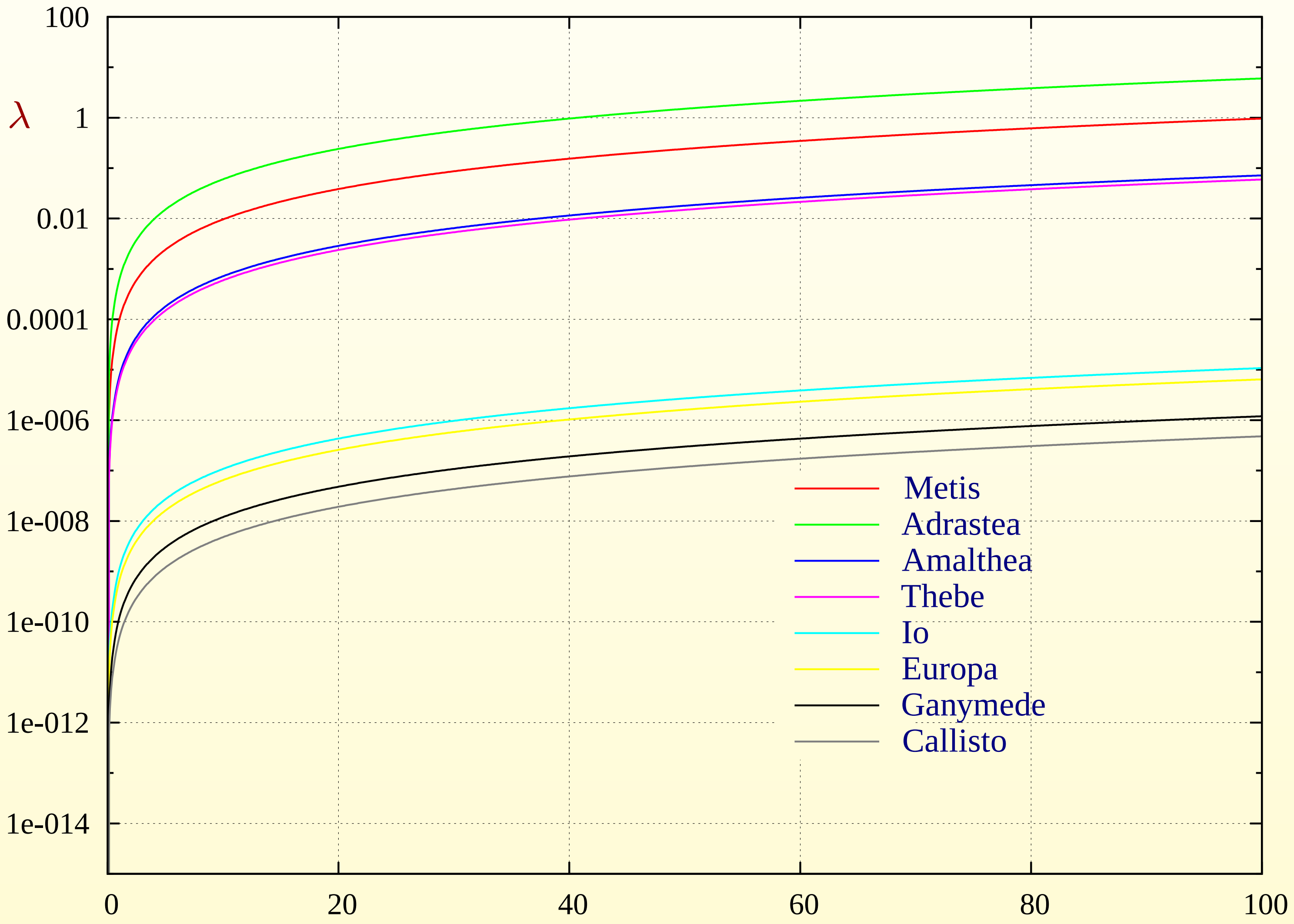

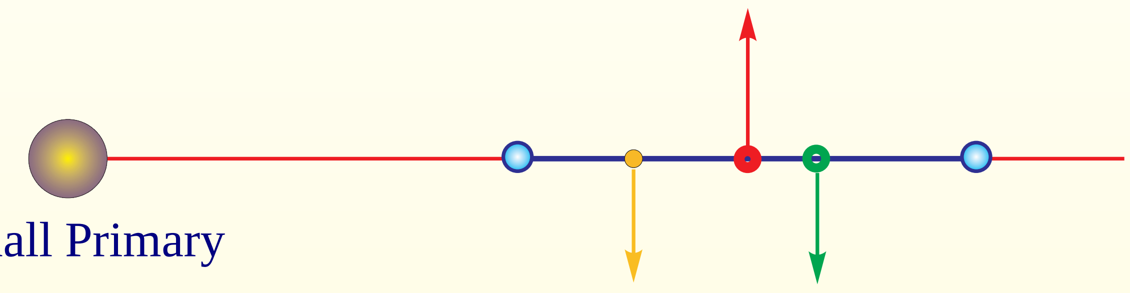

Sketch of the equilibrium position E_2 in the neighborhood of L_2.
There is another one, similar to this, *on the left* of L_1.

$$\xi_e = \pm\rho_e, \qquad \eta_e = \zeta_e = \varphi_e = 0, \qquad \theta_e = 0, \pi, \qquad \lambda = \frac{\rho_e^2}{3}\left(3\,\rho_e^3 - 1\right), \qquad \rho_e^3 > 1/3$$

This expression can be expanded when $\lambda \ll 1$ is small and provide the asymptotic solution

$$\xi_e \approx (\frac{1}{3})^{\frac{1}{3}} + 3^{\frac{1}{3}}\,\lambda - 9\,\lambda^2 + \mathcal{O}(\lambda^3)$$

The convergence of this serie is poor but, for really small values of λ the two first terms give a useful approximation.

A linear stability analysis shows that the equilibrium positions of that family are unstable for any value of λ.

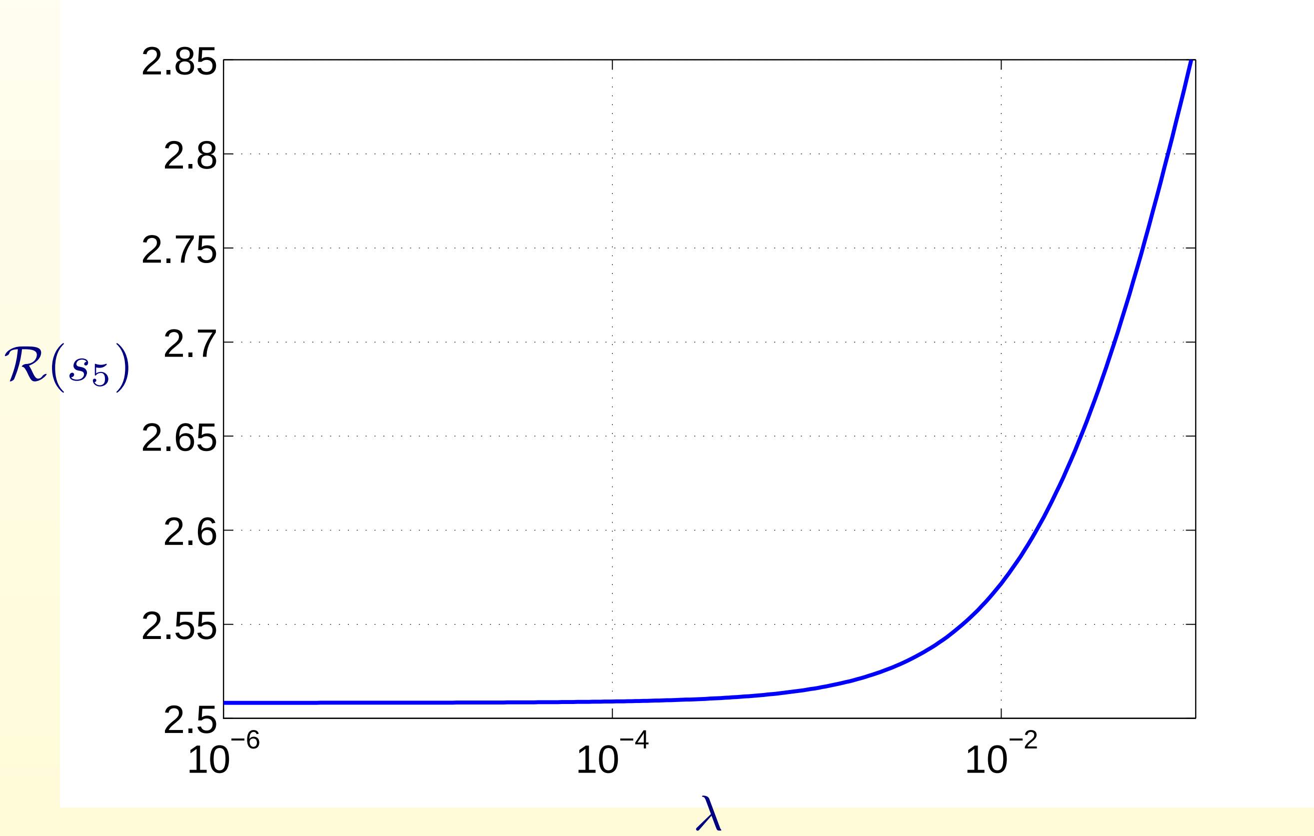

Real part of the unstable eigenvalue as a function of λ

Non Rotating Tethers. Variable Length

The idea original of Colombo and Farquhar is as follows: let us assume that the tether length is L and for that length we have the equilibrium position labeled with (1) in this figure. On the right of such a position, the system center of mass G is acted by a force that impulses it toward the right. By increasing the tether length up to $L^{(1)} = L + \Delta^{(1)}L$ we move the equilibrium position up to the point labeled with (2) in figure; now the force acting on G impulses it toward the left. Then we decrease the tether length, $L^{(2)} = L^{(1)} + \Delta^{(2)}L$ in order to move the equilibrium position on the left side of $G \ldots$ Thus, by changing the tether length in an appropriate way the center of mass G can be *stabilized* and kept in the neighborhood of the collinear lagrangian point L_2.

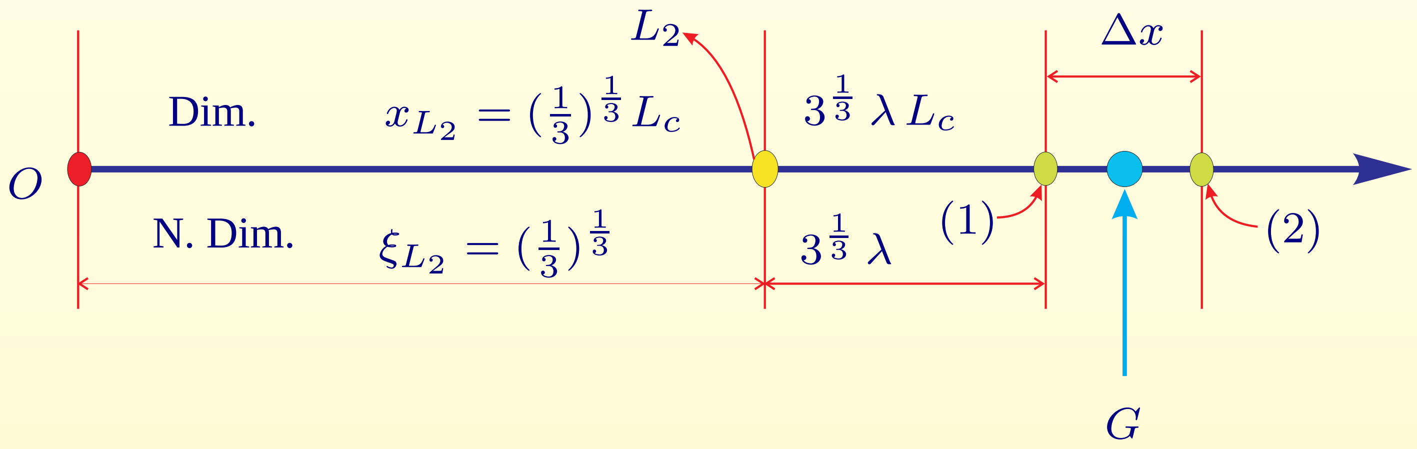

Distances from the small primary and from the collinear point L_2 when $\lambda \ll 1$ ($L_c = \ell\nu^{1/3}$)

NON ROTATING TETHERS. VARIABLE LENGTH

We carried out two different analysis:

- Linear approximation for small values of λ
- Full problem. Proportional control

We finish the analysis of non rotating tethers pointing to some drawbacks associated with this kind of control

- Control drawbacks

LINEAR APPROXIMATION FOR SMALL VALUES OF λ

$$\xi = \xi_L + 3^{1/3}\,\lambda_0(1+u(\tau))\,, \quad \eta = 3^{1/3}\,\lambda_0\,v(\tau)\,, \quad \lambda = \lambda_0(1+s(\tau))$$

$$\frac{d^2 u}{d\tau^2} - 2\,\frac{d v}{d\tau} - 9\,u(\tau) + \frac{9}{2}\left(3\,\cos^2\theta\,\cos^2\varphi - 1\right)\,s(\tau) + \frac{27}{2}\left(\cos^2\theta\,\cos^2\varphi - 1\right) = 0$$

$$\frac{d^2 v}{d\tau^2} + 2\,\frac{d u}{d\tau} + 3\,v(\tau) - 9\,\cos^2\varphi\,\cos\theta\,\sin\theta\,\left(1+s(\tau)\right) = 0$$

$$\frac{d^2 w}{d\tau^2} + 4\,w(\tau) - 9\,\cos\varphi\,\cos\theta\,\sin\varphi\,\left(1+s(\tau)\right) = 0$$

$$(1+s(\tau))\frac{d^2\theta}{d\tau^2} + \frac{d s}{d\tau}(1+\frac{d\theta}{d\tau}) - 2\,\tan\varphi\,\frac{d\varphi}{d\tau}\left(1+\frac{d\theta}{d\tau}\right)\left(1+\frac{d s}{d\tau}\right) + 12\,\cos\theta\,\sin\theta\,(1+s(\tau)) = 0$$

$$(1+s(\tau))\frac{d^2\varphi}{d\tau^2} + \frac{d s}{d\tau}\frac{d\varphi}{d\tau} + (1+s(\tau))\,\sin\varphi\,\cos\varphi\left[\left(1+\frac{d\theta}{d\tau}\right)^2 + 12\,\cos^2\theta\right] = 0$$

$$s(\tau) = e^{-\beta\,\tau}\,(A\,\cos\Omega\tau + B\sin\Omega\tau)$$

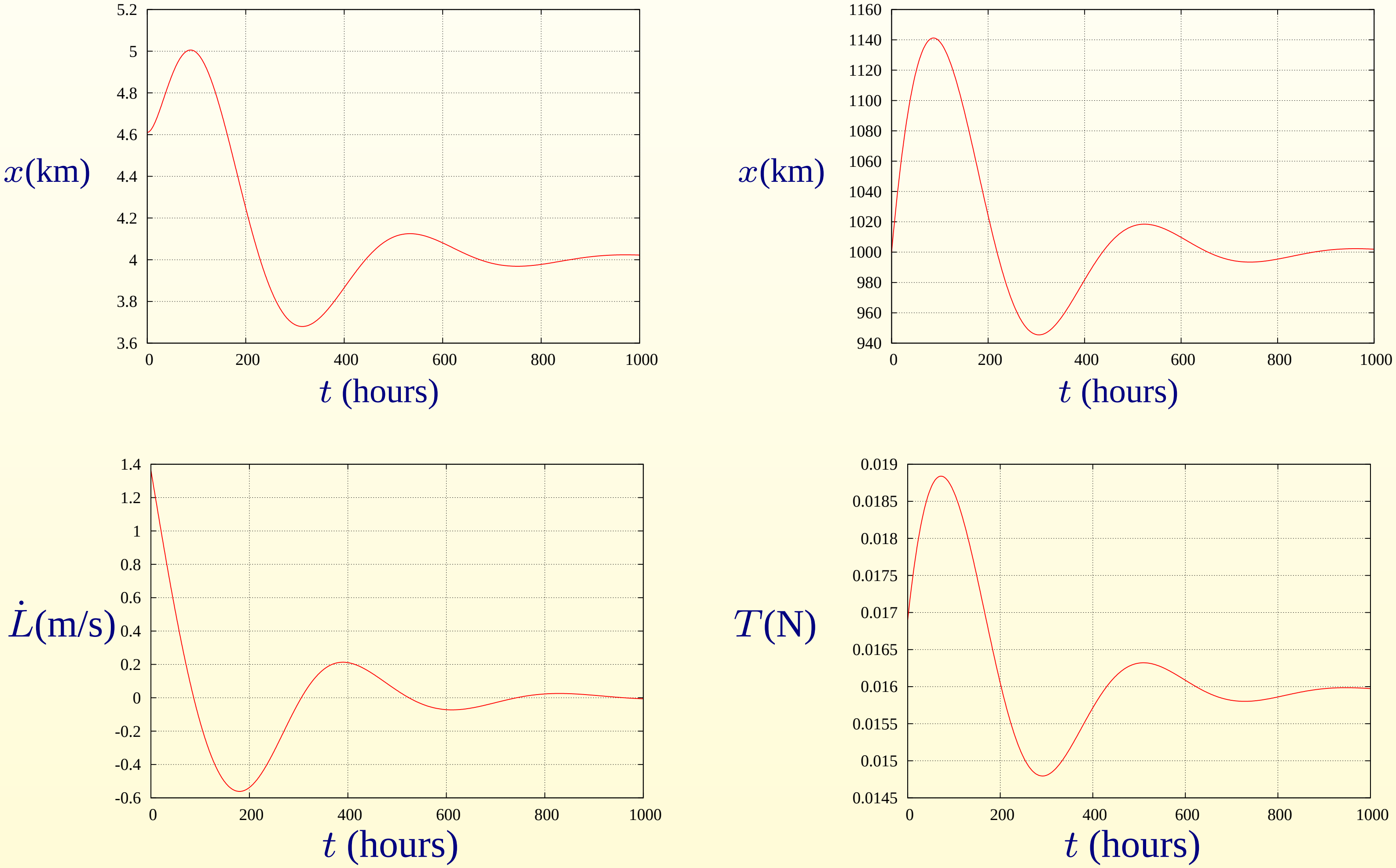

Massless tether with two equal masses (500 kg) at both ends in the Earth-Moon system. The selected parameters are $\beta = 0.5$, $\Omega = 1.5$, for the initial conditions $u_0 = 0.15$ and $\dot{u}_0 = 0$. The nominal tether length is $L = 1000$ km

Bi-dimensional motion

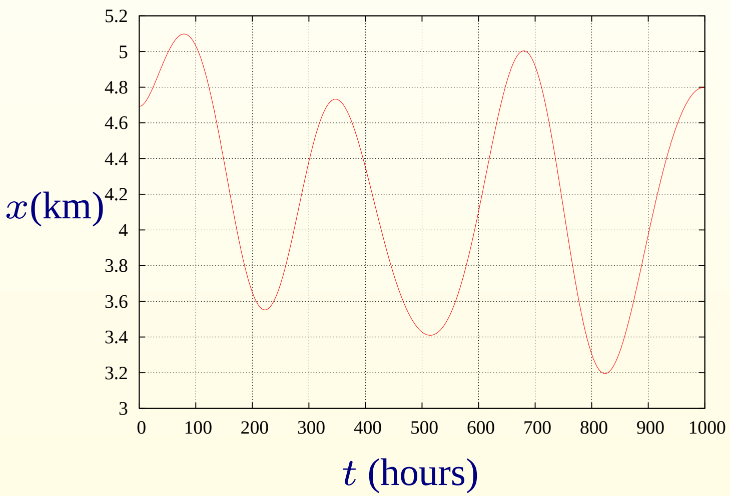

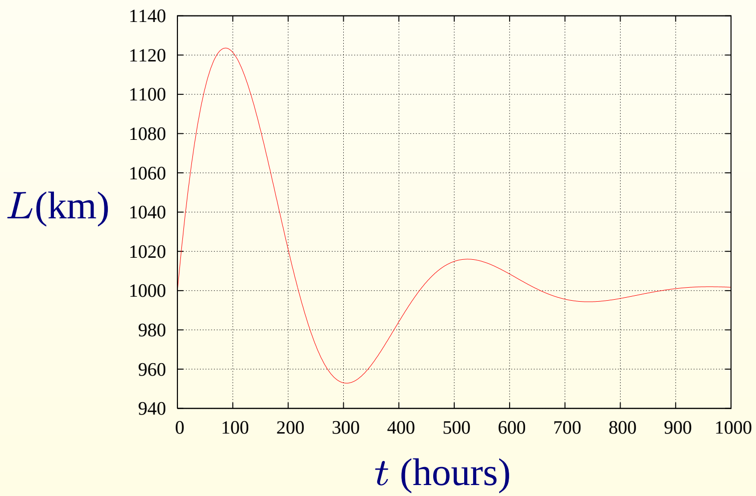

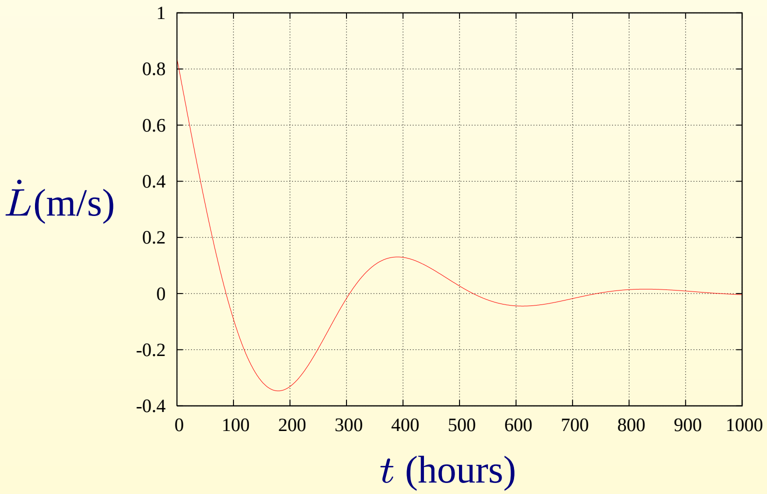

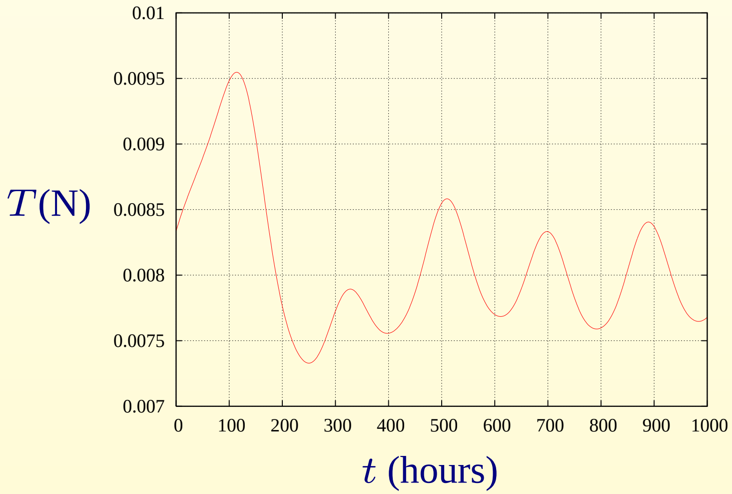

The length variation $\lambda(\tau)$ is governed by a proportional control law:

$$\lambda = \lambda_e + \sum K_i \left(x_i - x_{e,i}\right)$$

where K_i are gains and x_i stands for the variables ξ, η, θ.

$$\frac{d\,\boldsymbol{y}}{d\,t} = \mathcal{M}\,\boldsymbol{y}$$

where $\boldsymbol{y}^T = \left\{\delta\xi, \delta\eta, \delta\theta, \delta\dot{\xi}, \delta\dot{\eta}, \delta\dot{\theta}\right\}$.
The detailed stability analysis of this equation is cumbersome. Nevertheless, we firstly consider the simpler case in which only one gain K_ξ is different from zero. The characteristic polynomial takes the form:

$$s^3 + \left[\frac{3\,K_\xi}{\xi_e^4} - \left(2 - \frac{4}{\xi_e^3}\right)\right]\,s^2 + \left[\left(\frac{6\,J_g + 27}{\xi_e^4} + \frac{6}{\xi_e^7}\right)\,K_\xi - \left(105 - \frac{6}{\xi_e^3} + \frac{4}{\xi_e^6}\right)\right]\,s +$$
$$+6\left[\left(\frac{9}{\xi_e^4} - \frac{3}{\xi_e^7}\right)\,K_\xi - \left(45 + \frac{9}{\xi_e^3} - \frac{2}{\xi_e^6}\right)\right] = 0$$

The Descartes rule of signs provides **a sufficient condition for stability** to be fulfilled by K_ξ. Such a condition is drawn in figure as a function of the equilibrium value λ_e for a massless tether ($J_g = 1$).

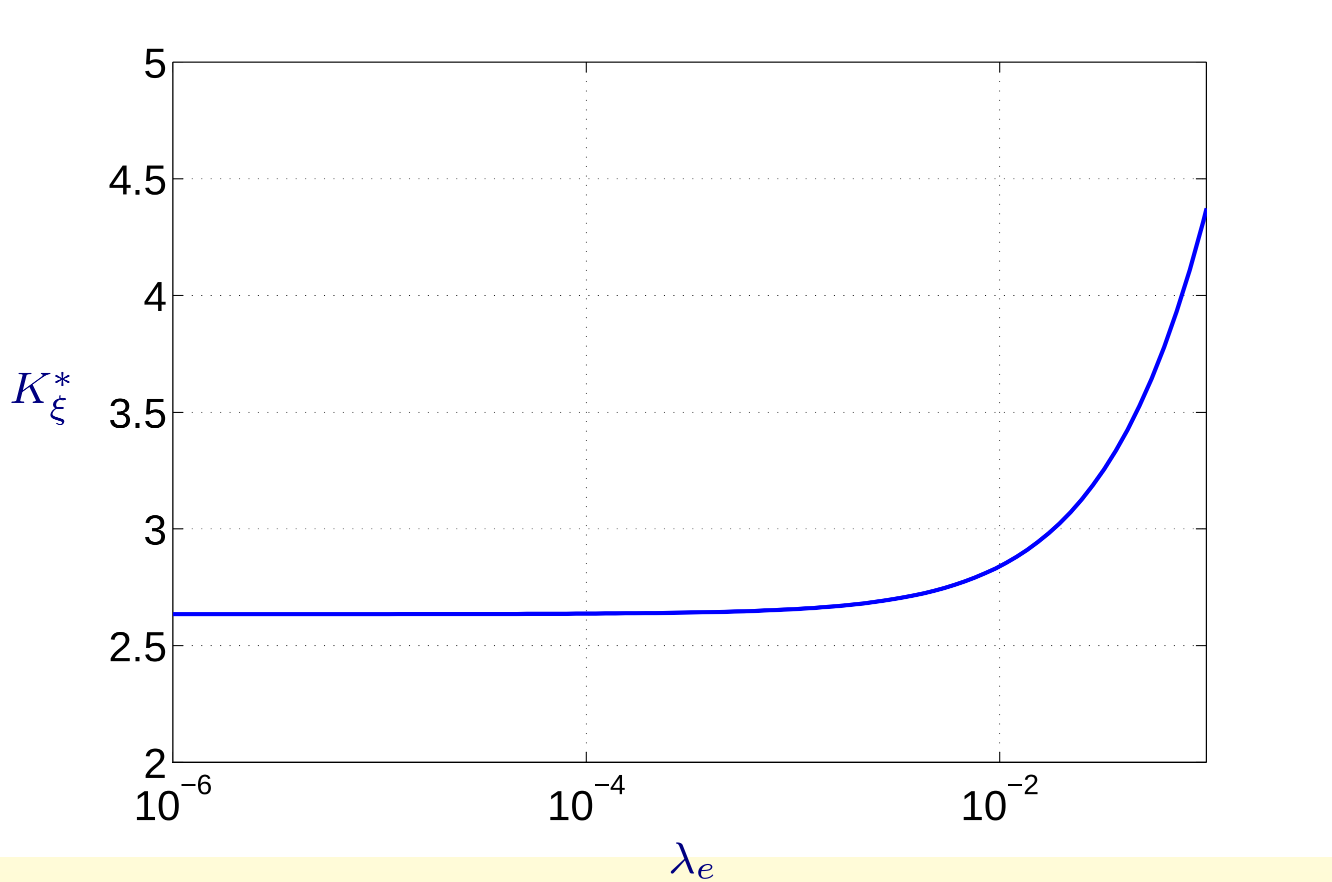

Sufficient condition for K_ξ to stabilize the system as a function of λ_e. Values over the curve ($K_\xi > K_\xi^*$) provide stability.

$$\frac{\Delta L}{\Delta x_e} = \frac{1}{2\,3^{\frac{1}{3}}\,\sqrt{a_2\,\lambda}}$$

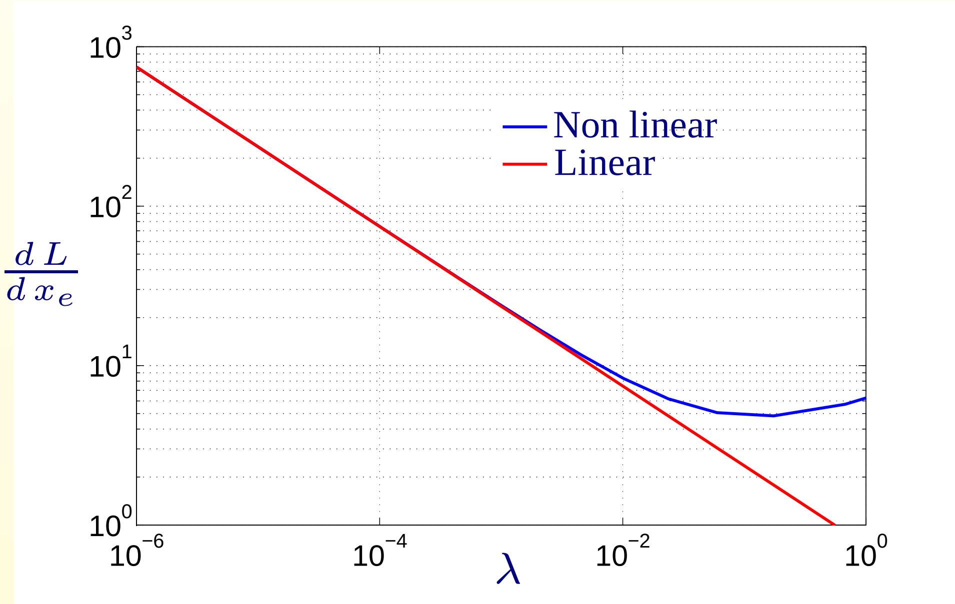

Ratio between variation of tether length and deviations of the center of mass vs. λ.

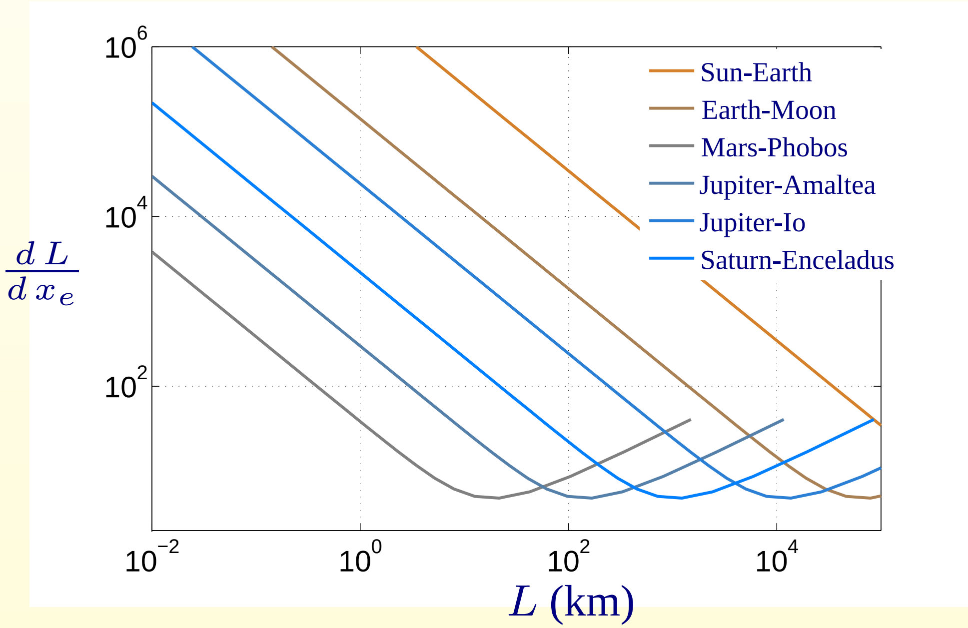

Ratio between variation of tether length and deviations of the center of mass vs. the tether length (km)

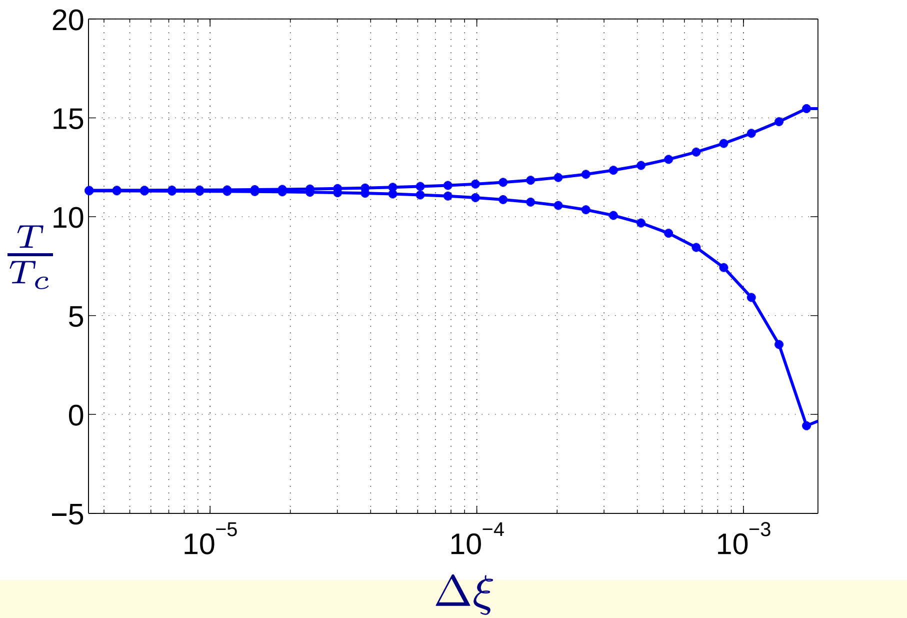

Maximum and minimum tether tension vs. the initial perturbation $\Delta\xi$ for $\lambda_e = 10^{-2}$.

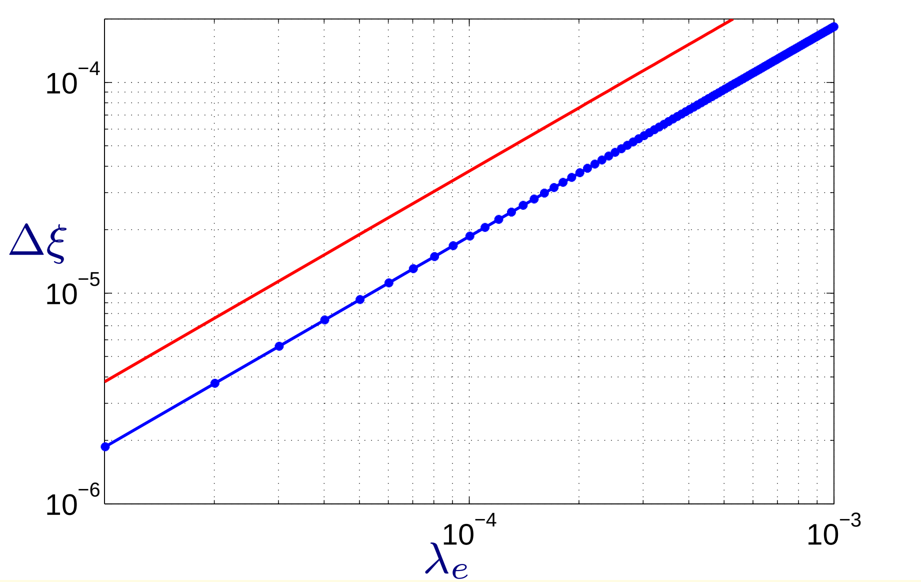

Zero tether tension $\Delta\xi$ vs. λ_e (blue line).

Zero tether length $\Delta\xi$ vs. λ_e (red line).

To avoid the zero tension problem (slack tether) is the most strong requirement of this control strategy

$$\xi_e = \pm\rho_e, \qquad \eta_e = \zeta_e = 0, \qquad \lambda_e = \frac{4\rho_e^5}{3}\left(3 - \frac{1}{\rho_e^3}\right), \qquad \rho_e^3 > 1/3$$

For small values of λ the above solution provides the asymptotic solution

$$\xi_e \approx (\frac{1}{3})^{\frac{1}{3}} + 3^{\frac{1}{3}}\,\frac{\lambda}{4} - 9\,(\frac{\lambda}{4})^2 + \mathcal{O}(\lambda^3)$$

Comparing with the same results for a non-rotating tether

$$\xi_e = \pm\rho_e, \qquad \eta_e = \zeta_e = 0, \qquad \lambda = \frac{\rho_e^2}{3}\left(3\,\rho_e^3 - 1\right), \qquad \rho_e^3 > 1/3$$

$$\xi_e \approx (\frac{1}{3})^{\frac{1}{3}} + 3^{\frac{1}{3}}\,\lambda - 9\,\lambda^2 + \mathcal{O}(\lambda^3)$$

ROTATING TETHERS. PROPORTIONAL CONTROL

$$\lambda = \lambda_e + K_\xi \delta\xi + K_{\dot\xi}\delta\dot\xi + K_\eta \delta\eta + K_{\dot\eta}\delta\dot\eta$$

Through the Routh-Hurwitz theorem, it has been found that **asymptotic stability** is guaranteed if the gains of the control law satisfy the relations

$$K_\xi \geq \frac{4}{3}\rho_e\left(15\rho_e^3 - 2\right) \qquad K_{\dot\xi} > 0 \qquad K_\eta = 0 \qquad K_{\dot\eta} = 0$$

We carried out two simulations of a rotating tether with different values of K_ξ and $K_{\dot\xi}$ in order to see the qualitative behavior of the system. The characteristics of the simulations are:
$\lambda_e = 0.0401$ ($\xi_e = 0.707$); $\xi_0 - \xi_e = 10^{-3}$, $\eta_e = 10^{-3}$; $\Omega_\perp = 50$.

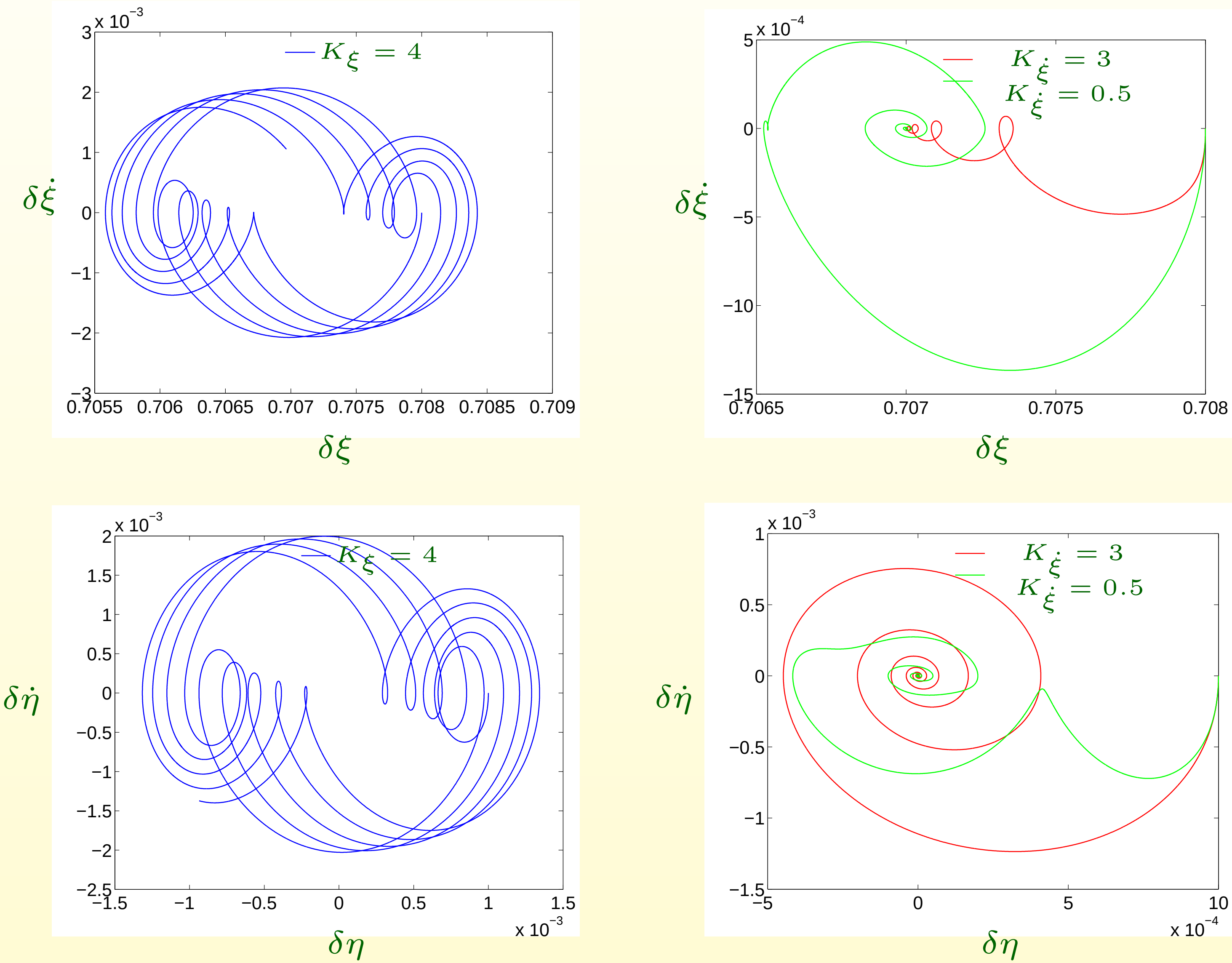

$$\lambda_e = 0.0401\ (\xi_e = 0.707);\ \xi_0 - \xi_e = 10^{-3},\ \eta_e = 10^{-3};\ \Omega_\perp = 50$$

SIMULATIONS

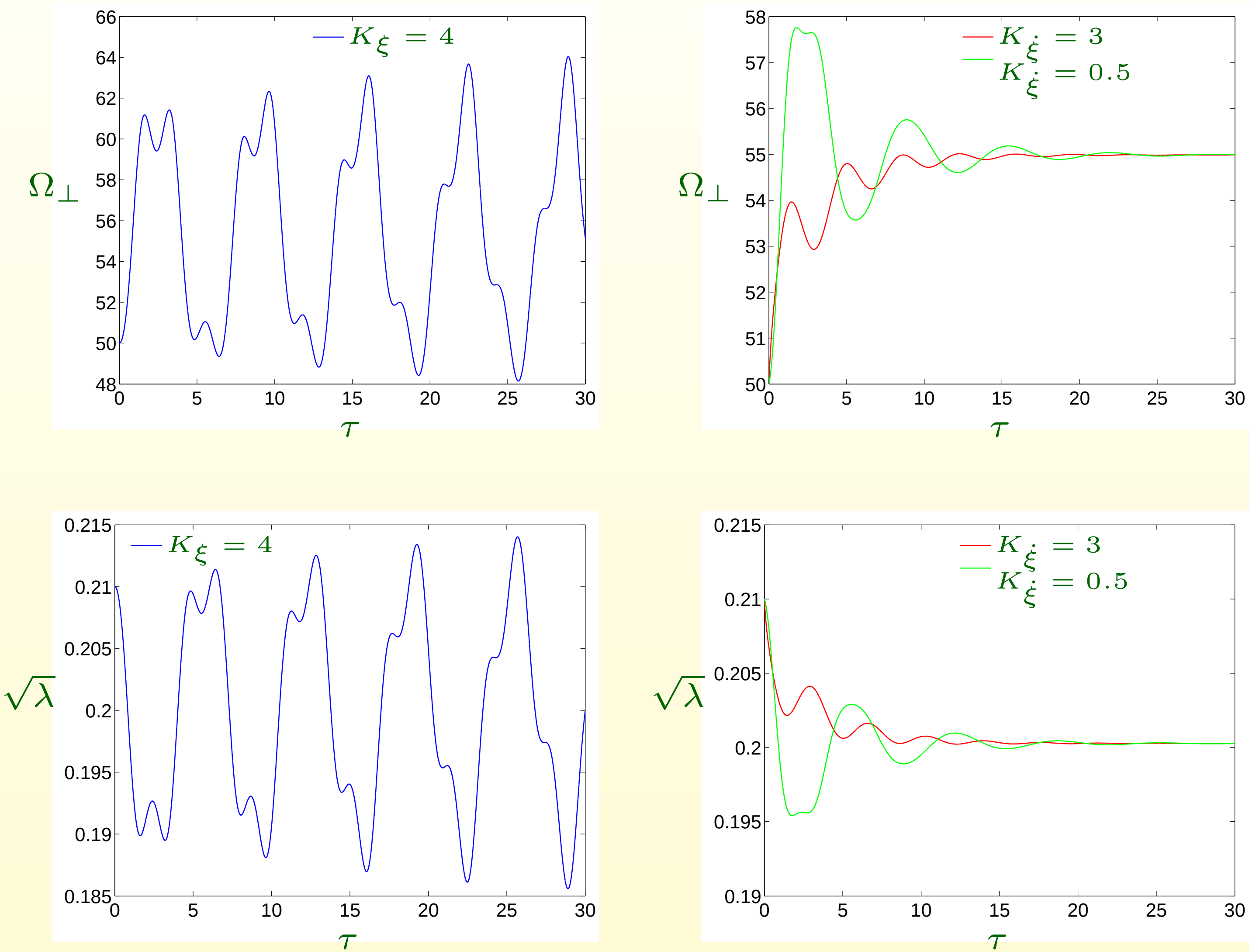

The END of
Stability of tethered satellites
at collinear lagrangian points

Lyapunov orbits

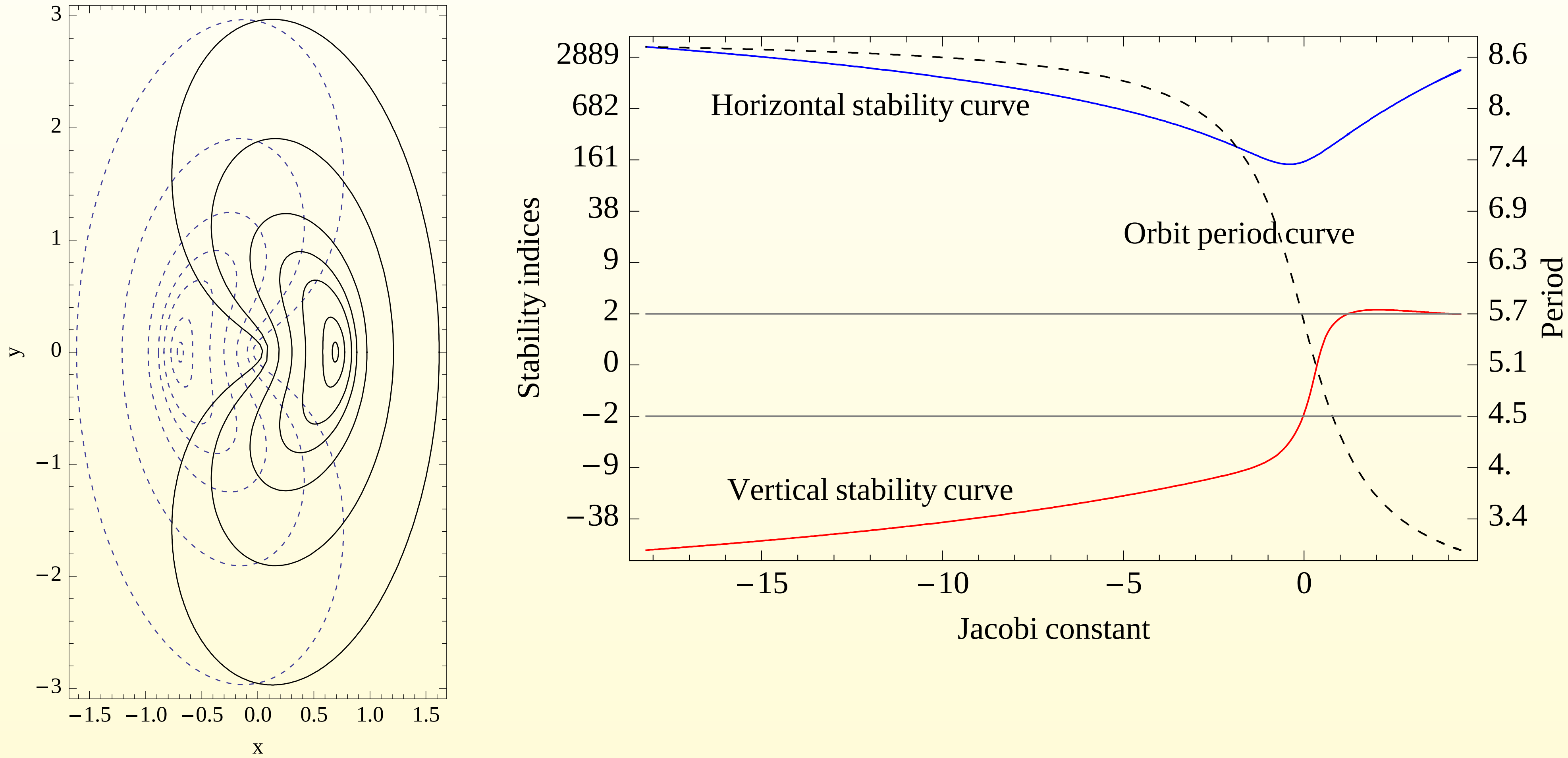

- Left: sample orbits of the family of Lyapunov orbits around L_1 (dashed) and L_2 (full line) for, from larger to smaller, $C = -1, 0, 1, 2, 3, 4$. Right: stability-period diagram of the family of Lyapunov orbits of the Hill problem. Note the $\mathrm{arcsinh}$ scale used for the stability curves. (C is the Jacobi constant)

Tethered family of Lyapunov orbits: unstable

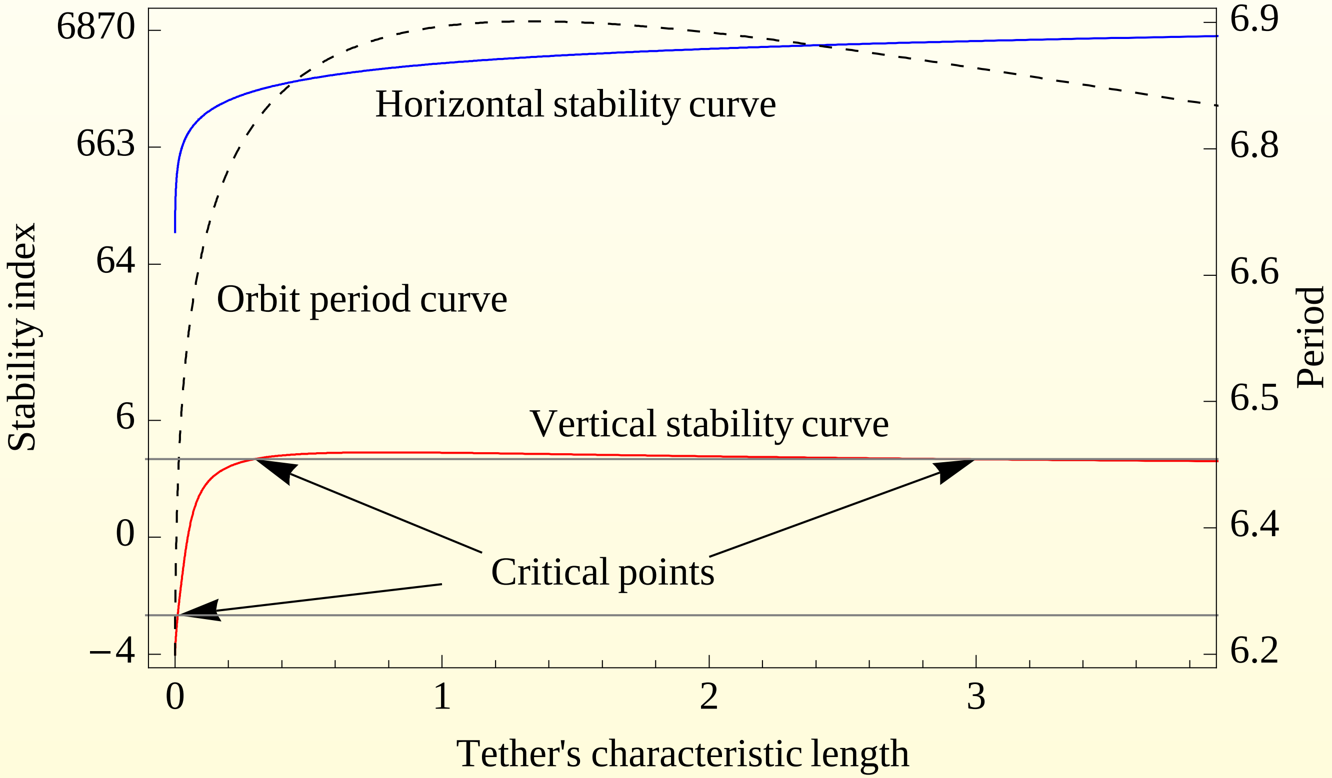

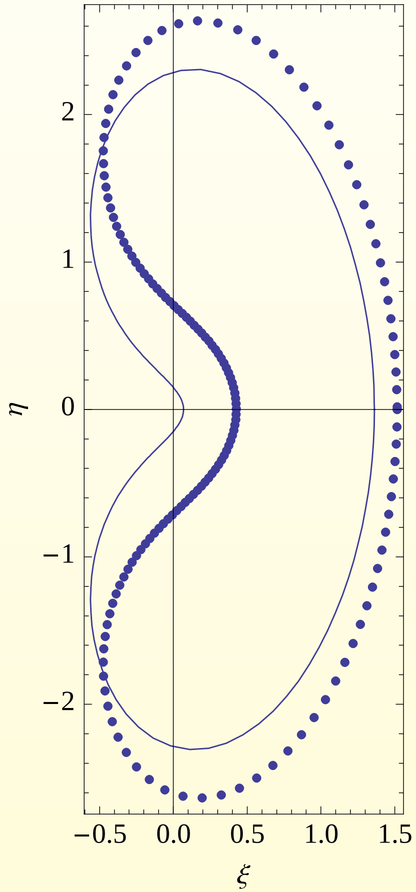

- Left: stability-period diagram of the family of Lyapunov orbits with Jacobi constant $C = -0.408295$ for tether's length variations; the horizontal gray lines correspond to the critical values $k = \pm 2$ (in the $\operatorname{arcsinh}$ scale). Rigth: Hill's problem Lyapunov orbit ($\lambda = 0$, full line) and an orbit with a tehter's characteristic lenght $\lambda = 1$ (dotted). (C is the Jacobi constant)

Tethered family of Lyapunov orbits: unstable

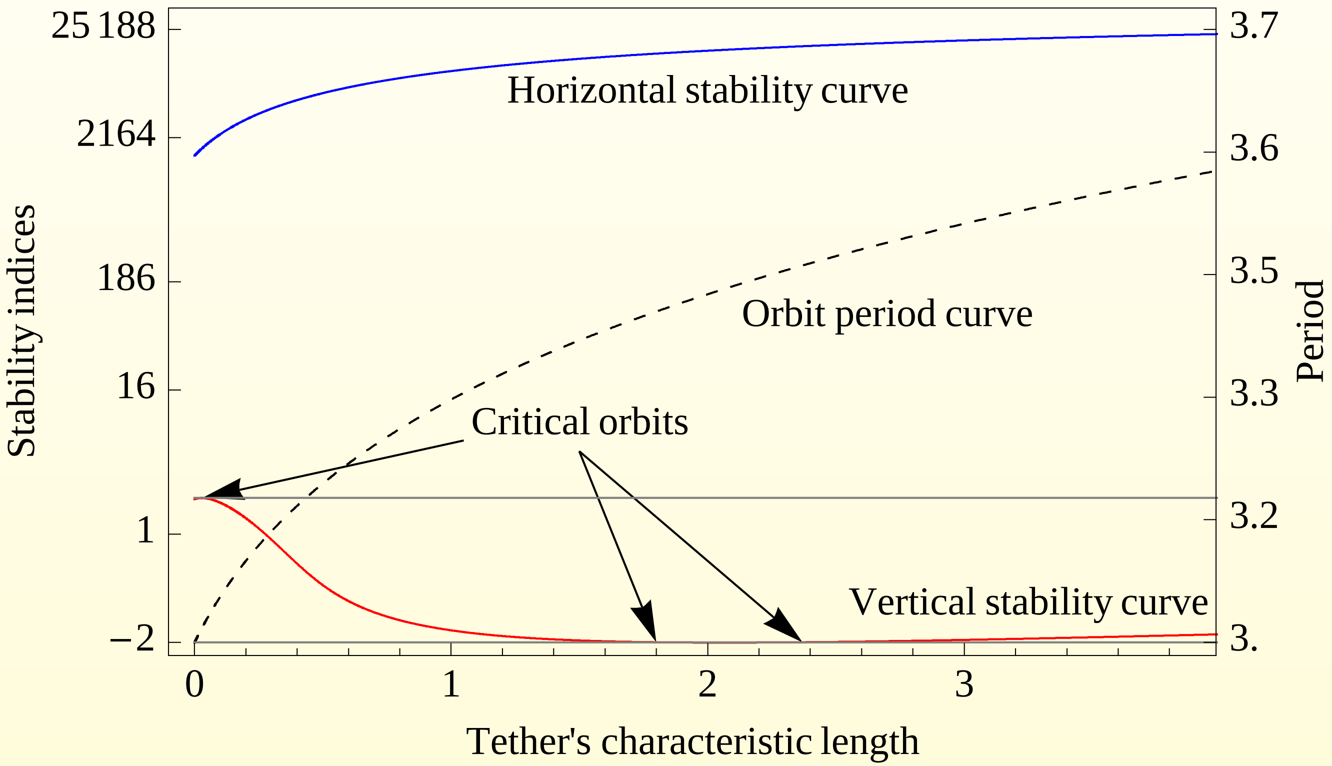

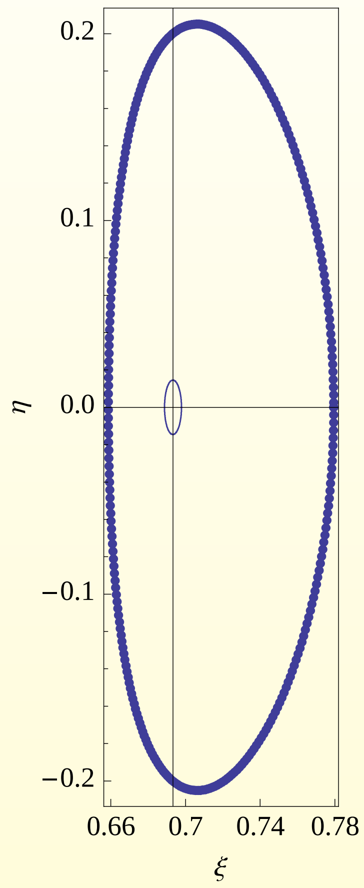

• Left: stability-period diagram of a family of Lyapunov orbits close to L_2 for tether's length variations; the horizontal gray lines correspond to the critical values $k = \pm 2$ (in the $\operatorname{arcsinh}$ scale). Rigth: starting orbit ($\lambda = 0$, full line) and an orbit with $\lambda = 0.1$ (dotted). (C is the Jacobi constant)

Family of eight-shaped orbits

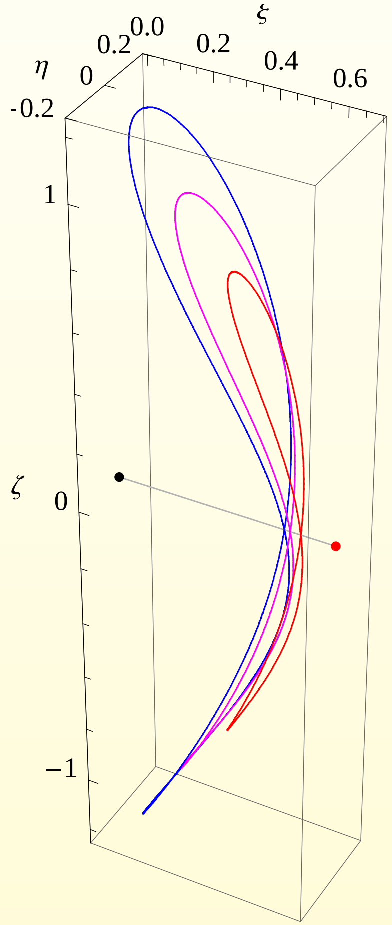

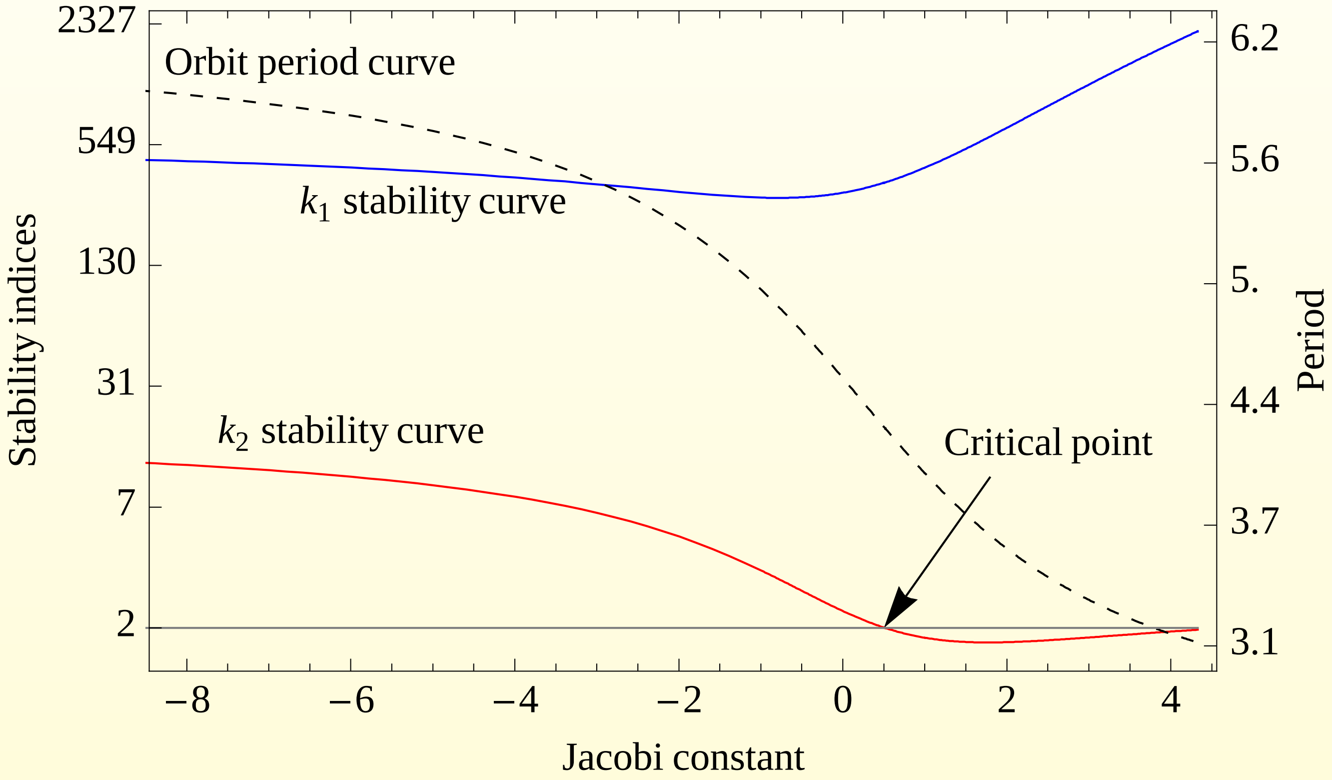

- Left: sample eight-shaped orbits for $C = 2$ (red), 1 (magenta), and 0 (blue). Right: stability-period diagram of the family of eight-shaped orbits of the Hill problem. (C is the Jacobi constant)

Tethered family of eight-shaped orbits

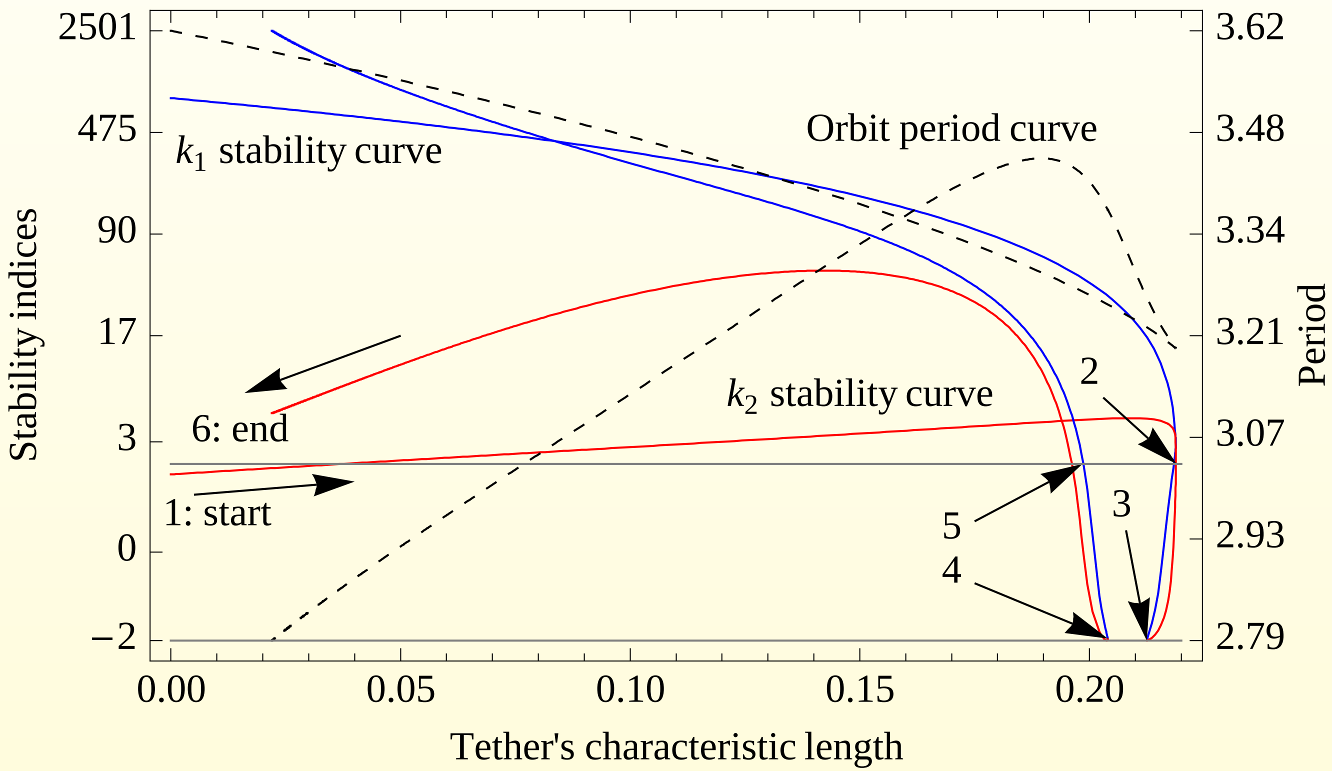

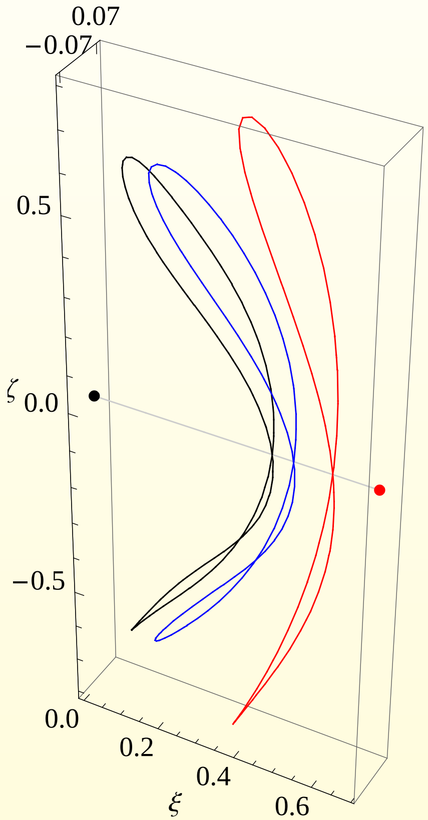

• Left: stability-period diagram of a family of eight-shaped, periodic orbits with constant $C = 2$ for tether's length variations; the horizontal gray lines correspond to the critical values $k = \pm 2$. Rigth: stable orbits for $\lambda = 0.2$ (left) $\lambda = 0.215$ (center), and unstable orbit of the Hill problem ($\lambda = 0$, right). (C is the Jacobi constant)

Tethered family of eight-shaped orbits

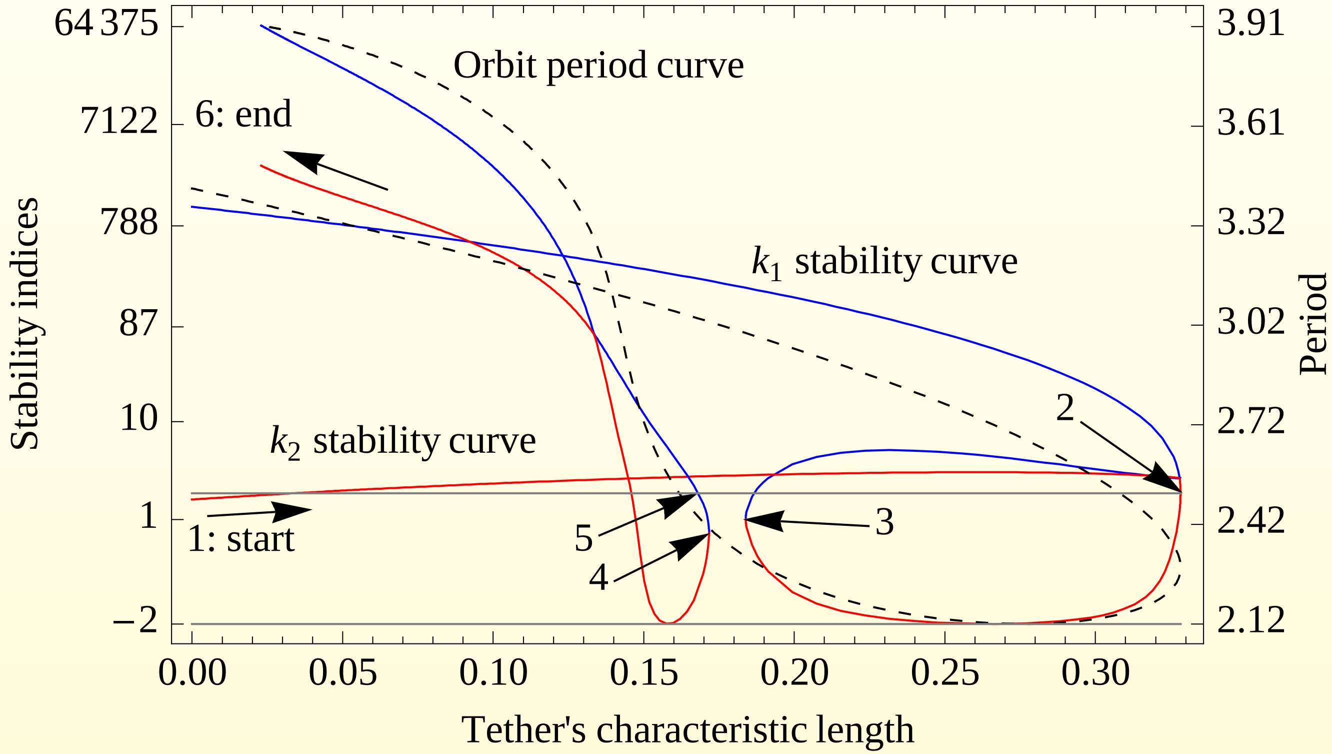

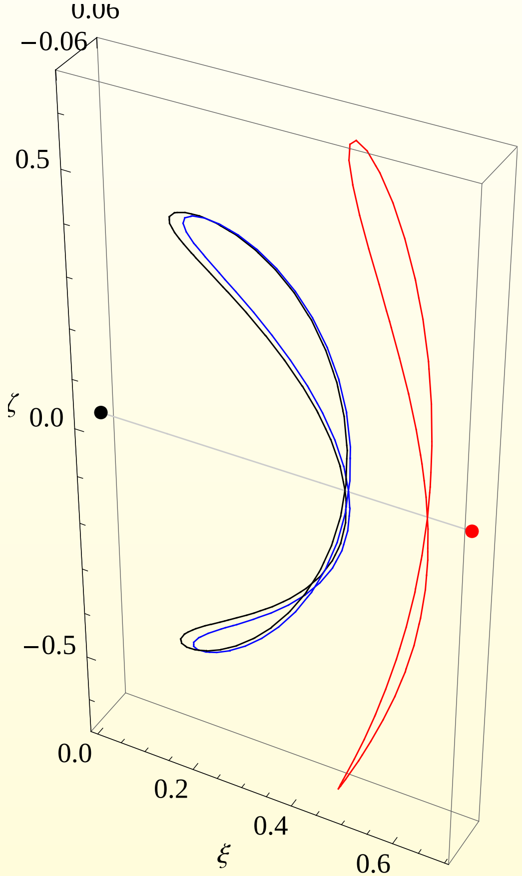

• Left: stability-period diagram of a family of eight-shaped, periodic orbits with constant $C = 2.7$ for tether's length variations; the horizontal gray lines correspond to the critical values $k = \pm 2$. Right: stable orbits for $\lambda = 0.17$ (left, black) $\lambda = 0.184$ (center, blue), and unstable orbit of the Hill problem ($\lambda = 0$, right). (C is the Jacobi constant)

Tethered family of eight-shaped orbits

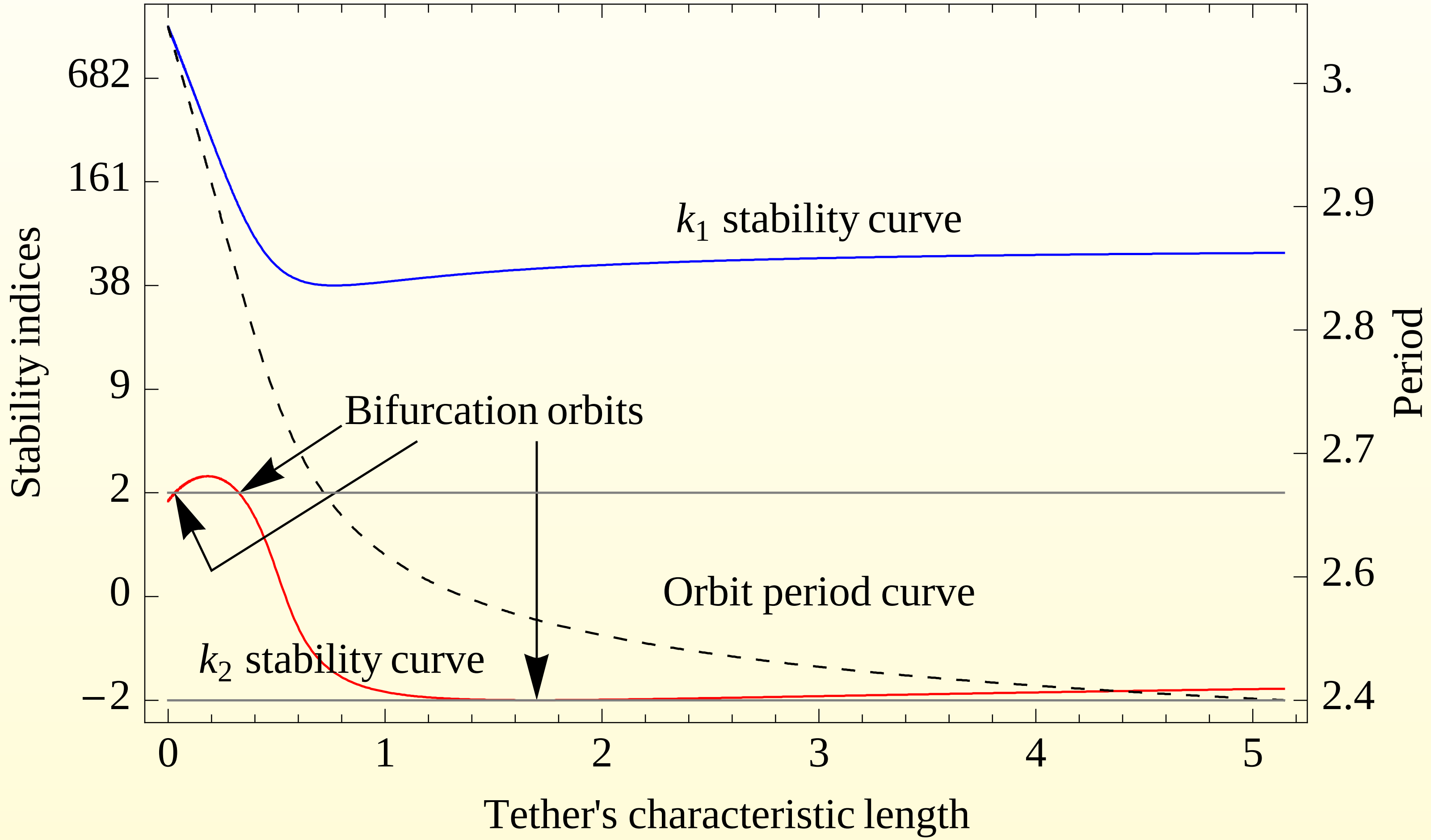

- Stability-period diagram of a family of eight-shaped, periodic orbits with constant $C = 3$ for tether's length variations; the horizontal gray line corresponds to the critical values $k = +2$. (C is the Jacobi constant)

Family of Halo orbits

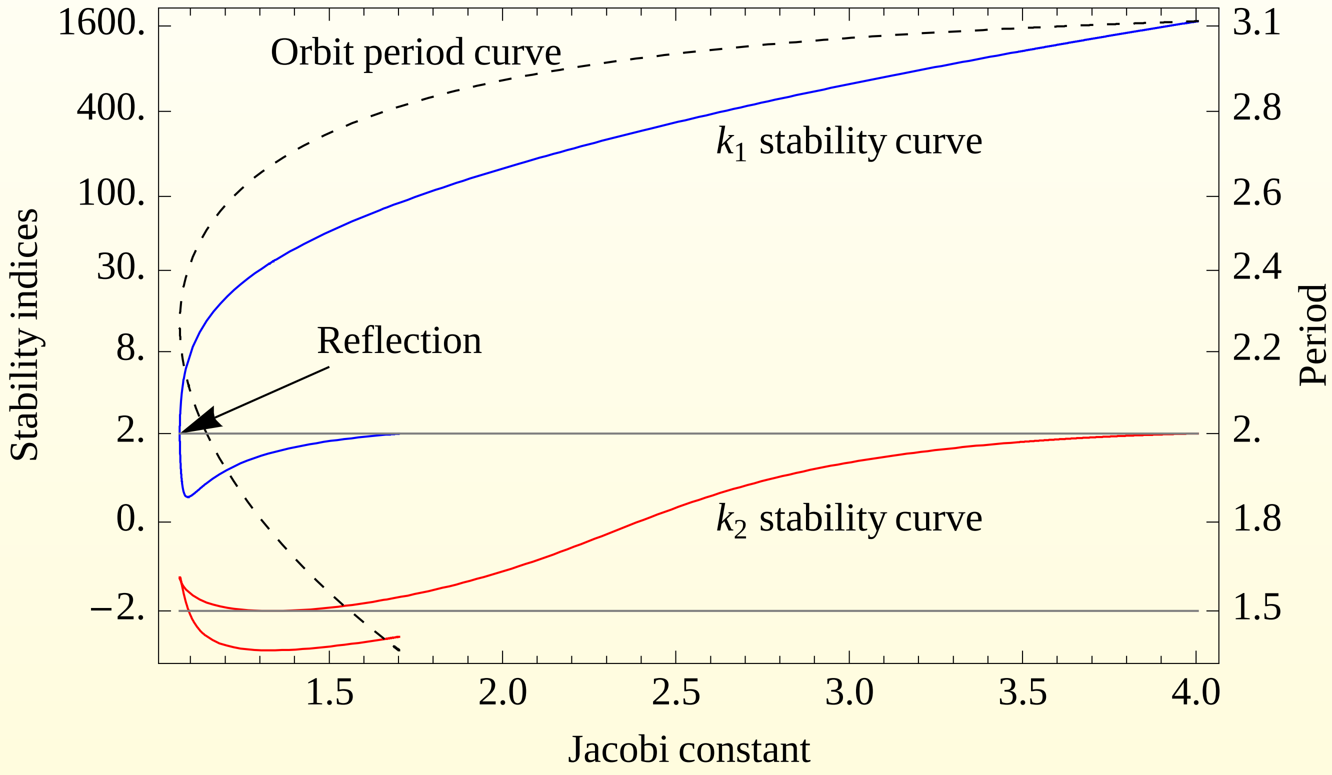

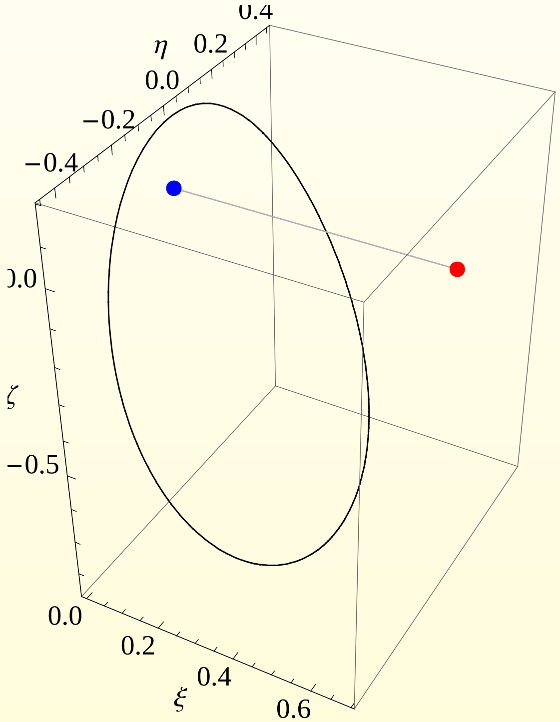

- Left: stability-period diagram of the family of Halo orbits of the Hill problem. Right: sample stable orbit for $C = 1.08$ (the blue and red dots linked by a gray line are the origin and L_2 point, respectively). (C is the Jacobi constant)

Tethered family of Halo orbits

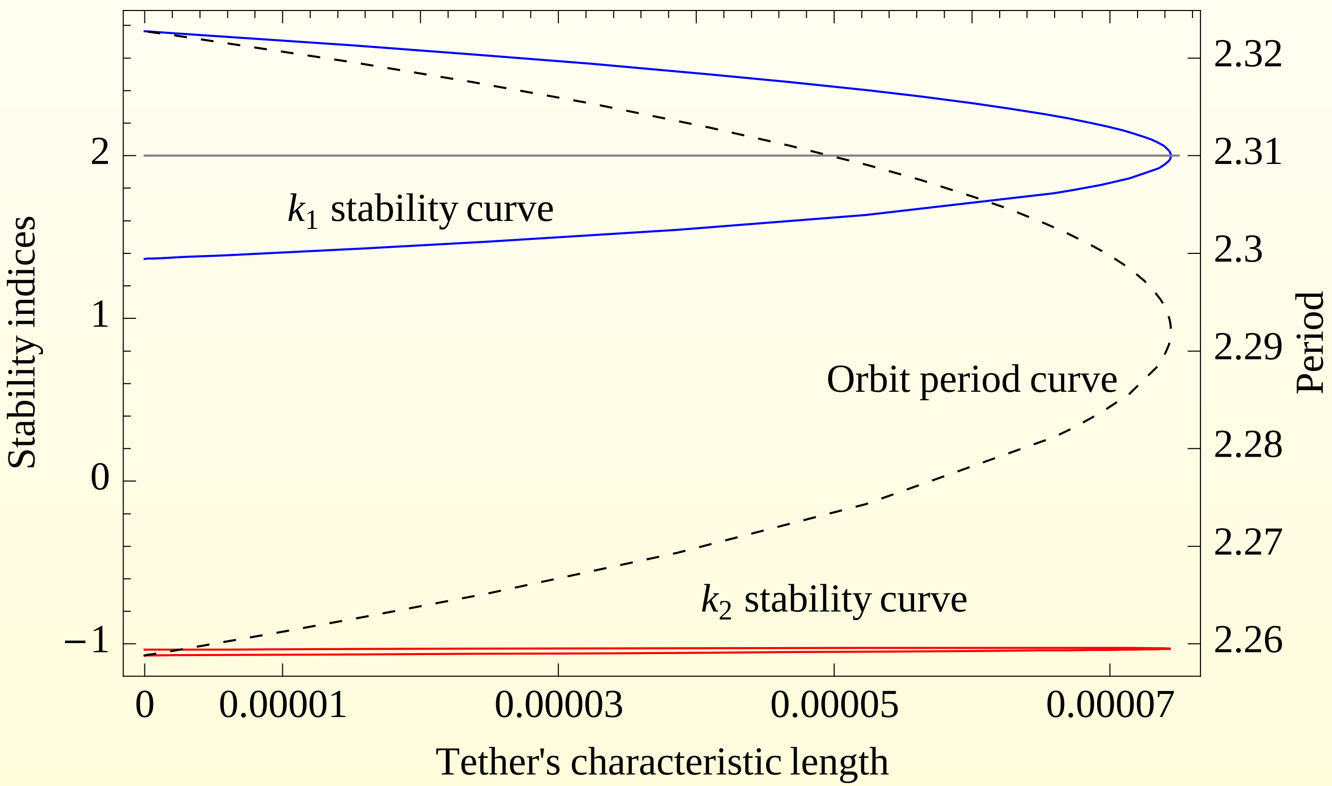

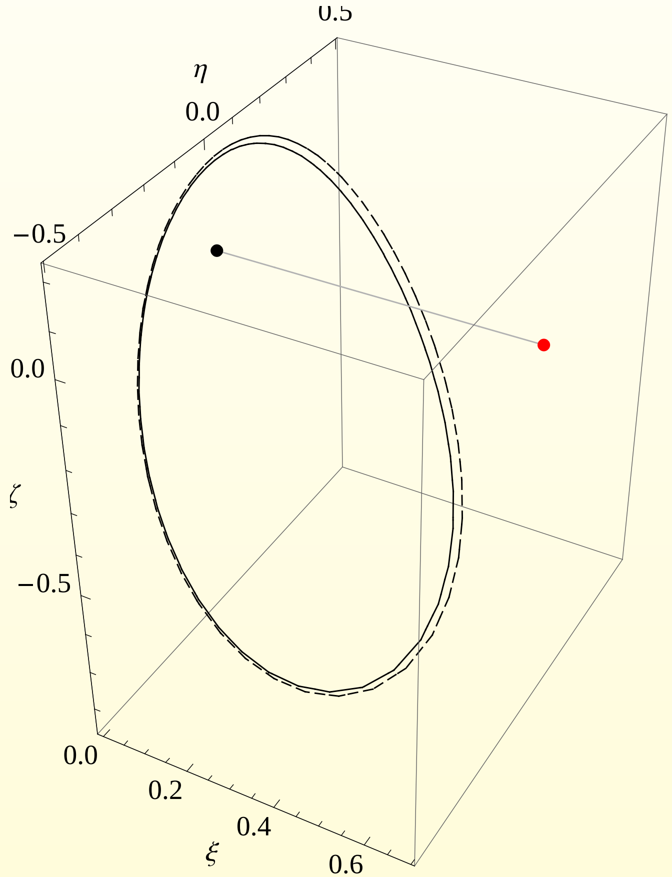

• Left: Stability-period diagram of the family of Halo orbits with $C = 1.07$ for tether's length variations.
Right: stable (full line) and unstable (dashed) Halo orbits of the Hill problem. (C is the Jacobi constant)

Tethered family of Halo orbits

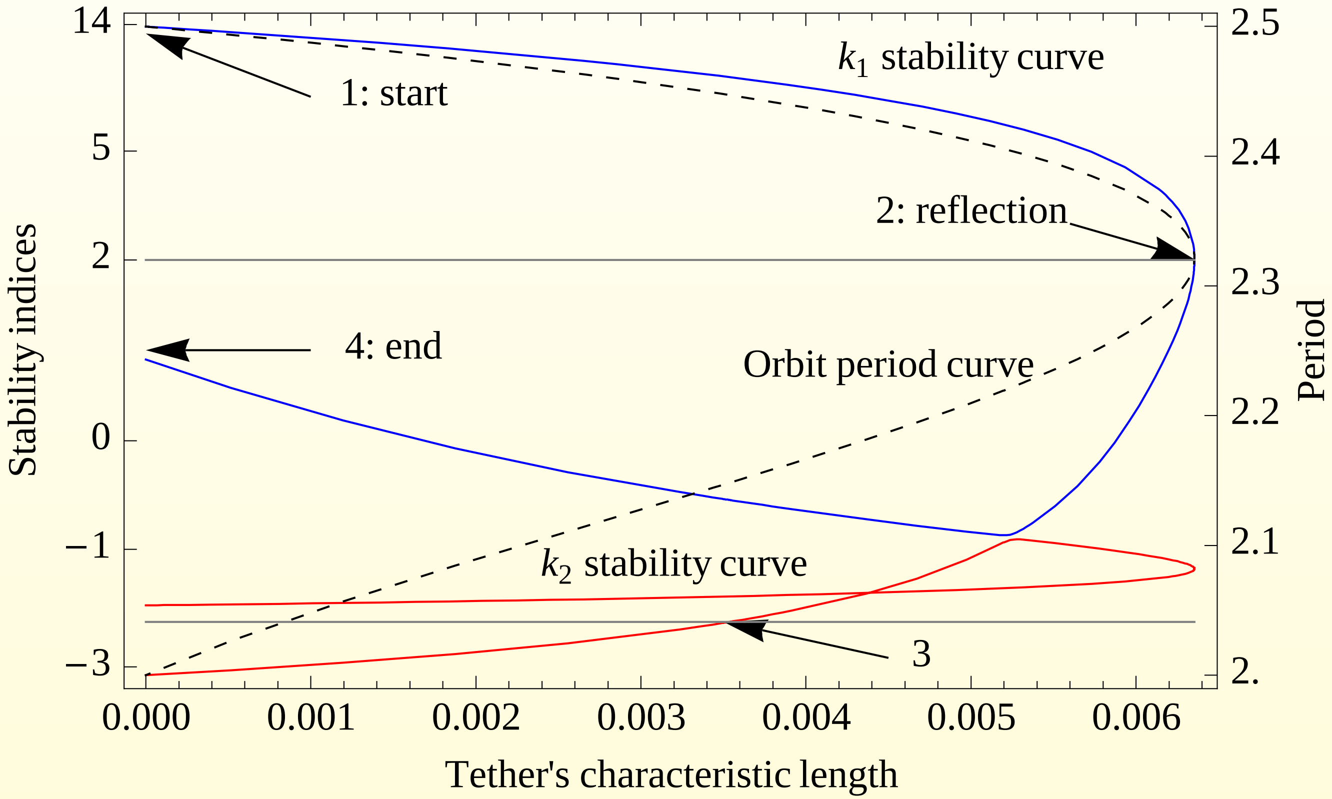

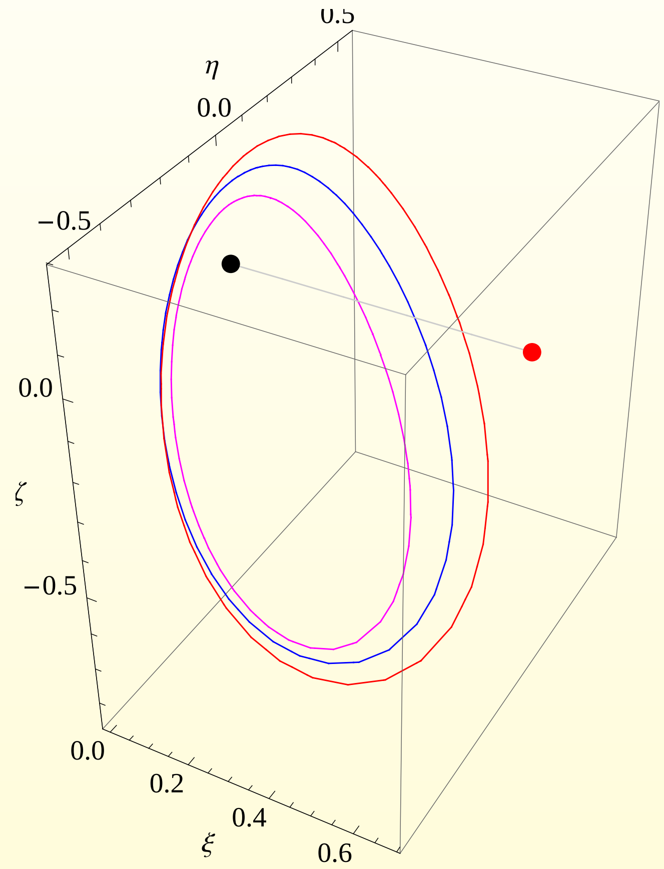

● Stability-period diagram of the family of Halo orbit with $C = 1.15$ for tether's length variations. Right: unstable Halo orbits of the Hill problem (red and magenta) and stable (blue) Halo orbits with a tethers characteristic length $\lambda = 0.0052$. (C is the Jacobi constant)

Tethered family of Halo orbits

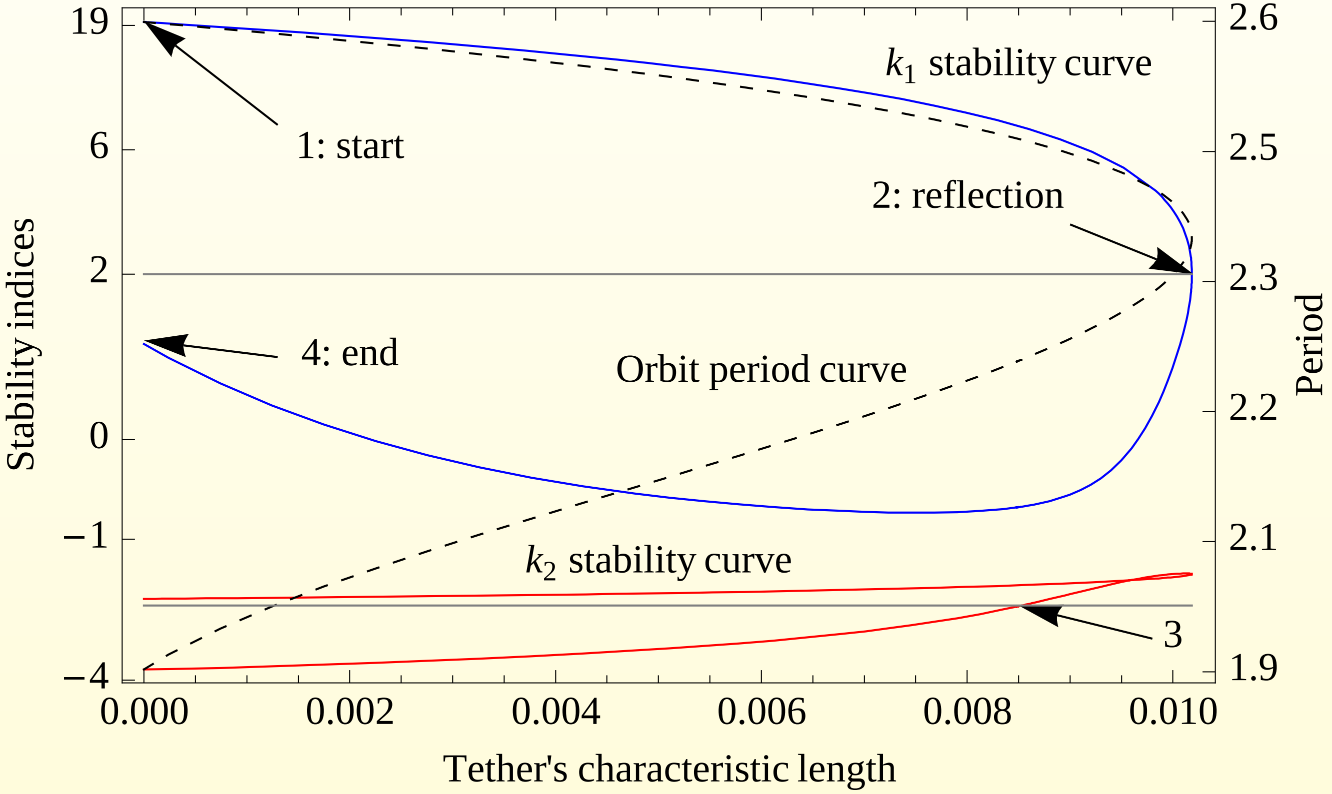

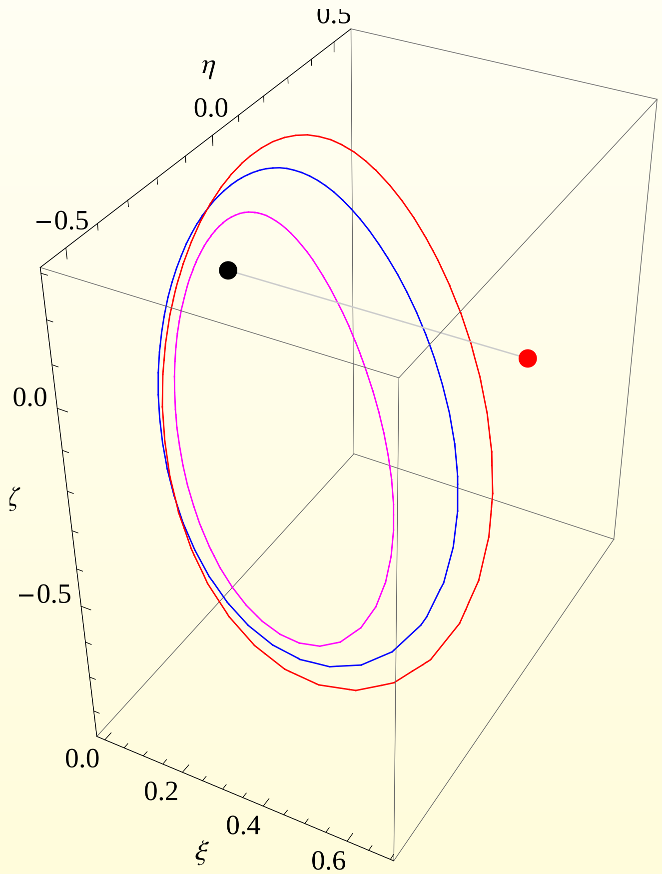

• Stability-period diagram of the family of Halo orbit with $C = 1.2$ for tether's length variations. Right: unstable Halo orbits of the Hill problem (red and magenta) and stable (blue) Halo orbits with a tethers characteristic length $\lambda = 0.009$. (C is the Jacobi constant)

Tethered family of Halo orbits

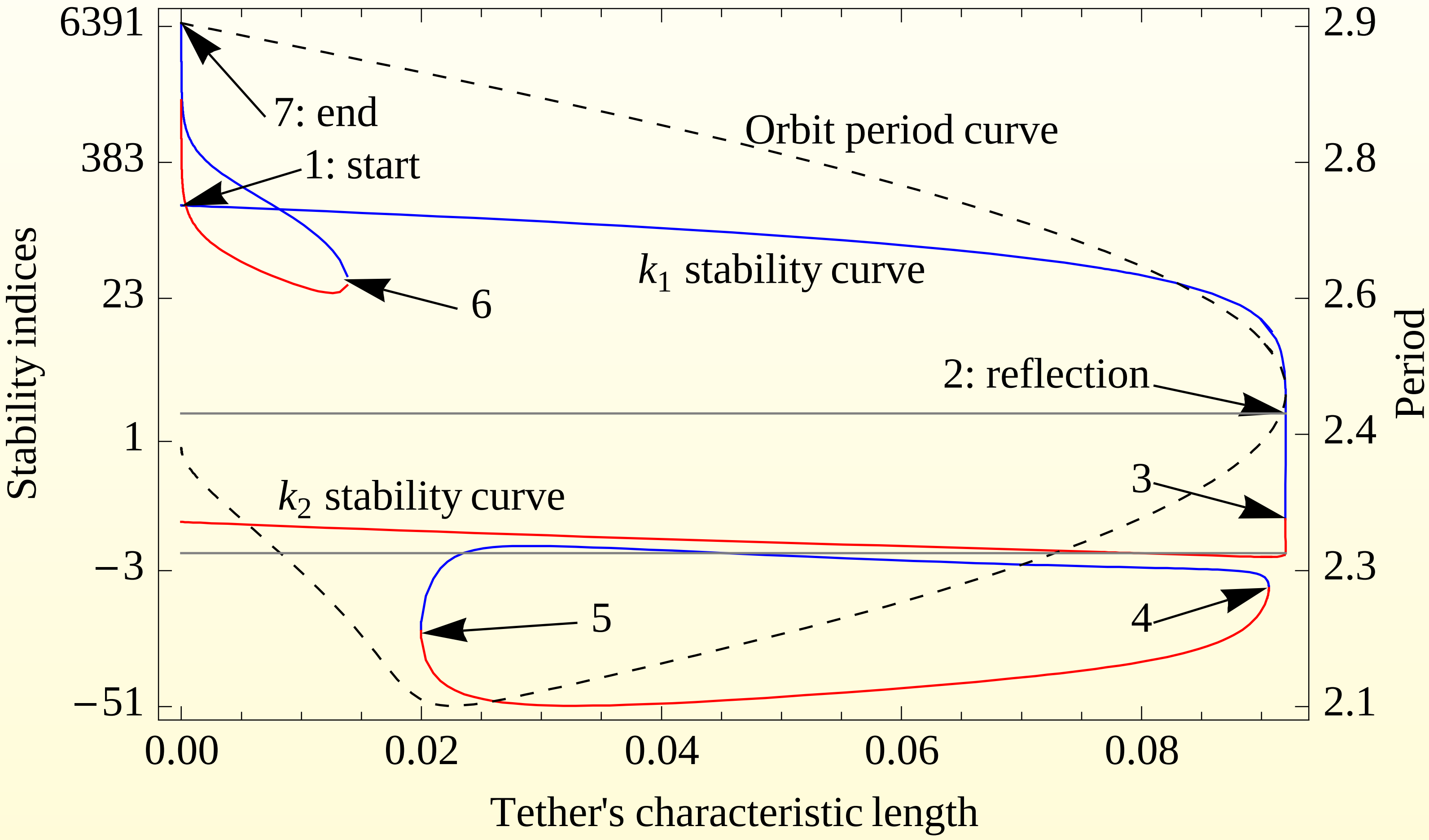

- Stability-period diagram of the family of Halo orbit with $C = 2$ for tether's length variations. The horizontal, gray lines mark the critical values $k = \pm 2$ in the $\operatorname{arcsinh}$ scale. (C is the Jacobi constant)